Results in Physics 30 (2021) 104690

Contents lists available at ScienceDirect

Results in Physics

journal homepage: www.elsevier.com/locate/rinp

The physical origin of a photon-number parity effect in cavity quantum electrodynamics

Agostino Migliore [a,*], Anna Napoli [b,c], Antonino Messina [d]

[a] Department of Chemical Sciences, University of Padova, Via Marzolo 1, 35131 Padova, Italy
[b] Dipartimento di Fisica e Chimica Emilio Segrè, Università degli Studi di Palermo, Via Archirafi 36, I-90123 Palermo, Italy
[c] Istituto Nazionale di Fisica Nucleare, Sezione di Catania, Via Santa Sofia 64, I-95123 Catania, Italy
[d] Dipartimento di Matematica ed Informatica, Università degli Studi di Palermo, Via Archirafi, 34, I-90123 Palermo, Italy

ARTICLE INFO

Keywords:
Quantum optics
Parity effect
Atom-field interaction
Quantum entanglement
Entropy

ABSTRACT

The rapidly increasing capability to modulate the physicochemical properties of atomic groups and molecules by means of their coupling to radiation, as well as the revolutionary potential of quantum computing for materials simulation and prediction, fuel the interest for non-classical phenomena produced by atom-radiation interaction in confined space. One of such phenomena is a "parity effect" that arises in the dynamics of an atom coupled to two degenerate cavity field modes by two-photon processes and manifests itself as a strong dependence of the field dynamics on the parity of the initial number of photons. Here we identify the physical origin of this effect in the quantum correlations that produce entanglement among the system components, explaining why the system evolution depends critically on the parity of the total number of photons. Understanding the physical underpinnings of the effect also allows us to characterize it within the framework of quantum information theory and to generalize it. Since a single photon addition/removal has dramatic effects on the system behavior, this effect may be usefully applied, also for amplification purposes, to optoelectronics and quantum information processing.

Introduction

The past decade has witnessed a rapidly growing interest in quantum coherence that may be used to enhance the physicochemical function in novel electronic materials or in biomolecular systems, where coherence can be detected against the typical incoherent background using spectroscopic techniques such as, e.g., two-dimensional electronic spectroscopy [1]. The debate on long-lived quantum coherence in photosynthetic energy transfer processes [2–4] has significantly contributed to spark such interest. The main approaches to the investigation of quantum coherence (which is akin to quantum correlations and thus also important for quantum information purposes) include: (i) the use and mimic of efficient biological processes that involve both tunneling and quantum correlations, such as charge separation and proton-coupled electron transfer [5,6]; (ii) the quantum confinement and coupling in low-dimension electronic materials [7–12]; (iii) the tuning of atomic and molecular properties by interaction with light [13–15]. Many studies use combinations of these approaches [13,16–18]. Recent experiments show the feasibility of the emission of quantum light from 2D materials [19–21] and cavity quantum electrodynamics between atomic arrays (acting as mirrors) to which the Jaynes-Cummings model [22] has been applied [14,23].

The ability to produce and detect single photons (hence, quantum light) supports fundamental studies aimed at probing quantum rules [24,25], revealing significant effects of individual photons [25,26], and using them in technology that is also relevant to quantum information processing [26–30]. Within this context, we describe giant single-photon effects on the dynamics of two field modes of an ideal cavity coupled to an atom (modeled as a two-effective level system, which can also represent a quantum dot or generally a fermionic exciton interacting with cavity field) by two-photon processes. We demonstrate why the addition/removal of one photon in any of the two field modes dramatically changes the evolution of the photon distribution over the field modes, thus significantly extending the quantum optics parity effect [31,32]. The thus generalized parity effect is explained using equations of motion and the analytical solution of the Hamiltonian model of the system. Furthermore, by means of entropy measures such as the quantum (von Neumann) mutual entropy [33], we obtain signatures of the

* Corresponding author.
E-mail address: agostino.migliore@unipd.it (A. Migliore).

https://doi.org/10.1016/j.rinp.2021.104690
Received 19 July 2021; Accepted 11 August 2021
Available online 23 August 2021

crucial entanglement at the core of the system dynamic evolution, which fosters future studies aiming to use the single-photon magnification in quantum information and computation applications.

System Hamiltonian and parity effect

The system consists of a two-level atom coupled to two field modes of an ideal cavity with the same frequency ω_F and orthogonal polarizations. The propagation directions of the two modes can differ. The lower and upper atomic states (denoted $|-\rangle$) and $|+\rangle$, respectively) have the same parity and an energy separation $\hbar\omega_0$ that satisfies the resonance condition $\omega_0 \cong 2\omega_F$ and thus implies a two-photon resonant interaction between atom and radiation field. The relevance of the two-level approximation for practical applications has been greatly expanded by recent experiments showing that an organic molecule within an optical cavity can behave like a two-level quantum system with a high degree of coherent evolution [34]. The system is described by the effective Hamiltonian [31] ($\hbar = 1$)

$$H = 2\omega S_z + \omega \sum_{\mu=1}^{2} \widehat{n}_\mu + \lambda \sum_{\mu=1}^{2} \left(a_\mu^2 S_+ + a_\mu^{\dagger 2} S_- \right) \tag{1}$$

Appendix A (which extends previous analysis of this Hamiltonian [31] and a strictly related one [32]) provides new insights into the range of physical conditions that are appropriately described by this interaction model (including the absence of Stark shift terms and one-photon interactions of the atom with both modes) and into the relations among ω_F, ω_0 and the effective frequency $\omega \approx \omega_F$. H acts on the atomic state through the ½ pseudospin operators S_z and $S_\pm$ ($S_z|\pm\rangle = \pm\frac{1}{2}|\pm\rangle$, $S_\pm|\pm\rangle = 0$, and $S_\pm|\mp\rangle = |\pm\rangle$ describes the atom excitation or de-excitation). The annihilation (creation) operator a_μ ($a^\dagger_\mu$) determines the photon removal from (addition to) field mode μ ($\mu = 1, 2$) and satisfies Bose's commutation relation $[a_\mu, a_\mu^\dagger] = 1$. $\widehat{n}_\mu = a_\mu^\dagger a_\mu$ is the photon number operator for mode μ ($\mu = 1, 2$). The first two terms in the expression of H are the Hamiltonians of isolated atom and field, while the last term describes the interaction between atom and field, as well as, implicitly, the interaction between the two modes, which is necessarily mediated by the atom through a coupling constant λ. In particular, $a_\mu^2 S_+$ causes a two-photon transition from mode μ to the atom, while $a_\mu^{+2} S_-$ de-excites the atom by transferring two photons to mode μ.

It was shown that the system evolution from the initial state

$$|\psi(0)\rangle = |n\rangle|0\rangle|-\rangle \equiv |n, 0, -\rangle \tag{2}$$

(i.e., one mode is excited in a Fock state with n photons, the other mode is empty, and the atom is in its ground state) shows a parity effect: the population of mode 1 reaches a plateau value of $\sim n/2$ and, after a 'lethargy' period, a revival of the field dynamics leads to significant depletion or repopulation of field mode 1 depending on the parity of n (Fig. 1a and 1d) [31,32]. For $\lambda t \ll n^{3/2}/2$, this behavior is approximately described by (cf. references [31,32] and see the exact expression in Appendix D, where it is derived after defining a new class of polynomials that enable the simplification of multiple summations)

$$n_1(t) \equiv \left\langle \widehat{n}_1(t) \right\rangle \equiv \langle \psi(t)|\widehat{n}_1|\psi(t)\rangle \cong \frac{n}{2}\left[1 + cos^{n-1}\left(\frac{2\lambda t}{n}\right)\right] \tag{3}$$

Furthermore, at the middle of the lethargy period, the covariance $\sigma_{12}(t) \equiv \left\langle \widehat{n}_1(t)\widehat{n}_2(t) \right\rangle - n_1(t)n_2(t)$ shows a maximum anticorrelation between the populations of the modes for even n and a minimum degree of correlation for odd n (Fig. 1b and 1e). However, σ_{12} gives very little information on the correlations at the heart of the system dynamics, especially since $\sigma_{12} \approx -(\sigma_1^2 + \sigma_2^2)/2$ (see Appendix C) and hence the σ_{12} main evolution can be seen as a result of the variances σ_1^2 and σ_2^2 of the individual mode populations (Fig. 1c and f). In fact, the physical origin of the parity effect has been elusive, thus hindering our understanding of whether this effect could survive the many possible perturbations that may affect the purity of the selective initial population of one field mode. Here (i) we find this physical origin in the (quantum) entanglement between the states of the subsystems and its interplay with the

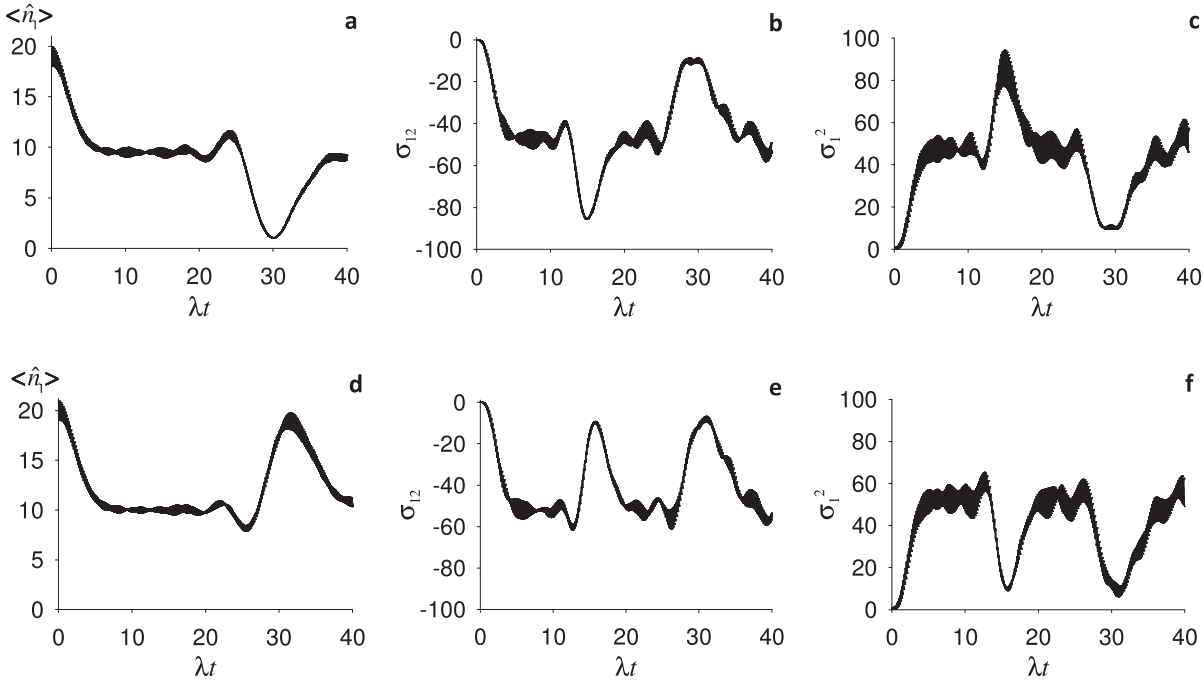

Fig. 1. Field population dynamics from the initial condition of Eq. (2). (a) Mean photon number in mode 1 $\left\langle \widehat{n}_1 \right\rangle$, (b) covariance of the two mode populations σ_{12}, and (c) variance of the mode 1 photon number σ_1^2 vs. λt for the initial condition of Eq. (2) with $n = 20$. (d–f) Corresponding quantities for $n = 21$ (cf. references [31;32]).

symmetry properties of the initial condition. (ii) We identify the quantum correlations responsible for the system dynamics and (iii) quantify them so as to link the quantum optics parity effect to quantum information theory approaches. (iv) With clear relevance to potential applications, we show that the essence of the effect is in the relative parity of the initial populations n and m of the two modes (which can be restated in terms of the parity of the total photon number $n+m$ because only two modes are considered here), thereby generalizing the parity effect to the initial condition

$$|\psi(0)\rangle = |n,\, m,\, -\rangle \tag{4}$$

Such generalization is important for potential applications of the optical effect, where environmental perturbations may undermine the selective population of the modes.

System symmetry and equations of motion

Fig. 1a and d show a lethargy period of the field dynamics between 'macroscopic revivals' of the photon redistribution. The existence of plateaus in $n_1(t)$ and $n_2(t)$, as well as their value (namely, about half the total excitation number) are nontrivial aspects of the system dynamics (e.g., a priori one could not exclude a different type of evolution of the field population without plateaus or with an oscillation between two different plateaus symmetric with respect to $n/2$). To gain insight into the physical origin of the observed features, we examine the equation of motion (Appendix E)

$$\frac{dn_\mu(t)}{dt} = -2\lambda \mathrm{Im}\left\langle \left[a_\mu^2(t) - a_\nu^2(t)\right] S_+(t) \right\rangle - \frac{d\langle S_z(t)\rangle}{dt} \qquad (\nu \neq \mu = 1,2) \tag{5}$$

Eq. (5) highlights the competing photon-transfer processes between the two field modes and the atom that entangle the states of the field and atom subsystems, thus enabling the photon redistribution. The first term on the right-hand side of Eq. (5) vanishes (or rapidly oscillates around zero; *vide infra*) if the system approaches a state that is symmetric with respect to the two field modes (hereafter referred to as field symmetry), which thus have similar propensity to exchange photons with the atom. Then, the populations of the field modes experience small and fast oscillations strictly related to the atomic inversion evolution (see Fig. D1), but their coarse-grained dynamics slows down until substantial quenching, consistent with the plateaus in Fig. 1a and d. The field-atom correlation term is also zero in the initial factorized state, for which $\langle a_1^2 S_+\rangle = \langle a_2^2 S_+\rangle = 0$. However, the asymmetry of the initial photon distribution triggers the system evolution, as one can see from the second derivative

$$\begin{aligned} \frac{1}{4\lambda^2}\frac{d^2\langle \Delta\hat{n}(t)\rangle}{dt^2} &= 2N\langle S_z(t)\Delta\hat{n}(t)\rangle + \langle \Delta\hat{n}(t)\rangle \\ &= N\left[\sigma_2^2(t) - \sigma_1^2(t)\right] + \left[2N\langle S_z(t)\rangle + 1\right]\langle \Delta\hat{n}(t)\rangle \end{aligned} \tag{6}$$

(see derivation in Appendix E), where $\Delta\hat{n} \equiv \hat{n}_1 - \hat{n}_2$ and N is the value of the total excitation number operator $\hat{N} = \hat{n}_1 + \hat{n}_2 + 2S_z + 1$, which is a constant of motion. In particular, N is n and $n+m$ starting from the initial conditions (2) and (4), respectively.

$d^2\langle \Delta\hat{n}(t)\rangle/dt^2$ is approximately zero, on average, during the plateaus of $n_1(t)$ and $n_2(t)$. This implies similar correlations between the two field modes and the atom (in particular, $\langle S_z\Delta\hat{n}\rangle \approx 0$ after coarse graining the field dynamics) and $\langle \Delta\hat{n}\rangle \approx 0$ (Fig. D2), which approximately sets the value of the mode populations during their plateaus.

Eqs. (5) and (6) explain the existence of plateaus in Fig. 1a and d and the slow evolution of the photon population towards and from states of high symmetry with respect to the two field modes. Given the field symmetry of the Hamiltonian, the large photon redistribution after the plateaus implies that an exact field symmetry is never achieved. In Eq. (6), $\langle \Delta\hat{n}\rangle$ and $\langle S_z\Delta\hat{n}\rangle$, or $\sigma_2^2 - \sigma_1^2$, embody the residual field asymmetry necessary for the subsequent evolution of the system, but the reason and physical underpinnings for this evolution back to states of high field asymmetry (which manifests the parity effect) remain to be explained.

Parity effect from (pseudo)symmetry-entanglement interplay

The inspection of Eqs. (5) and (6) suggests that, since the interaction Hamiltonian is symmetric with respect to the field modes, the evolution of the system from an asymmetric condition such as in Eq. (2) or (4) drives the system to states of the highest symmetry compatible with the initial condition, as well as with the revival dynamics that follows the plateaus of Fig. 1a and d. Therefore, in order to understand the giant single-photon effects of Fig. 1a and d, we search for mid-plateau states of the system that have the maximum field symmetry compatible with the subsequent dynamics, taking into account that the symmetry and correlation properties of the mid-plateau states have to depend on the initial condition so as to produce the parity effect. The system evolution from the initial condition (2) or (4) to such maximally symmetric states requires entanglement between the field modes, which implies entanglement of the field and the atom because the atom mediates the interaction between the two modes, as described by the interaction Hamiltonian. This is consistent with the form of the system state at a generic time t,

$$|\psi(t)\rangle = \sum_{r=0}^{r_{max}} P_r^{(-)}(t)|n-2r,\, 2r,\, -\rangle + \sum_{s=1}^{s_{max}} P_s^{(+)}(t)|n-2s,\, 2s-2,\, +\rangle \tag{7}$$

where $2r_{max} = 2s_{max}$ is the largest even integer not exceeding n (a complete derivation of the expansion coefficients [31] for initial condition (2) is provided in Appendix B). Moreover, for even n, the peaks in $\sigma_1^2(t) = \langle\psi(t)|\hat{n}_1^2|\psi(t)\rangle - \langle\psi(t)|\hat{n}_1|\psi(t)\rangle^2$ and $\sigma_2^2(t)$ (Fig. 1c and Fig. C1) mark the center of the plateau in Fig. 1a as the point of maximum anticorrelation between the mode populations (Fig. 1b). We will show that this is the turning point of the system dynamics leading to a generalized parity effect. To this end, we search for entangled states of the system such that

$$\begin{cases} \left\langle \hat{n}_\mu \right\rangle = \dfrac{n}{2} - \varepsilon \qquad (\mu = 1,2) \\ \left\langle \hat{n}_1\, \hat{n}_2 \right\rangle = 0 \;\Rightarrow\; \sigma_{12} = -\left(\dfrac{n}{2} - \varepsilon\right)^2 \end{cases} \tag{8}$$

where ε is the departure of the mode populations from $n/2$ and the second condition expresses their maximum (negative) anticorrelation. Given N conservation, the first condition implies $\langle S_z\rangle = \varepsilon - 1/2$ ($0 \le \varepsilon \le 1$). Thus, ε is also a measure of atom-field entanglement: $\varepsilon = 0$, 1 means zero entanglement, while $\varepsilon = 1/2$ corresponds to the quenching of the atomic inversion (as the reduced atomic density is a mixture with equal weights of $|+\rangle\langle+|$ and $|-\rangle\langle-|$) and to the maximum entanglement between atom (A) and field (F). In fact, the mutual entropy [33,35]

$$S_{A:F}(\varepsilon) = S_A(\varepsilon) + S_F(\varepsilon) - S_{AF}(\varepsilon) = 2S_A(\varepsilon) = -2[\varepsilon ln\varepsilon + (1-\varepsilon)ln(1-\varepsilon)] \tag{9}$$

takes its quantum maximum value of $2ln2$ for $\varepsilon = 1/2$ (the second equality holds because the overall system is in a pure state [36]; note that we do not consider local nonunitary operations, which may change the amount of entanglement [28,37], and thus the mutual entropy is a proper measure of entanglement).

The maximally symmetric states (see Appendix F for derivation)

$$\begin{cases} |\psi_a\rangle = \dfrac{1}{\sqrt{2(n-1)}}\left(\sqrt{n-2}\,|n,\,0,\,-\rangle + i\sqrt{n}\,|0,\,n-2,\,+\rangle\right) \\ |\psi_b\rangle = \dfrac{1}{\sqrt{2(n-1)}}\left(\sqrt{n-2}\,|0,\,n,\,-\rangle - i\sqrt{n}\,|n-2,\,0,\,+\rangle\right) \end{cases} \tag{10}$$

make the correlation terms in Eq. (5) vanish, satisfy Eq. (8), and maxi-

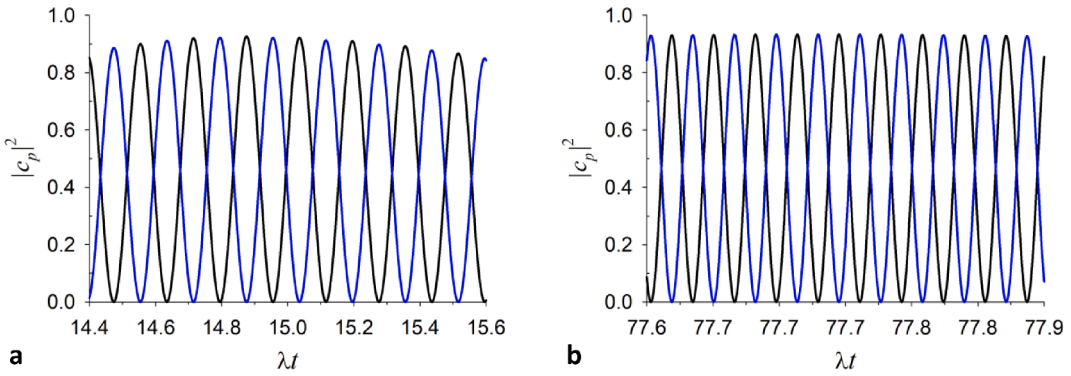

Fig. 2. Time evolution of the system at mid-plateau. (a) $|c_p|^2$ $(p = a, b)$ as a function of the effective time λt, over a time interval surrounding the centers of the plateaus in the mean photon numbers of the field modes. $|c_a|^2$(blue line) and $|c_b|^2$ (black line) are obtained from Eq. (11) for $n = 20$ and the initial condition (2), using the closed-form expressions for the expansion coefficients of $|\psi(t)\rangle$ in Appendix B. (b) Same quantities as in (a) for $n = 100$. (For interpretation of the references to colour in this figure legend, the reader is referred to the web version of this article.)

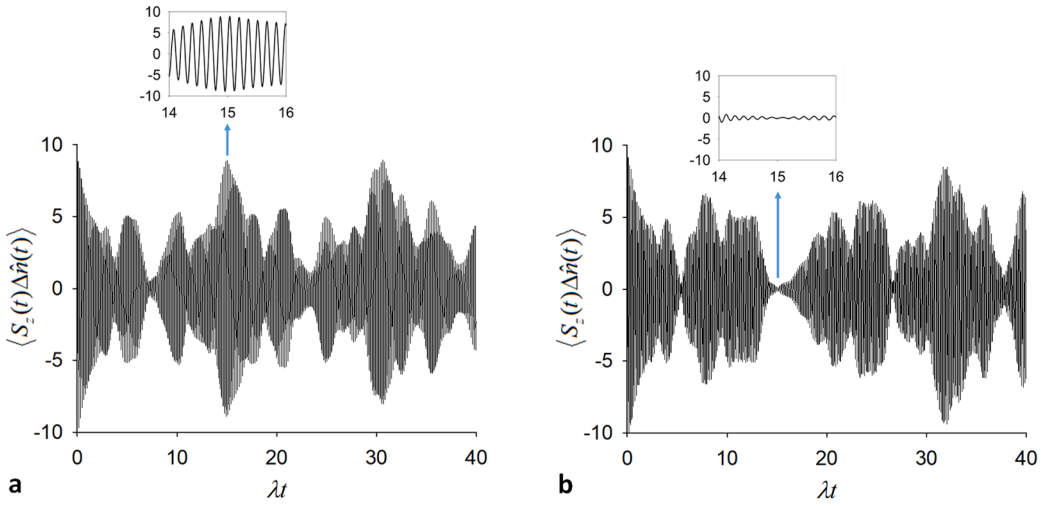

Fig. 3. Field-atom correlation difference $\langle S_z(t)\Delta\hat{n}(t)\rangle$. (a) $\langle S_z(t)\Delta\hat{n}(t)\rangle$ versus λt for $n = 20$. The inset highlights the maximal mid-plateau oscillation of the quantity, which is approximately described by Eq. (15). (b) Same quantity as in (a) for $n = 21$.

mize $S_{A:F}$. Such states tend to field-atom Bell states as $n\to\infty$. Given the expansion $|\psi(t)\rangle = c_a(t)|\psi_a\rangle + c_b(t)|\psi_b\rangle + |\Delta\psi(t)\rangle$ for the system state, we find that its mid-plateau evolution is approximately a Rabi oscillation between $|\psi_a\rangle$ and $|\psi_b\rangle$. That is, the sum of

$$\begin{cases} |c_a(t)|^2 = \dfrac{1}{2(n-1)}\left[\sqrt{n-2}\,P_0^{(-)}(t) + \sqrt{n}\,\mathrm{Im}\left(P_{n/2}^{(+)}(t)\right)\right]^2 \\ |c_b(t)|^2 = \dfrac{1}{2(n-1)}\left[\sqrt{n-2}\,P_{n/2}^{(-)}(t) - \sqrt{n}\,\mathrm{Im}\left(P_1^{(+)}(t)\right)\right]^2 \end{cases} \tag{11}$$

is near unity. Approximations valid at mid-plateau give (Appendix F)

$$\begin{cases} |c_a(t)|^2 \cong \dfrac{1}{2}\{1 + sin[2\pi\nu_n(t - n\pi/4\lambda)]\} \\ |c_b(t)|^2 \cong \dfrac{1}{2}\{1 - sin[2\pi\nu_n(t - n\pi/4\lambda)]\} \end{cases} \tag{12}$$

The frequency of oscillation is $\nu_n = |\langle\psi_b|H_{\mathrm{int}}|\psi_a\rangle|/\pi = \frac{n\lambda}{\pi}\sqrt{\frac{n-2}{n-1}} \cong n\lambda/\pi$, where H_{int} is the interaction Hamiltonian. The exact coefficients are smaller, but such that $|c_a(t)|^2 + |c_b(t)|^2 > 0.9$ (Fig. 2). $|\Delta\psi(t)\rangle$ never vanishes, as is expected since the energy of a ground state built as a linear combination of $|\psi_a\rangle$ and $|\psi_b\rangle$ would be $(n-1)\omega - |\langle\psi_b|H_{\mathrm{int}}|\psi_a\rangle|$, while Eq. (2) implies an energy of $(n-1)\omega$ (Appendix A). The insensitivity of $|\Delta\psi(t)\rangle$ to the n value reflects the fact that the expansion coefficients of $|\psi_a\rangle$ and $|\psi_b\rangle$ are virtually constant for sufficiently large n.

$|\psi_a\rangle$ is the linear combination of the initial state and another state with almost inverted photon distribution between the two modes. Moreover, the photon-number probability distributions of $|\psi_a\rangle$ and $|\psi_b\rangle$ are obtained from each other exchanging the two field modes, and a two-photon transfer is sufficient to cause this exchange. These two facts cause the large covariance and anticorrelation (Fig. 1b and c) at mid-plateau for even n. Importantly,

$$\langle\psi_b|\,a_1^2 S_+|\psi_a\rangle = \langle\psi_b|\,a_2^{\dagger 2} S_-|\psi_a\rangle = \frac{1}{2\lambda}\langle\psi_b|H_{\mathrm{int}}|\psi_a\rangle = i\frac{n}{2}\sqrt{\frac{n-2}{n-1}} \tag{13}$$

Eq. (13) and its complex conjugate describe an equality of field mode-atom interaction strengths such that the mode 1-to-atom and atom-to-mode 2 photon transfers, as well as the converse processes, contribute in phase and equally to the coupling between ψ_a and ψ_b, while the dynamics of the atomic inversion is quenched, as $\langle S_z\rangle = 0.5/(n-1)$ and $d\langle S_z\rangle/dt = 0$ in both states, in good agreement with the exact $\langle S_z(t)\rangle$ evolution at mid-plateau (Fig. D1).

The matching of mode-atom interaction strengths selects ψ_a and ψ_b as the predominant states in the mid-plateau evolution of $|\psi(t)\rangle$, enabling the role exchange between the modes and hence the depletion of the initially populated mode. In fact, $|\psi_a\rangle$ and $|\psi_b\rangle$ have similar (equal

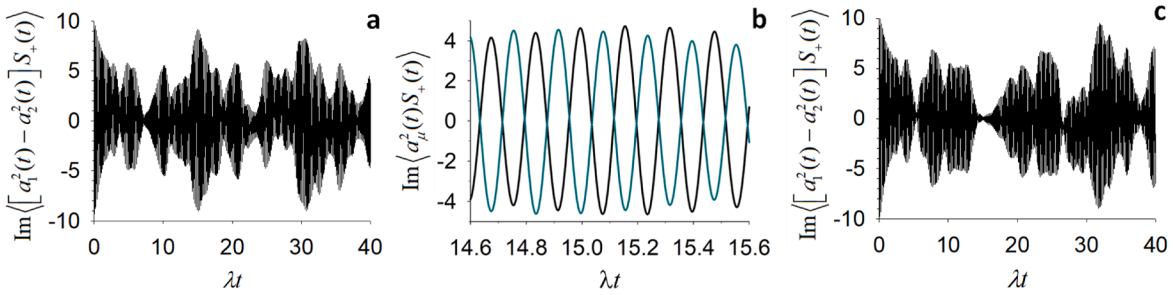

Fig. 4. Field-atom correlation difference $\mathrm{Im}\langle[a_1^2(t)-a_2^2(t)]S_+(t)\rangle$. (a) $\mathrm{Im}\langle[a_1^2(t)-a_2^2(t)]S_+(t)\rangle$ vs. λt for $n=20$. (b) Mid-plateau temporal evolution of $\mathrm{Im}\langle a_1^2(t)S_+(t)\rangle$ (black) and $\mathrm{Im}\langle a_2^2(t)S_+(t)\rangle$ (cyan). Given the opposite phase, the peaks in the correlation difference are close to $n/2$, as is shown in (a) and also predicted by Eq. (17). (c) Same quantity as in (a) for $n=21$. (For interpretation of the references to colour in this figure legend, the reader is referred to the web version of this article.)

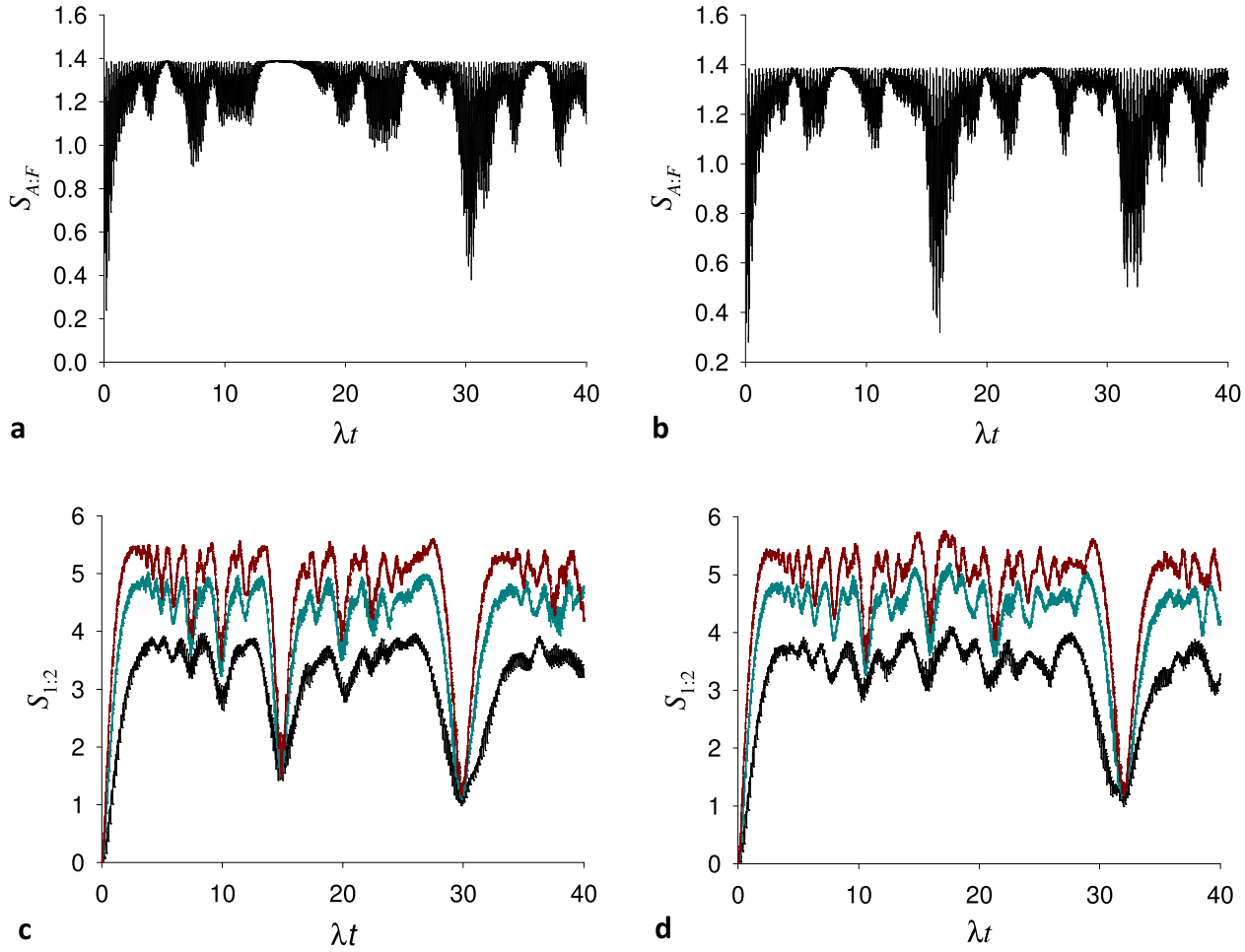

Fig. 5. Mutual entropies in the tripartite atom-radiation system. (a and b) Mutual atom-field entropy $S_{A:F}$ vs. scaled time λt, as given by Eq. (18) for (a) $n=20$ and (b) $n=21$. (c and d) Mutual entropy of the two cavity field modes $S_{1:2}$ vs. λt, as obtained for (c) $n=20$ and (d) $n=21$ from Eqs. (H10) and (H11), after tracing over the atomic degrees of freedom.

for $n\to\infty$) Fock space distributions, but anticorrelated interactions of the two modes with the atom, which can be seen from the correlations in Eqs. (5) and (6). We find

$$\langle S_z(t)\Delta\widehat{n}(t)\rangle = \frac{n}{2^n}\sum_{p=0}^{n-1}\binom{n-1}{p}\Big\{-cos[f(p)t]cos[f(p+1)t] + \sqrt{\frac{p}{p+1}\left(1-\frac{1}{n-p}\right)}\,sin[f(p)t]sin[f(p+1)t]\Big\} \tag{14}$$

with $f(p)=2\lambda\sqrt{p(n-p)}$ (Fig. 3), for the exact $|\psi(t)\rangle$ evolution (Appendix G), with an oscillation amplitude near the maximum of $n/2$ around the center of the plateau, as expected from the approximation $|\psi(t)\rangle \cong |\psi(t)\rangle_{\text{two - state}} = c_a(t)|\psi_a\rangle + c_b(t)|\psi_b\rangle$:

$$\begin{cases}\langle\psi_b|S_z\Delta\widehat{n}|\psi_b\rangle = -\langle\psi_a|S_z\Delta\widehat{n}|\psi_a\rangle = \dfrac{n(n-2)}{2(n-1)} \cong \dfrac{n}{2}\\ \langle S_z(t)\,\Delta\widehat{n}(t)\rangle_{\text{two-state}} \cong \dfrac{n}{2}sin[2\pi\nu_n(t-n\pi/4\lambda)+\pi]\end{cases} \tag{15}$$

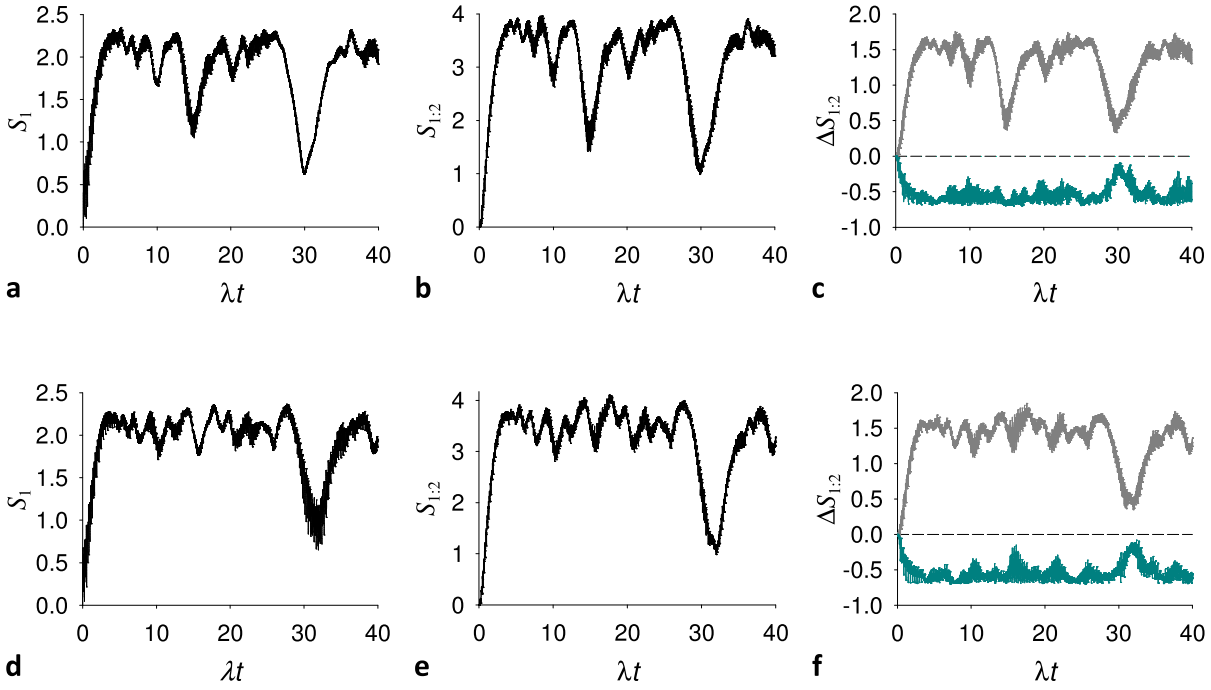

Fig. 6. Entropies of the field modes. (a) Entropy associated with mode 1, S_1, vs. scaled time λt, as obtained from Eq. (H10) for $n = 20$. (b) Mutual entropy of the two cavity field modes, $S_{1:2}$, vs. λt for $n = 20$. (c)$\Delta S_{1:2}$, defined as $S_{1:2} - min\{S_1, S_2\}$ (gray) or as $S_{1:2} - 2min\{S_1, S_2\}$ (cyan), vs. λt for $n = 20$. (d–f) Same quantities as in (a-c) for $n = 21$. The time evolution of S_2 is shown in Fig. H1. (For interpretation of the references to colour in this figure legend, the reader is referred to the web version of this article.)

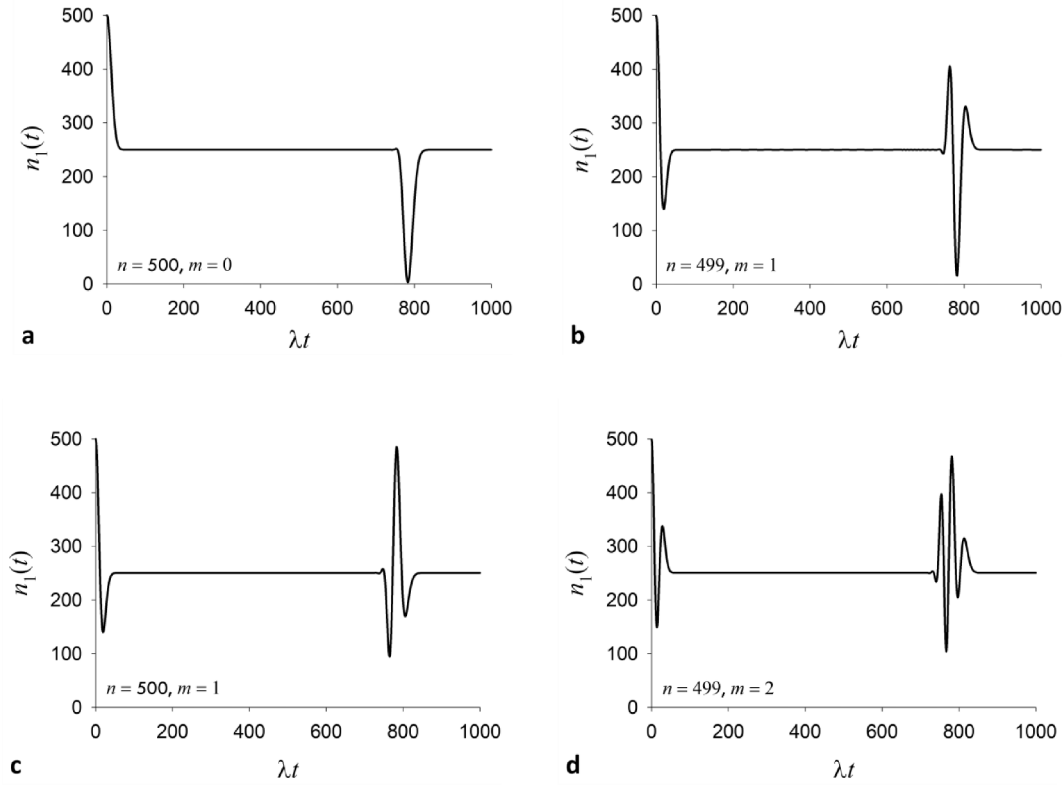

Fig. 7. Generalized quantum optics parity effect. (a–d) Average number of photons in field mode 1 vs. scaled time λt for $|\psi(0)\rangle = |n, m, -\rangle$ with the indicated values of n and m. Mode 1 is substantially emptied (refilled) after the plateau if n and m have the same (different) parity.

The coarse-grained value of $\langle S_z(t)\Delta\hat{n}(t)\rangle$ is about zero at mid-plateau, but the oscillation peaks mean large and opposite mode-atom correlations: $\left|\left\langle S_z\hat{n}_1\right\rangle\right| \cong \left|\left\langle S_z\hat{n}_2\right\rangle\right| \approx \frac{1}{2}\frac{n}{2} = n/4$ and $\left\langle S_z\hat{n}_1\right\rangle \cong -\left\langle S_z\hat{n}_2\right\rangle$. Also, Eqs. (6) and (15) imply that $d^2\langle\Delta\hat{n}(t)\rangle/dt^2$ has opposite signs for $|\psi_a\rangle$ and $|\psi_b\rangle$.

At mid-plateau, large oscillations (Fig. 4) are also experienced, for even n, by

$$\mathrm{Im}\left\langle \left[a_1^2(t) - a_2^2(t)\right] S_+(t)\right\rangle = \frac{n}{2^n}\sum_{p=0}^{n-1}\binom{n-1}{p}\left\{\sqrt{\frac{p}{n-p}}\sin[f(p)t]\cos[f(p+1)t] + \sqrt{\frac{n-p-1}{p+1}}\cos[f(p)t]\sin[f(p+1)t]\right\} \tag{16}$$

While $\langle\psi_a|a_\mu^2 S_+|\psi_a\rangle = \langle\psi_b|a_\mu^2 S_+|\psi_b\rangle = 0$ ($\mu = 1, 2$) (and thereby, $dn_\mu(t)/dt$ vanishes in both states), during the approximate two-state oscillation it is

$$\begin{cases} < a_1^2(t)\, S_+(t) >_{\text{two-state}} = - < a_2^2(t)\, S_+(t) >_{\text{two-state}} \\ \mathrm{Im}\left\langle \left[a_1^2(t) - a_2^2(t)\right] S_+(t)\right\rangle_{\text{two-state}} \cong \frac{n}{2}\cos[2\pi\nu_n(t - n\pi/4\lambda)] \end{cases} \tag{17}$$

which highlights the instantaneous opposite propensities of the two modes to exchange photons with the atom that are maximized and synchronized by the achievement of condition (13). This is the core dynamic evolution that establishes an approximate pseudo time reversal symmetry with respect to the two field modes, i.e., the population of each mode begins to experience, in the opposite direction, the temporal evolution that the other mode had up to mid-plateau.

For odd n, two-photon processes clearly cannot evolve the system from state (2) to states (10); hence, the anticorrelation in (8) and the interaction-matching condition (13) are never achieved (Fig. 1e and Appendix F). Accordingly, the atomic inversion is not quenched; in fact, it shows oscillations with peak values close to ½ that correspond to substantial field-atom disentanglement. In between, the mode-atom correlations are in phase and produce the very small differences in Figs. 3b and 4c, in contrast to the large oscillations of these correlation differences predicted by Eqs. (15) and (17) for even n. Thus, the atom-mediated transfer of photons (and of the related information; *vide infra*) from one mode to the other as described by Eq. (13) is inhibited, and the roles of the field modes in the system dynamics cannot be exchanged.

Entropic signatures of the parity effect

The atom-mediated exchange of mode populations corresponding to the oscillation between ψ_a and ψ_b implies large population variances (Fig. 1 and Fig. C1) and the maximal uncertainty in the atomic state described by $\langle S_z\rangle \cong 0$. Thus, the atom-field mutual entropy $S_{A:F}$ (which can be defined as the entropy S_A of the atom minus its conditional entropy $S_{A|F}$ given the field state [33,36]) is expected to be large at mid-plateau. In fact, the mutual entropy (Appendix H)

$$S_{A:F}(t) = S_A(t) - S_{A|F}(t) = -\frac{1}{2^{n-1}}\sum_{p=0}^{n}\binom{n}{p}\cos^2[f(p)t]\ln\left\{\frac{1}{2^n}\sum_{p=0}^{n}\binom{n}{p}\cos^2[f(p)t]\right\} - \frac{1}{2^{n-1}}\sum_{p=0}^{n}\binom{n}{p}\sin^2[f(p)t]\ln\left\{\frac{1}{2^n}\sum_{p=0}^{n}\binom{n}{p}\sin^2[f(p)t]\right\} = 2S_F(t) \tag{18}$$

persists at its maximum value at mid-plateau (Fig. 5a) for even n, in agreement with Eq. (9) for $\varepsilon = \frac{1}{2}$, a signature of maximum atom-field quantum information trade. This is a consequence of the fact that $|\psi_a\rangle$ and $|\psi_b\rangle$ are maximally entangled states with respect to the atom and field subsystems.

On the contrary, the large mid-plateau oscillation of $\langle S_z\rangle$ for odd n correlates with a (coarse-grained) minimum in $S_{A:F}(t)$ (Fig. 5b), similarly to what is observed for the atom interacting with a single mode in Jaynes-Cummings models [38]. Net of the difference in the type of atom-field interaction, this similarity indicates that the atom-mediated communication between the modes required for their exchange in Fock space does not occur for odd n. Rather, the two similarly populated modes interact similarly and in phase with the atom, as described by vanishing differences in dynamically relevant atom-field correlations (Figs. 3b, 4c), and each mode population is reverted approximately to its initial value after the plateau.

The mid-plateau mutual entropy of the two modes, $S_{1:2}(t)$, remains above the upper bound in classically correlated systems for both even and odd n (Figs. 5-6 and H1), as quantum entanglement is necessary for the system evolution from an initially factorized state and back to states in which one mode is predominantly populated. In fact, Fig. 6c and f show that [33,36]

$$min\{S_1(t), S_2(t)\} \le S_{1:2}(t) \le 2min\{S_1(t), S_2(t)\} \tag{19}$$

that is, $S_{1:2}(t)$ is between the classical and quantum upper bounds of the mutual entropy, which define a regime of pure quantum entanglement. However, for even n, $S_{1:2}(t)$ has a minimum at mid-plateau, because $|\psi_a\rangle$ and $|\psi_b\rangle$ correspond approximately to the maximum classical-type correlation among all pairs of subsystems. In fact, from Eqs. (H10) and (H11), for $|\psi\rangle = |\psi_a\rangle$ or $|\psi\rangle = |\psi_b\rangle$ one obtains

$$S_1 = S_2 = S_{1:2} = -\frac{n-2}{2(n-1)}\ln\frac{n-2}{2(n-1)} - \frac{n}{2(n-1)}\ln\frac{n}{2(n-1)} \underset{n\to\infty}{\to} \ln 2 \tag{20}$$

The minima in S_1 and S_2 are also expression, in terms of information, of the maximal anticorrelation between the modes,

$$\sigma_{12} = -\left[\frac{n(n-2)}{2(n-1)}\right]^2 \underset{n\to\infty}{\to} -\frac{n^2}{4} \tag{21}$$

which is enabled by the synchronism of the two mode-atom interactions described by Eq. (13). Fig. 6a-b show that the system state does not reach an exact oscillation between $|\psi_a\rangle$ and $|\psi_b\rangle$, and the minimum of either the mode entropies or their mutual entropy define the point of closest approach to this oscillation. Moreover, Fig. 5c shows in agreement with Fig. 2 that the ability of the system to approach a Rabi-like oscillation between $|\psi_a\rangle$ and $|\psi_b\rangle$ is insensitive to the value of n, although the time required for the closest approach scales linearly with n. The pronounced mid-plateau minimum in $S_{1:2}(t)$ is the entropic manifestation of the parity effect and sharply defines the center of the plateau. For odd n, the states (10), which satisfy condition (13), are never approached and, at mid-plateau, the achievement of nearly equal populations of the modes requires the contribution of many similarly populated states to the linear combination of Eq. (7), with accordingly large entropies (Figs. 5d and 6d-e).

Generalized parity effect

The basis states in Eq. (10) are also achievable starting from state (4) with even n and $m \neq 0$. Also, for odd n and m, an analysis similar to that leading to states (10) in Appendix F produces the states

$$\begin{cases} |\psi_c\rangle = \frac{1}{\sqrt{2(n-2)}}\left(\sqrt{n-3}\,|n,\,1,\,-\rangle + e^{i\theta}\sqrt{n-1}\,|1,\,n-2,\,+\rangle\right) \\ |\psi_d\rangle = \frac{1}{\sqrt{2(n-2)}}\left(\sqrt{n-3}\,|1,\,n,\,-\rangle + e^{-i\theta}\sqrt{n-1}\,|n-2,\,1,\,+\rangle\right) \end{cases} \tag{22}$$

which satisfy the interaction-matching condition

$$\langle\psi_d|\, a_1^2 S_+|\psi_c\rangle = \langle\psi_d|\, a_2^{\dagger 2} S_-|\psi_c\rangle = e^{i\theta}\frac{n-1}{2(n-2)}\sqrt{n(n-3)} \tag{23}$$

For these states, $\left\langle \hat{n}_1\, \hat{n}_2 \right\rangle$ is nonzero, but $\left\langle \hat{n}_1\, \hat{n}_2 \right\rangle \approx n$ and thus it is still $\sigma_{12} \approx -n^2/4$. The states satisfying condition (13) or (23) cannot be achieved unless n and m have the same parity, that is, unless $n+m$ is even. Thus, we expect the occurrence of a generalized parity effect, which is confirmed by the time evolution of $|\psi(t)\rangle$ derived in Appendix I and shown in Fig. 7. For $|\psi(0)\rangle = |n, 1, -\rangle$, one also obtains the approximate expression (Appendix I)

$$n_1(t) \cong \frac{n}{2} + \frac{n}{2} cos^{n-2}\left(\frac{2\lambda t}{n}\right)\left[1 - n sin^2\left(\frac{2\lambda t}{n}\right)\right] \tag{24}$$

Eq. (24) shows that the predominant population dynamics for odd n is the same as that predicted by Eq. (3) for even n. This dynamics is complicated by higher frequency oscillations that make the parity effect more visible at larger n values. However (and with relevance to future applications), the generalized effect can also be seen, for any n, in terms of mirror revivals in the mode populations with respect to $n_1 \cong n_2 \cong (n+m)/2$, as the number of photons in the initially more populated mode is changed by one photon, while m controls the number of oscillations in the revival (compare Fig. 7b and c).

Conclusion

We explained the physical origin of the quantum optics parity effect [31,32], which manifests itself as the sensitivity of the atom-radiation dynamics in high-Q resonators to single-photon changes in the cavity field. We show how the parity effect arises from the quantum entanglement of the system components over time intervals in which the photon distribution is essentially at a standstill. The key determinant of the dynamic evolution is the ability of the system to synchronize the two-photon processes between the atom and the field modes, so as to select a predominant Rabi-like two-state oscillation at the heart of the system dynamics. Our analysis also brings to light a generalized form of the parity effect as a switching dynamics dependent on variations of one unit in the total photon number (with relevance to very similar parity effects later studied in other physical systems, such as in the evolution of interference in Bose condensates [39]). Therefore, potential uses of the quantum optics effect might also be devised for detection purposes [27], including the detection of single-photon cavity losses.

The parity effect and its generalization are observable in the full quantum regime (for example, for atom-field interaction strengths λ in the range $10^{-5}\omega$ to $10^{-4}\omega$, namely, well below the limit for spectral collapse [40]), over a ns time scale in cavities with well-feasible Q factors [41,42] of 10^7 (Appendix J). Advances in generating Fock states [43], and the remarkable progress in realizing nanostructures with quantum confinement properties [10] (including quantum light emission from 2D materials [18,20]), qubits or atom-like systems interacting with quantized fields [14,15,44], single-photon experiments [19,24–26,45–49] and theory [46,47,49] provide a feasibility background to investigate potential applications of the generalized parity effect as a switching and amplification mechanism in future optoelectronics. The here explained role for quantum entanglement in the effect generation and its entropy characterization provide the starting point for considering its relevance to the research area of quantum computing [50,51].

CRediT authorship contribution statement

Agostino Migliore: Conceptualization, Formal analysis, Investigation, Methodology, Data curation, Software, Visualization, Writing - original draft, Writing - review & editing. **Anna Napoli:** Conceptualization, Investigation, Methodology, Writing - review & editing. **Antonino Messina:** Conceptualization, Investigation, Methodology, Writing - review & editing.

Declaration of Competing Interest

The authors declare that they have no known competing financial interests or personal relationships that could have appeared to influence the work reported in this paper.

Acknowledgment

The authors thank Prof. Jean-Michel Raimond and Prof. Nicolay Vitanov for stimulating discussions.

Appendix A

Hamiltonian model and constants of motion

In this section, we present a detailed analysis of the effective Hamiltonian model in Eq. (1), thus providing new insights into its range of applicability.

Fig. A1 illustrates the relationship between the relevant portion of the atomic energy spectrum and the frequency ω_F of the two field modes (note that ω_F also represents the photon energy because we use units such that $\hbar = 1$). $|-\rangle$ and $|+\rangle$ denote the ground and excited atomic states (with energies E_- and E_+, respectively) within the effective single-particle, two-level model adopted here. E_- and E_+ satisfy the resonance condition $\omega_0 \equiv E_+ - E_- \approx 2\omega_F$. $|s\rangle$ is one of the atomic intermediate states, with energy E_s. The detuning $\Delta_s = \omega_F - (E_s - E_-)$ of the photon energy with respect to the excitation energy $E_s - E_-$ prevents the actual population of state $|s\rangle$, and thus $|s\rangle$ behaves as a virtual state that can assist two-photon transitions between states $|-\rangle$ and $|+\rangle$.

We assume the existence of at least one intermediate state such as $|s\rangle$. As in previous analysis of the Hamiltonian in Eq. (1) [31] and the strictly related Hamiltonian of reference [32], we assume that $|-\rangle$ and $|+\rangle$ have the same parity. Therefore, the pertinent transition dipole moment is zero and the direct transition between these two states is forbidden within the dipole approximation. While this transition is anyway not allowed by the radiation frequency used (because our model implicitly assumes that the radiation is approximately monochromatic and $\omega_0 - \omega_F > \Delta_s$ for any $|s\rangle$), the above condition on the parity enables virtual transitions to intermediate states $|s\rangle$ of opposite parity.

The Hamiltonian of the system is

$$H_{\text{atom - field}} = H_0 + H_{\text{int}} \tag{A1a}$$

where the unperturbed Hamiltonian is

$$H_0 = E_-|-\rangle\langle -| + E_+|+\rangle\langle +| + \omega_F(\hat{n}_1 + \hat{n}_2) \tag{A1b}$$

and, in the dipole approximation, the interaction Hamiltonian is [52]

$$H_{\text{int}} = -\boldsymbol{d}\cdot\boldsymbol{E} = -i\sqrt{\frac{2\pi\omega_F}{V}}\boldsymbol{d}\cdot\sum_{\mu=1}^{2}\boldsymbol{\varepsilon}_\mu(a_\mu - a_\mu^\dagger) \tag{A1c}$$

In Eq. (A1), $\mathbf{d}$ is the electric dipole moment operator of the atom, $\mathbf{E}$ is the electric field operator, V is the volume of the cavity, and $\boldsymbol{\varepsilon}_\mu$ is the polarization vector of field mode μ. The transitions induced by H_{int} are described by two-photon matrix elements of the form [53]

$$M_{IF} = \sum_s \frac{\langle F|H_{\text{int}}|S\rangle\langle S|H_{\text{int}}|I\rangle}{E_I - E_S} \tag{A2}$$

where $|I\rangle$ and $|F\rangle$ are the initial and final states of the atom-radiation field system connected by the transition (note that these are eigenstates of the full non-interacting system, which thus have the same energy), $|S\rangle$ are the intermediate states involved in the two component virtual transitions, and s is an index (in general, s can be a set of quantum numbers) that distinguishes the intermediate states. Here we are assuming that H_{int} is sufficiently small not to allow multiphoton transitions that could lead to atomic states lower in energy than $|-\rangle$ or higher than $|+\rangle$, so that the two-state approximation applies to the atom. Then, the action of the interaction Hamiltonian on the evolution of the atom-field system remains defined by the transition amplitudes among all eigenstates $|n-k, k\mp 2, \pm\rangle$ of the unperturbed Hamiltonian, which provide a basis set for the expansion of the atom-field state at any time. Next, we will calculate all such transition amplitudes and build an effective Hamiltonian that gives, to the first order, the same transition amplitudes as those produced by the Hamiltonian (A1) to the second order and describes the system dynamics within the rotating-wave approximation [54].

Transition amplitudes and effective Hamiltonian

We first consider the transitions in which the field loses two photons that excite the atom (two-photon absorption). These transitions connect states $|I\rangle = |n_1, n_2, -\rangle$ and $|F\rangle = |p_1, p_2, +\rangle$ for which n_1, n_2, p_1 and p_2 satisfy the relation $p_1 + p_2 = n_1 + n_2 - 2$. The intermediate states are $|S\rangle = |m_1, m_2, s\rangle$, with m_1 and m_2 such that $min(n_1, p_1) \le m_1 \le max(n_1, p_1)$ and $min(n_2, p_2) \le m_2 \le max(n_2, p_2)$, respectively. Moreover, since the virtual transition to any of the intermediate states implies a change of one unit in the total population of the two field modes, it is $|n_1 + n_2 - m_1 - m_2| = |p_1 + p_2 - m_1 - m_2| = 1$. Therefore, the denominator of Eq. (A2) is $E_I - E_S = E_- - E_s + (n_1 + n_2 - m_1 - m_2)\omega = E_- - E_s + \omega = \Delta_s$.

For $m_1 = n_1 - 1, m_2 = n_2, p_1 = n_1 - 2$ and $p_2 = n_2$ (namely, the atom absorbs two photons from field mode 1, through a virtual intermediate state in which one photon is in the atom), Eq. (A2) gives

$$\begin{aligned} M_{IF}^{(1)} &= \frac{2\pi\omega_F}{V}\sum_s \frac{\langle n_1 - 2, n_2, +|(-i\mathbf{d}\cdot\boldsymbol{\varepsilon}_1 a_1)|n_1 - 1, n_2, s\rangle\langle n_1 - 1, n_2, s|(-i\mathbf{d}\cdot\boldsymbol{\varepsilon}_1 a_1)|n_1, n_2, -\rangle}{\Delta_s} \\ &= -\frac{2\pi\omega_F}{V}\sqrt{n_1(n_1-1)}\sum_s \frac{(\mathbf{d}_{+s}\cdot\boldsymbol{\varepsilon}_1)(\mathbf{d}_{s-}\cdot\boldsymbol{\varepsilon}_1)}{\Delta_s} \end{aligned} \tag{A3}$$

where $\mathbf{d}_{+s} = \langle +|\mathbf{d}|s\rangle$ and $\mathbf{d}_{s-} = \langle s|\mathbf{d}|-\rangle$ are the atomic transition dipole moments. By introducing the atom-mode 1 coupling strength parameter (note that the detuning parameter is defined with opposite sign compared to reference [32])

$$\lambda_1 = -\frac{2\pi\omega_F}{V}\sum_s \frac{(\mathbf{d}_{+s}\cdot\boldsymbol{\varepsilon}_1)(\mathbf{d}_{s-}\cdot\boldsymbol{\varepsilon}_1)}{\Delta_s} \tag{A4}$$

the second-order matrix element in Eq. (A3) can be obtained to the first order from the operator $\lambda_1 a_1^2 S_+$:

$$M_{IF}^{(1)} = \langle F|\lambda_1 a_1^2 S_+|I\rangle \tag{A5}$$

For $m_1 = n_1, m_2 = n_2 - 1, p_1 = n_1$ and $p_2 = n_2 - 2$ (that is, the case analogous to the previous one for mode 2), one obtains

$$M_{IF}^{(2)} = -\frac{2\pi\omega_F}{V}\sqrt{n_2(n_2-1)}\sum_s \frac{(\mathbf{d}_{+s}\cdot\boldsymbol{\varepsilon}_2)(\mathbf{d}_{s-}\cdot\boldsymbol{\varepsilon}_2)}{\Delta_s} = \langle F|\lambda_2 a_2^2 S_+|I\rangle \tag{A6}$$

where

$$\lambda_2 = -\frac{2\pi\omega_F}{V}\sum_s \frac{(\mathbf{d}_{+s}\cdot\boldsymbol{\varepsilon}_2)(\mathbf{d}_{s-}\cdot\boldsymbol{\varepsilon}_2)}{\Delta_s} \tag{A7}$$

For $m_1 = n_1, m_2 = n_2 - 1, p_1 = n_1 - 1$ and $p_2 = n_2 - 1$ (that is, the atom absorbs one photon from each field mode), the relevant second-order matrix element is

$$M_{IF}^{(3)} = -\frac{2\pi\omega_F}{V}\sqrt{n_1 n_2}\sum_s \frac{(\mathbf{d}_{+s}\cdot\boldsymbol{\varepsilon}_1)(\mathbf{d}_{s-}\cdot\boldsymbol{\varepsilon}_2)}{\Delta_s} \tag{A8}$$

If the intermediate state is given by $m_1 = n_1 - 1, m_2 = n_2$, one obtains

$$M_{IF}^{(4)} = -\frac{2\pi\omega_F}{V}\sqrt{n_1 n_2}\sum_s \frac{(\mathbf{d}_{+s}\cdot\boldsymbol{\varepsilon}_2)(\mathbf{d}_{s-}\cdot\boldsymbol{\varepsilon}_1)}{\Delta_s} \tag{A9}$$

The sum of the second-order matrix elements in Eqs. (A8) and (A9) is given, to the first order, as

$$M_{IF}^{(3)} + M_{IF}^{(4)} = \langle F|g a_1 a_2 S_+|I\rangle \tag{A10}$$

where

$$g = -\frac{2\pi\omega_F}{V}\sum_s \frac{(\mathbf{d}_{+s}\cdot\boldsymbol{\varepsilon}_1)(\mathbf{d}_{s-}\cdot\boldsymbol{\varepsilon}_2) + (\mathbf{d}_{+s}\cdot\boldsymbol{\varepsilon}_2)(\mathbf{d}_{s-}\cdot\boldsymbol{\varepsilon}_1)}{\Delta_s} \tag{A11}$$

By exchanging the initial and final states, one obtains the Hermitian conjugates of $M_{IF}^{(1)}$, $M_{IF}^{(2)}$, $M_{IF}^{(3)}$ and $M_{IF}^{(4)}$.

Next, we consider the second-order matrix elements corresponding to Rayleigh scattering (for which $\omega_F << E_s - E_- \approx \Delta_s$ and the atom remains in its initial state, while a photon transfers from a mode to another) and the Stark effect (which involves virtual transitions to intermediate atomic states and back to the initial state). For such terms, $|I\rangle = |n_1, n_2, u\rangle$, $|S\rangle = |m_1, m_2, s\rangle$ and $|F\rangle = |p_1, p_2, u\rangle$, with $u = \pm$, $n_1 + n_2 = p_1 + p_2$ and the $\{m_1, m_2\}$ values intermediate between $\{n_1, n_2\}$ and $\{p_1, p_2\}$. For $u = -$, $m_1 = n_1 - 1$, $m_2 = n_2$, $p_1 = n_1$ and $p_2 = n_2$, we obtain

$$M_{IF}^{(5)} = \frac{2\pi\omega_F}{V} n_1 \sum_s \frac{(\mathbf{d}_{-s}\cdot\boldsymbol{\varepsilon}_1)(\mathbf{d}_{s-}\cdot\boldsymbol{\varepsilon}_1)}{\Delta_s} \equiv \widetilde{M}_{IF}^{(5)} n_1 \tag{A12}$$

where $\widetilde{M}_{IF}^{(5)}$ remains clearly defined by the above equation.

$u = -$, $m_1 = n_1$, $m_2 = n_2 - 1$, $p_1 = n_1$ and $p_2 = n_2 \rightarrow$

$$M_{IF}^{(6)} = \frac{2\pi\omega_F}{V} n_2 \sum_s \frac{(\mathbf{d}_{-s}\cdot\boldsymbol{\varepsilon}_2)(\mathbf{d}_{s-}\cdot\boldsymbol{\varepsilon}_2)}{\Delta_s} \equiv \widetilde{M}_{IF}^{(6)} n_2 \tag{A13}$$

$u = -$, $m_1 = n_1$, $m_2 = n_2 - 1$, $p_1 = n_1 + 1$ and $p_2 = n_2 - 1 \rightarrow$

$$M_{IF}^{(7)} = \frac{2\pi\omega_F}{V} \sqrt{(n_1+1)n_2} \sum_s \frac{(\mathbf{d}_{-s}\cdot\boldsymbol{\varepsilon}_1)(\mathbf{d}_{s-}\cdot\boldsymbol{\varepsilon}_2)}{\Delta_s} \equiv \widetilde{M}_{IF}^{(7)} \sqrt{(n_1+1)n_2} \tag{A14}$$

$u = -$, $m_1 = n_1 - 1$, $m_2 = n_2$, $p_1 = n_1 - 1$ and $p_2 = n_2 + 1 \rightarrow$

$$M_{IF}^{(8)} = \frac{2\pi\omega_F}{V} \sqrt{n_1(n_2+1)} \sum_s \frac{(\mathbf{d}_{-s}\cdot\boldsymbol{\varepsilon}_2)(\mathbf{d}_{s-}\cdot\boldsymbol{\varepsilon}_1)}{\Delta_s} \equiv \widetilde{M}_{IF}^{(8)} \sqrt{n_1(n_2+1)} \tag{A15}$$

$u = +$, $m_1 = n_1 + 1$, $m_2 = n_2$, $p_1 = n_1$ and $p_2 = n_2 \rightarrow$

$$M_{IF}^{(9)} = \frac{2\pi\omega_F}{V} (n_1+1) \sum_s \frac{(\mathbf{d}_{+s}\cdot\boldsymbol{\varepsilon}_1)(\mathbf{d}_{s+}\cdot\boldsymbol{\varepsilon}_1)}{\Delta_s} \equiv \widetilde{M}_{IF}^{(9)} (n_1+1) \tag{A16}$$

where we used the (exact) resonance condition $E_+ - E_- = 2\omega_F$.

$u = +$, $m_1 = n_1$, $m_2 = n_2 + 1$, $p_1 = n_1$ and $p_2 = n_2 \rightarrow$

$$M_{IF}^{(10)} = \frac{2\pi\omega_F}{V} (n_2+1) \sum_s \frac{(\boldsymbol{d}_{+s}\cdot\boldsymbol{\varepsilon}_2)(\boldsymbol{d}_{s+}\cdot\boldsymbol{\varepsilon}_2)}{\Delta_s} \equiv \widetilde{M}_{IF}^{(10)} (n_2+1) \tag{A17}$$

$u = +$, $m_1 = n_1$, $m_2 = n_2 + 1$, $p_1 = n_1 - 1$ and $p_2 = n_2 + 1 \rightarrow$

$$M_{IF}^{(11)} = \frac{2\pi\omega_F}{V} \sqrt{n_1(n_2+1)} \sum_s \frac{(\mathbf{d}_{+s}\cdot\boldsymbol{\varepsilon}_1)(\mathbf{d}_{s+}\cdot\boldsymbol{\varepsilon}_2)}{\Delta_s} \equiv \widetilde{M}_{IF}^{(11)} \sqrt{n_1(n_2+1)} \tag{A18}$$

$u = +$, $m_1 = n_1 + 1$, $m_2 = n_2$, $p_1 = n_1 + 1$ and $p_2 = n_2 - 1 \rightarrow$

$$M_{IF}^{(12)} = \frac{2\pi\omega_F}{V} \sqrt{(n_1+1)n_2} \sum_s \frac{(\mathbf{d}_{+s}\cdot\boldsymbol{\varepsilon}_2)(\mathbf{d}_{s+}\cdot\boldsymbol{\varepsilon}_1)}{\Delta_s} \equiv \widetilde{M}_{IF}^{(12)} \sqrt{(n_1+1)n_2} \tag{A19}$$

Note that the matrix elements in Eqs. (A12) and (A13) can be added to give the overall matrix element responsible for two-photon virtual transitions that bring the system back to its original state with the atom in state $|-\rangle$. A similar consideration applies to Eqs. (A16) and (A17) with respect to atomic state $|+\rangle$. Moreover,

$$\widetilde{M}_{IF}^{(7)} = \widetilde{M}_{IF}^{(8)^*}, \widetilde{M}_{IF}^{(12)} = \widetilde{M}_{IF}^{(11)^*} \tag{A20}$$

The matrix elements in Eqs. (A12) to (A19) can all be written in terms of operators that add up to

$$\begin{aligned} H_{RS} \;=\; & \left(\widetilde{M}_{IF}^{(5)}\widehat{n}_1 + \widetilde{M}_{IF}^{(6)}\widehat{n}_2 + \widetilde{M}_{IF}^{(7)} a_1^\dagger a_2 + \widetilde{M}_{IF}^{(8)} a_1 a_2^\dagger\right)|-\rangle\langle -| \\ & + \left[\widetilde{M}_{IF}^{(9)}(\widehat{n}_1+1) + \widetilde{M}_{IF}^{(10)}(\widehat{n}_2+1) + \widetilde{M}_{IF}^{(11)} a_1 a_2^\dagger + \widetilde{M}_{IF}^{(12)} a_1^\dagger a_2\right]|+\rangle\langle +| \end{aligned} \tag{A21}$$

which produces, to the first order, the above matrix elements and related transition amplitudes for all different pairs of initial and final states of the atom-field system. Since $S_z = (|+\rangle\langle +| - |-\rangle\langle -|)/2$ and the atomic inversion operators can be written as $S_- = |-\rangle\langle +|$ and $S_+ = |+\rangle\langle -|$, we have $|-\rangle\langle -| = S_- S_+ = \frac{1}{2} - S_z$ and $|+\rangle\langle +| = S_+ S_- = \frac{1}{2} + S_z$. Thus, we can write the sum of the unperturbed Hamiltonian in Eq. (A1b) and the Rayleigh-Stark Hamiltonian in equation (A21) as follows:

$$
\begin{aligned}
H_0 + H_{RS} \quad &= \frac{1}{2}\left(E_- + E_+ + \widetilde{M}_{IF}^{(9)} + \widetilde{M}_{IF}^{(10)}\right) + \left(\omega_0 + \widetilde{M}_{IF}^{(9)} + \widetilde{M}_{IF}^{(10)}\right)S_z \\
&+ \left[\omega_F + \frac{1}{2}\left(\widetilde{M}_{IF}^{(5)} + \widetilde{M}_{IF}^{(9)}\right)\right]\widehat{n}_1 + \left[\omega_F + \frac{1}{2}\left(\widetilde{M}_{IF}^{(6)} + \widetilde{M}_{IF}^{(10)}\right)\right]\widehat{n}_2 \\
&+ \left[\left(\widetilde{M}_{IF}^{(9)} - \widetilde{M}_{IF}^{(5)}\right)\widehat{n}_1 + \left(\widetilde{M}_{IF}^{(10)} - \widetilde{M}_{IF}^{(6)}\right)\widehat{n}_2\right]S_z \\
&+ \frac{1}{2}\left[\left(\widetilde{M}_{IF}^{(8)} + \widetilde{M}_{IF}^{(11)}\right)a_1 a_2^{\dagger} + HC\right] + \left[\left(\widetilde{M}_{IF}^{(11)} - \widetilde{M}_{IF}^{(8)}\right)a_1 a_2^{\dagger} + HC\right]S_z
\end{aligned}
\tag{A22}
$$

where HC denotes the Hermitian conjugate operator. The first term on the right-hand side of Eq. (A22) is the half-sum of the atomic energy in the ground state and in the excited state corrected with Stark shift. This constant term will be dropped in the following analysis.

Using Eqs. (A5), (A6), (A10) and (A22), we obtain the effective Hamiltonian (cf. reference [32])

$$
\begin{aligned}
H_{eff} = \widetilde{\omega}_0 S_z + \sum_{\mu=1}^{2}\omega_\mu \widehat{n}_\mu + \left[\left(\sum_{\mu=1}^{2}\lambda_\mu a_\mu^2 + g a_1 a_2\right)S_+ + HC\right] \\
+ S_z\sum_{\mu=1}^{2}s_\mu \widehat{n}_\mu + \left[\left(r_- a_1 a_2^{\dagger} + r_+ a_1 a_2^{\dagger} S_z\right) + HC\right]
\end{aligned}
\tag{A23}
$$

in which λ_1 and λ_2 are given by Eqs. (A4) and (A7), respectively, g is provided by Eq. (A11) and

$$
\widetilde{\omega}_0 = \omega_0 + \widetilde{M}_{IF}^{(9)} + \widetilde{M}_{IF}^{(10)} = \omega_0 + \frac{2\pi\omega_F}{V}\sum_s \frac{(\mathbf{d}_{+s}\cdot\boldsymbol{\varepsilon}_1)(\mathbf{d}_{s+}\cdot\boldsymbol{\varepsilon}_1) + (\boldsymbol{d}_{+s}\cdot\boldsymbol{\varepsilon}_2)(\boldsymbol{d}_{s+}\cdot\boldsymbol{\varepsilon}_2)}{\Delta_s} \tag{A24}
$$

$$
\omega_\mu = \omega_F + \frac{\pi\omega_F}{V}\sum_s \frac{(\mathbf{d}_{-s}\cdot\boldsymbol{\varepsilon}_\mu)(\mathbf{d}_{s-}\cdot\boldsymbol{\varepsilon}_\mu) + (\mathbf{d}_{+s}\cdot\boldsymbol{\varepsilon}_\mu)(\mathbf{d}_{s+}\cdot\boldsymbol{\varepsilon}_\mu)}{\Delta_s} \qquad (\mu = 1, 2) \tag{A25}
$$

$$
s_\mu = \frac{2\pi\omega_F}{V}\sum_s \frac{(\mathbf{d}_{+s}\cdot\boldsymbol{\varepsilon}_\mu)(\mathbf{d}_{s+}\cdot\boldsymbol{\varepsilon}_\mu) - (\mathbf{d}_{-s}\cdot\boldsymbol{\varepsilon}_\mu)(\mathbf{d}_{s-}\cdot\boldsymbol{\varepsilon}_\mu)}{\Delta_s} \qquad (\mu = 1, 2) \tag{A26}
$$

$$
r_- = \frac{1}{2}\left(\widetilde{M}_{IF}^{(11)} + \widetilde{M}_{IF}^{(8)}\right) = \frac{\pi\omega_F}{V}\sum_s \frac{(\mathbf{d}_{+s}\cdot\boldsymbol{\varepsilon}_1)(\mathbf{d}_{s+}\cdot\boldsymbol{\varepsilon}_2) + (\mathbf{d}_{-s}\cdot\boldsymbol{\varepsilon}_2)(\mathbf{d}_{s-}\cdot\boldsymbol{\varepsilon}_1)}{\Delta_s} \tag{A27}
$$

$$
r_+ = \widetilde{M}_{IF}^{(11)} - \widetilde{M}_{IF}^{(8)} = \frac{2\pi\omega_F}{V}\sum_s \frac{(\mathbf{d}_{+s}\cdot\boldsymbol{\varepsilon}_1)(\mathbf{d}_{s+}\cdot\boldsymbol{\varepsilon}_2) - (\mathbf{d}_{-s}\cdot\boldsymbol{\varepsilon}_2)(\mathbf{d}_{s-}\cdot\boldsymbol{\varepsilon}_1)}{\Delta_s} \tag{A28}
$$

A more elemental Hamiltonian model for the two-photon atom-radiation interaction

Next, we describe physical conditions under which the Hamiltonian of Eq. (A23) is well approximated by a more elemental Hamiltonian model that fundamentally describes two-photon exchange processes (that is, absorption or emission) between the atom and the two field modes.

We consider two field modes with orthogonal polarization vectors. We orient the unit vectors of the reference coordinate system so that (see Fig. A1b)

$$
\boldsymbol{\varepsilon}_1 = \mathbf{x}, \qquad \boldsymbol{\varepsilon}_2 = \mathbf{y} \tag{A29}
$$

We assume that the atom has two intermediate states $|s\rangle$ and $|s'\rangle$ that can support its interaction with the radiation field and the pertinent transitions. The detuning parameters associated with the two states are denoted Δ and Δ', respectively. We assume that two states are almost degenerate and are related to $|\pm\rangle$ by transition dipole moments of the same (or sufficiently similar) size (Fig. A1b):

$$
\begin{aligned}
\mathbf{d}_{s-} &= d_-(cos\theta\,\mathbf{x} + sin\theta\,\mathbf{y}), \\
\mathbf{d}_{+s} &= d_+[cos(-\theta)\mathbf{x} + sin(-\theta)\mathbf{y}]
\end{aligned}
\tag{A30a}
$$

and

$$
\begin{aligned}
\mathbf{d}_{s'-} &= d_-\left[cos\left(\frac{\pi}{2} + \theta\right)\mathbf{x} + sin\left(\frac{\pi}{2} + \theta\right)\mathbf{y}\right], \\
\mathbf{d}_{+s'} &= d_+\left[cos\left(\frac{\pi}{2} - \theta\right)\mathbf{x} + sin\left(\frac{\pi}{2} - \theta\right)\mathbf{y}\right]
\end{aligned}
\tag{A30b}
$$

with

$$
d_+ - d_- << \; d_-, d_+ \tag{A31}
$$

The condition of near degeneracy is written

$$\delta \equiv \Delta^{'} - \Delta << \Delta \tag{A32}$$

The insertion of Eqs. (A29) and (A30) into Eqs. (A4), (A7) and (A11) gives

$$\lambda_1 = \frac{2\pi\omega_F}{V} d_- d_+ \left(\frac{sin^2\theta}{\Delta^{'}} - \frac{cos^2\theta}{\Delta}\right), \quad \lambda_2 = \frac{2\pi\omega_F}{V} d_- d_+ \left(\frac{sin^2\theta}{\Delta} - \frac{cos^2\theta}{\Delta^{'}}\right), \quad g = 0 \tag{A33}$$

If $\Delta = \Delta^{'}$, the common value of λ_1 and λ_2 is

$$\lambda(\theta) = -\frac{2\pi\omega_F}{V\Delta} d_- d_+ cos(2\theta) \tag{A34}$$

For $\Delta \neq \Delta^{'}$, the difference between thet two coupling strengths is

$$\lambda_1 - \lambda_2 = \frac{2\pi\omega_F}{V} d_- d_+ \left(\frac{1}{\Delta^{'}} - \frac{1}{\Delta}\right) \cong -\frac{2\pi\omega_F}{V} \frac{\delta}{\Delta^2} d_- d_+ = \frac{\delta}{\Delta cos(2\theta)} \lambda(\theta) \tag{A35}$$

Based on Eq. (A32), $\lambda_1 - \lambda_2$ is much smaller than $\lambda(\theta)$ if $cos(2\theta) >> \delta/\Delta$. This condition can be easily achieved by suitable orientation of the field mode polarization vectors, because of the small value of δ/Δ. Where the pertinent orientation degrees of freedom of the two-level system (that is, an atom or molecule with appropriate energy spectrum) cannot be sufficiently controlled, this condition is anyway satisfied most of the time. Then, to the first order in δ/Δ we obtain

$$\frac{\lambda_1 - \lambda(\theta)}{\lambda(\theta)} \cong \frac{1 - cos(2\theta)}{2cos(2\theta)} \frac{\delta}{\Delta}, \quad \frac{\lambda_2 - \lambda(\theta)}{\lambda(\theta)} \cong -\frac{1 + cos(2\theta)}{2cos(2\theta)} \frac{\delta}{\Delta} \tag{A36}$$

Eqs. (A35) and (A36) imply that $\lambda_1 - \lambda_2 << \lambda_1, \lambda_2$. We assume that the two intermediate states are close enough to degeneracy to neglect the first-order terms in δ/Δ. Thus, we take $\lambda \equiv \lambda_1 = \lambda_2$.

Using equations (A29) to (A34), and neglecting all terms that contain δ/Δ, $(d_+ - d_-)/d_-$ and $(d_+ - d_-)/d_+$, Eqs. (A24) to (A28) give

$$\omega_2 \cong \omega_1 = \omega_F + \frac{\pi\omega_F}{V}\left(d_-^2 + d_+^2\right)\left(\frac{cos^2\theta}{\Delta} + \frac{sin^2\theta}{\Delta^{'}}\right) \cong \omega_F + \frac{\lambda(\theta)}{cos(2\theta)} \equiv \omega \tag{A37}$$

$$\widetilde{\omega}_0 = \omega_0 + \frac{2\pi\omega_F}{V} d_+^2 \left(\frac{1}{\Delta} + \frac{1}{\Delta^{'}}\right) \cong \omega_0 + \frac{2\lambda(\theta)}{cos(2\theta)} = 2\omega \tag{A38}$$

$$s_2 \cong s_1 = \frac{2\pi\omega_F}{V}\left(d_+^2 - d_-^2\right)\left(\frac{cos^2\theta}{\Delta} + \frac{sin^2\theta}{\Delta^{'}}\right) \cong 0 \tag{A39}$$

$$r_- = \frac{\pi\omega_F}{2V}\left(d_+^2 - d_-^2\right)\left(\frac{1}{\Delta^{'}} - \frac{1}{\Delta}\right) sin(2\theta) \cong 0 \tag{A40}$$

$$r_+ = \frac{\pi\omega_F}{V}\left(d_-^2 + d_+^2\right)\left(\frac{1}{\Delta^{'}} - \frac{1}{\Delta}\right) sin(2\theta) \cong 0 \tag{A41}$$

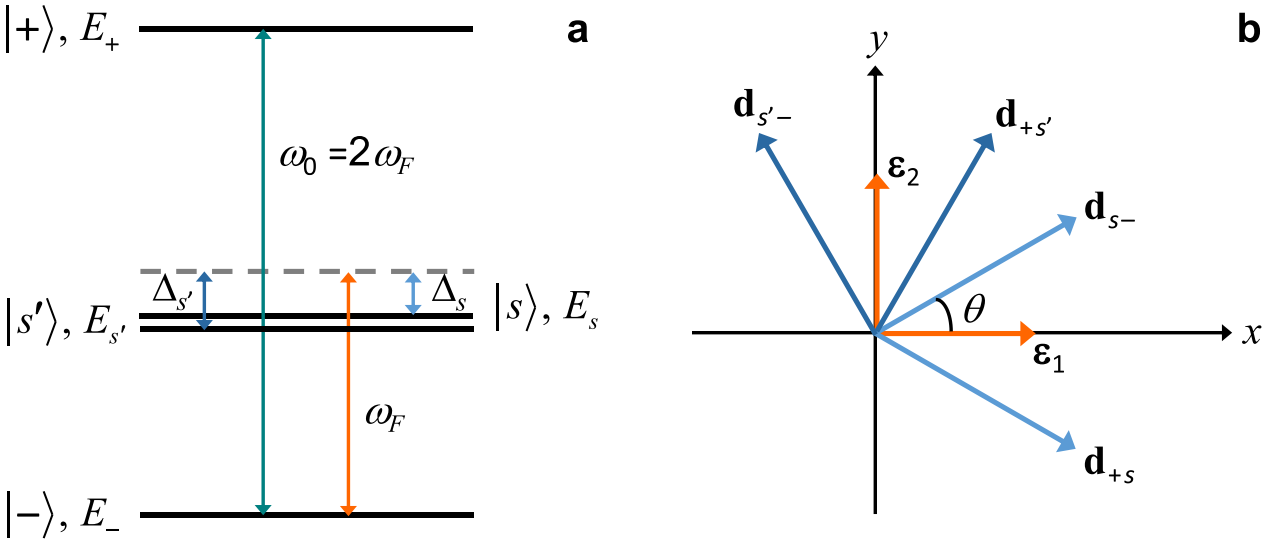

Fig. A1. Physical properties of the atom-radiation system. (*a*) Relationship between the portion of atom energy spectrum relevant to the interaction with the radiation field and the field frequency ω_F. The two intermediate virtual states of the atom, $|s\rangle$ and $|s^{'}\rangle$, are almost degenerate (or degenerate). (*b*) Polarization vectors of the field modes and transition dipole moments that connect the ground and excited states of the atom with its intermediate states. θ defines the reciprocal orientation of the dipole moments and the polarization vectors.

The insertion of Eqs. (A37) to (A41) into Eq. (A23) provides Eq. (1). Furthermore, Eqs. (A37) and (A38) relate the effective frequency ω in Eq. (1) to ω_0 and ω_F.

It is worth noting that, using Eqs. (A24) and (A38), the value of the (constant) energy term dropped in Eq. (A22) is ω and the ground state energy for the Hamiltonian of Eq. (1) is $(N-1)\omega$, where N is the total number of photons in the system.

Appendix B

Expansion of the system state at time t in the eigenstates of the non-interacting Hamiltonian for $|\psi(0)\rangle = |n,0,-\rangle$

We reobtain the expansion coefficients in Eq. (7) for the initial condition $|\psi(0)\rangle = |n,0,-\rangle$ [31] in a way amenable to generalizations to different initial conditions. To this aim, we make use of the unitary operator (which is related to the operator defined in reference [55])

$$U = exp\Big[-i\frac{\pi}{4}\left(a_1^\dagger a_2 + a_1 a_2^\dagger\right)\Big] \tag{B1}$$

Using the commutation relations for the annihilation and creation operators a_μ and $a_\mu^\dagger$, we obtain

$$\begin{cases} U^\dagger a_\mu U = \dfrac{1}{\sqrt{2}}\left(a_\mu - i a_\nu\right) \\ U^\dagger a_\mu^\dagger U = \dfrac{1}{\sqrt{2}}\left(a_\mu^\dagger + i a_\nu^\dagger\right) \end{cases} \qquad (\mu,\nu = 1,2; \mu \neq \nu) \tag{B2}$$

By repeated use of the property $UU^\dagger = \widehat{1}$, we find

$$U^\dagger\left(a_1^2 + a_2^2\right)U = \frac{1}{2}\left[(a_1 - i a_2)(a_1 - i a_2) + (a_2 - i a_1)(a_2 - i a_1)\right] = -2i a_1 a_2 \tag{B3}$$

The action of U on the interaction Hamiltonian (apart from the coupling constant) is thus given by

$$U^\dagger\left[\left(a_1^2 + a_2^2\right)S_+ + \left(a_1^{\dagger 2} + a_2^{\dagger 2}\right)S_-\right]U = -2i\left(a_1 a_2 S_+ - a_1^\dagger a_2^\dagger S_-\right) \tag{B4}$$

Similarly, using the commutation relations $[a_\mu, \widehat{n}_\mu] = a_\mu$ and $[a_\mu^\dagger, \widehat{n}_\mu] = -a_\mu^\dagger$ $(\mu = 1,2)$, or the fact that $\widehat{N} \equiv \widehat{n}_1 + \widehat{n}_2 + 2S_z + 1$ is a constant of motion corresponding to the total excitation number, one can see that U commutes with the atom and field Hamiltonians and hence

$$\widetilde{H} \equiv U^\dagger H U = 2\omega S_z + \omega\left(\widehat{n}_1 + \widehat{n}_2\right) - 2\lambda i\left(a_1 a_2 S_+ - a_1^\dagger a_2^\dagger S_-\right) \tag{B5}$$

Next, we introduce the transform of the system state through the U operator:

$$|\varphi(t)\rangle \equiv U^\dagger|\psi(t)\rangle \tag{B6}$$

In particular, since $\left(a_1^\dagger a_2 + a_1 a_2^\dagger\right)|0,0,\pm\rangle = 0$, it is

$$U^\dagger|0,0,\pm\rangle = \left[\widehat{1} + i\frac{\pi}{4}\left(a_1^\dagger a_2 + a_1 a_2^\dagger\right) + \ldots\right]|0,0,\pm\rangle = |0,0,\pm\rangle \tag{B7}$$

and, for $|\psi(0)\rangle = |n,0,-\rangle$, the use of Eqs. (B2) and (B7) gives

$$|\varphi(0)\rangle = U^\dagger|n,0,-\rangle = U^\dagger\frac{\left(a_1^\dagger\right)^n}{\sqrt{n!}}UU^\dagger|0,0,-\rangle = \frac{\left(a_1^\dagger + i a_2^\dagger\right)^n}{\sqrt{2^n n!}}|0,0,-\rangle$$

$$= \frac{1}{\sqrt{2^n n!}}\sum_{k=0}^{n}\binom{n}{k}\left(i a_2^\dagger\right)^k\left(a_1^\dagger\right)^{n-k}|0,0,-\rangle = \sum_{k=0}^{n} i^k\binom{n}{k}\left[\frac{1}{2^n}\frac{(n-k)!k!}{n!}\right]^{1/2}|n-k,k,-\rangle \tag{B8a}$$

$$= \sum_{k=0}^{n} P_k|n-k,k,-\rangle$$

with

$$P_k = i^k\left[\frac{1}{2^n}\binom{n}{k}\right]^{1/2} \tag{B8b}$$

At time t, employing the constant of motion $\widehat{N}$ and Eq. (B5), we have

$$|\varphi(t)\rangle = e^{-i\widetilde{H}t}\sum_{k=0}^{n} P_k|n-k,k,-\rangle = e^{-i(n-1)\omega t}e^{-2\lambda(a_1a_2S_+ - a_1^\dagger a_2^\dagger S_-)t}\sum_{k=0}^{n} P_k|n-k,k,-\rangle$$
$$= e^{-i(n-1)\omega t}\sum_{k=0}^{n} P_k\sum_{l=0}^{\infty}\frac{(-2\lambda t)^l}{l!}(a_1a_2S_+ - a_1^\dagger a_2^\dagger S_-)^l|n-k,k,-\rangle \tag{B9}$$

It is easy to verify that, for$j \neq 0$,

$$(a_1a_2S_+ - a_1^\dagger a_2^\dagger S_-)^{2j}|n-k,k,-\rangle = (-1)^j[k(n-k)]^j|n-k,k,-\rangle \tag{B10a}$$

and, for any integer $j \geq 0$,

$$(a_1a_2S_+ - a_1^\dagger a_2^\dagger S_-)^{2j+1}|n-k,k,-\rangle = (-1)^j[k(n-k)]^{(2j+1)/2}|n-k-1,k-1,+\rangle \tag{B10b}$$

Therefore,

$$|\varphi(t)\rangle = e^{-i(n-1)\omega t}\left[\sum_{k=0}^{n} P_k\sum_{j=0}^{\infty}\frac{(-1)^j}{(2j)!}\left[2\lambda t\sqrt{k(n-k)}\right]^{2j}|n-k,k,-\rangle\right.$$
$$\left.-\sum_{k=1}^{n-1} P_k\sum_{j=0}^{\infty}\frac{(-1)^j}{(2j+1)!}\left[2\lambda t\sqrt{k(n-k)}\right]^{2j+1}|n-k-1,k-1,+\rangle\right] \tag{B11a}$$
$$= e^{-i(n-1)\omega t}\left\{\sum_{k=0}^{n} P_k cos[f(k)t]|n-k,k,-\rangle - \sum_{k=1}^{n-1} P_k sin[f(k)t]|n-k-1,k-1,+\rangle\right\}$$

with

$$f(k) = 2\lambda\sqrt{k(n-k)} \tag{B11b}$$

At this point, we consider the coefficients

$$\langle p,q,\pm|\psi(t)\rangle = \langle p,q,\pm|U|\varphi(t)\rangle \tag{B12}$$

First, we obtain a general expression for the action of the unitary operator on the eigenstates of the non-interacting Hamiltonian. For any given initial condition, the generic state $|p,q,\pm\rangle$ (where p and q are integers) in the expansion of $|\psi(t)\rangle$ can be written in the form

$$|p,q,\pm\rangle = \frac{(a_1^\dagger)^p(a_2^\dagger)^q}{\sqrt{p!q!}}|0,0,\pm\rangle \tag{B13}$$

Using Eq. (B2), we obtain

$$U^\dagger|p,q,\pm\rangle = \frac{U^\dagger(a_1^\dagger)^p UU^\dagger(a_2^\dagger)^q U}{\sqrt{p!q!}}U^\dagger|0,0,\pm\rangle$$
$$= \frac{2^{-\frac{p+q}{2}}}{\sqrt{p!q!}}(a_1^\dagger + ia_2^\dagger)^p(a_2^\dagger + ia_1^\dagger)^q|0,0,\pm\rangle$$
$$= \frac{2^{-\frac{p+q}{2}}}{\sqrt{p!q!}}\sum_{j=0}^{p}\sum_{k=0}^{q}\binom{p}{j}\binom{q}{k}i^{j+k}(a_1^\dagger)^{p-j+k}(a_2^\dagger)^{q+j-k}|0,0,\pm\rangle \tag{B14a}$$
$$= 2^{-\frac{p+q}{2}}\sum_{j=0}^{p}\sum_{k=0}^{q}\binom{p}{j}\binom{q}{k}i^{j+k}\sqrt{\frac{(p-j+k)!(q+j-k)!}{p!q!}}|p-j+k,q+j-k,\pm\rangle$$
$$= \sum_{j=0}^{p}\sum_{k=0}^{q} P_{jk}^{(p,q)}|p-j+k,q+j-k,\pm\rangle$$

with

$$P_{jk}^{(p,q)} = i^{j+k}\left[\frac{1}{2^{p+q}}\binom{p}{j}\binom{q}{k}\binom{p-j+k}{k}\binom{q+j-k}{j}\right]^{1/2} \tag{B14b}$$

Then, by inserting Eqs. (B8b), (B11) and (B14) into equation (B12) with the atom in state|–>, and thus with $p+q=n$, we obtain

$$\begin{aligned} e^{i(n-1)\omega t}\langle p,q,-|\psi(t)\rangle &= \sum_{k=0}^{n}\sum_{j=0}^{p}\sum_{l=0}^{q} P_k P_{jl}^{(p,q)\,*} cos[f(k)t]\delta_{n-k,p-j+l}\delta_{k,q+j-l} \\ &= \sum_{j=0}^{p}\sum_{l=0}^{q} P_{q+j-l} P_{jl}^{(p,q)\,*} cos[f(q+j-l)t]\delta_{n-q,p} = \sum_{j=0}^{n-q}\sum_{l=0}^{q} P_{q+j-l} P_{jl}^{(n-q,q)\,*} cos[f(q+j-l)t] \\ &= \frac{i^q}{2^n}\sum_{j=0}^{n-q}\sum_{l=0}^{q}(-1)^l\left[\binom{n}{q+j-l}\binom{n-q}{j}\binom{q}{l}\binom{n-q-j+l}{l}\binom{q+j-l}{j}\right]^{1/2} cos[f(q+j-l)t] \\ &= \frac{i^q}{2^n}\binom{n}{q}^{1/2}\sum_{j=0}^{n-q}\sum_{l=0}^{q}(-1)^{q-l}\binom{n-q}{j}\binom{q}{l} cos[f(j+l)t] \end{aligned} \tag{B15}$$

where the last expression results from the substitution $l \to q-l$ and the binomial property $\binom{q}{l} = \binom{q}{q-l}$. Because of the same property and the fact that $f(k) = f(n-k)$, for any given term $(j,l) = (j_0,l_0)$ in the summation, there is a term $(j,l) = (n-q-j_0, q-l_0)$ such that the ratio between the two terms is $(-1)^{q-2l}$; that is, the two terms cancel each other unless q is even. Therefore, the coefficients in Eq. (7) for the atom in state |–> have the form [31]

$$P_r^{(-)}(t) \equiv \langle n-2r, 2r, -|\psi(t)\rangle = e^{-i(n-1)\omega t}\frac{(-1)^r}{2^n}\binom{n}{2r}^{1/2}\sum_{l=0}^{2r}\sum_{j=0}^{n-2r}(-1)^l\binom{2r}{l}\binom{n-2r}{j} cos[f(j+l)t] \tag{B16}$$

with $r = 0,\ldots,r_{max}$. When the atom is in state |+>, and thus $p+q=n-2$, we similarly find

$$\begin{aligned} e^{i(n-1)\omega t}\langle p,q,+|\psi(t)\rangle &= \sum_{k=0}^{n}\sum_{j=0}^{p}\sum_{l=0}^{q} P_k P_{jl}^{(p,q)\,*} sin[f(k)t]\delta_{n-k-1,p-j+l}\delta_{k-1,q+j-l} \\ &= \sum_{j=0}^{p}\sum_{l=0}^{q} P_{q+j-l+1} P_{jl}^{(p,q)\,*} sin[f(q+j-l+1)t]\delta_{n-q-2,p} \\ &= \sum_{j=0}^{n-q-2}\sum_{l=0}^{q} P_{q+j-l+1} P_{jl}^{(n-q-2,q)\,*} sin[f(q+j-l+1)t] \\ &= \sum_{j=0}^{n-q'}\sum_{l=0}^{q'-2} P_{q'+j-l-1} P_{jl}^{(n-q',q'-2)\,*} sin[f(q'+j-l-1)t] \\ &= \frac{i^{q'-1}}{2^{n-1}}\sqrt{q'(q'-1)}\binom{n}{q'}^{1/2}\sum_{j=0}^{n-q'}\sum_{l=0}^{q'-2}(-1)^{q'-l}\binom{n-q'}{j}\binom{q'-2}{l}\frac{sin[f(j+l+1)t]}{\sqrt{(n-j-l-1)(j+l+1)}} \end{aligned} \tag{B17}$$

where $q' = q+2$, and the last expression results from the binomial property mentioned above and the substitution $l \to q'-2-l$. Since the terms such as $(j,l) = (j_0,l_0)$ and $(j,l) = (n-q'-j_0, q'-2-l_0)$ differ by a factor of $(-1)^{q'-2l}$, the nonzero coefficients in Eq. (7), for the atom in state |+>, are

$$\begin{aligned} P_s^{(+)}(t) &= -ie^{-i(n-1)\,\omega t}\frac{(-1)^s}{2^{n-1}}\sqrt{2s(2s-1)}\binom{n}{2s}^{1/2} \\ &\times\sum_{l=0}^{2s-2}\sum_{j=0}^{n-2s}(-1)^l\binom{2s-2}{l}\binom{n-2s}{j}\frac{sin[f(j+l+1)t]}{\sqrt{(j+l+1)(n-j-l-1)}} \end{aligned} \tag{B18}$$

with $s = 1,\ldots,s_{max}$.

Appendix C

Atomic state and second moments of the field population

In this section, we derive relations between the atom and field operators that are useful to characterize the entanglement of the atomic state with the degrees of freedom of the radiation field and to describe the coarse-grained dynamics of the field, with special attention to the correlations among subsystems.

The conservation of the total excitation number N implies that the mean values of the operators $S_x = \frac{1}{2}(S_+ + S_-) = \frac{1}{2}(|+\rangle\langle -| + |-\rangle\langle +|)$ and $S_y = \frac{1}{2i}(S_+ - S_-)$ are zero. Therefore, after tracing over the field (F) degrees of freedom to obtain the density operator of the atom (A) $\rho_A(t) = \mathrm{Tr}_F|\psi(t)\rangle\langle\psi(t)|$, the relationship between $Tr_A\rho_A^2(t)$ and the averages of the atomic spin operators [56] at time t reduces to

$$Tr_A\rho_A^2(t) = \frac{1}{2}\left[1 + 4\langle S_z(t)\rangle^2\right] \tag{C1}$$

Eq. (C1) clearly shows that S_z is sufficient to describe the degree of purity of the atomic state. In particular, $S_z = \pm 1/2$ corresponds to a pure atomic state. The distribution of the S_z values at time t can be characterized through the variance

$$\sigma_z^2(t) = \langle S_z^2(t)\rangle - \langle S_z(t)\rangle^2 = \frac{1}{4} - \langle S_z(t)\rangle^2 \tag{C2}$$

where the last expression is easily obtained using Eq. (B11), while the covariance of the atomic inversion and the photon number operator of field mode μ is

$$\sigma_{\mu z}(t) = \langle n_\mu(t)S_z(t)\rangle - \langle n_\mu(t)\rangle\langle S_z(t)\rangle \qquad (\mu = 1,2) \tag{C3}$$

Since we are interested in unraveling the key determinants of the system dynamics over time windows in which the evolutions of the field mode populations are essentially quenched, we introduce in the analysis the second moments of the photon distributions in the two modes, that is, the variances of the photon numbers

$$\sigma_\mu^2(t) = \left\langle \widehat{n}_\mu^2(t)\right\rangle - \left\langle \widehat{n}_\mu(t)\right\rangle^2 \qquad (\mu = 1,2) \tag{C4}$$

and their covariance

$$\sigma_{12}(t) = \sigma_{21}(t) = \left\langle \widehat{n}_1(t)\widehat{n}_2(t)\right\rangle - \left\langle \widehat{n}_1(t)\right\rangle\left\langle \widehat{n}_2(t)\right\rangle \tag{C5}$$

Inserting Eqs. (C3) and (C4) into (C5), and taking into account that $\widehat{n}_\nu = \widehat{N} - \widehat{n}_\mu - 2S_z - 1$, we obtain

$$\sigma_{\mu\nu}(t) = -\sigma_\mu^2(t) - 2\sigma_{\mu z}(t) \qquad (\mu = 1,2;\ \mu \neq \nu) \tag{C6}$$

Furthermore, since

$$\langle NS_z\rangle - N\langle S_z\rangle = \sigma_{1z} + \sigma_{2z} + 2\sigma_z^2 = 0 \tag{C7}$$

Eq. (C6) can be recast in the form

$$\sigma_{12}(t) = -\frac{1}{2}\left[\sigma_1^2(t) + \sigma_2^2(t)\right] + 2\sigma_z^2(t) \cong -\frac{1}{2}\left[\sigma_1^2(t) + \sigma_2^2(t)\right] \tag{C8}$$

The approximation that produces the rightmost expression is based on the fact that $\sigma_z^2 \leq \langle S_z^2\rangle \leq 1/4$. Eq. (C8) expresses an anti-correlation between the populations of the two field modes, (e.g., see Fig. 1b and e). It is also worth noting that Eq. (C6) implies that

$$\sigma_1^2(t) - \sigma_2^2(t) = -2[\sigma_{1z}(t) - \sigma_{2z}(t)] \tag{C9}$$

Therefore, while the variations of σ_1^2 and σ_2^2 during the evolution of the system are of the order of N^2 (more precisely, the variances span a range from 0 to $\sim N^2/4$ for odd N, as in Figs. 1c and C1a, and about half of that for even N, as in Figs. 1f and C1b), their difference $\sigma_1^2 - \sigma_2^2$ can undergo much smaller variations on the order of N. Thus, the relative difference between the variances of the photon numbers in the two field modes decrease as the inverse of N. The closed-form expressions of σ_1^2, σ_2^2 and σ_{12} represented in Figs. 1 and C1 are provided in the next section.

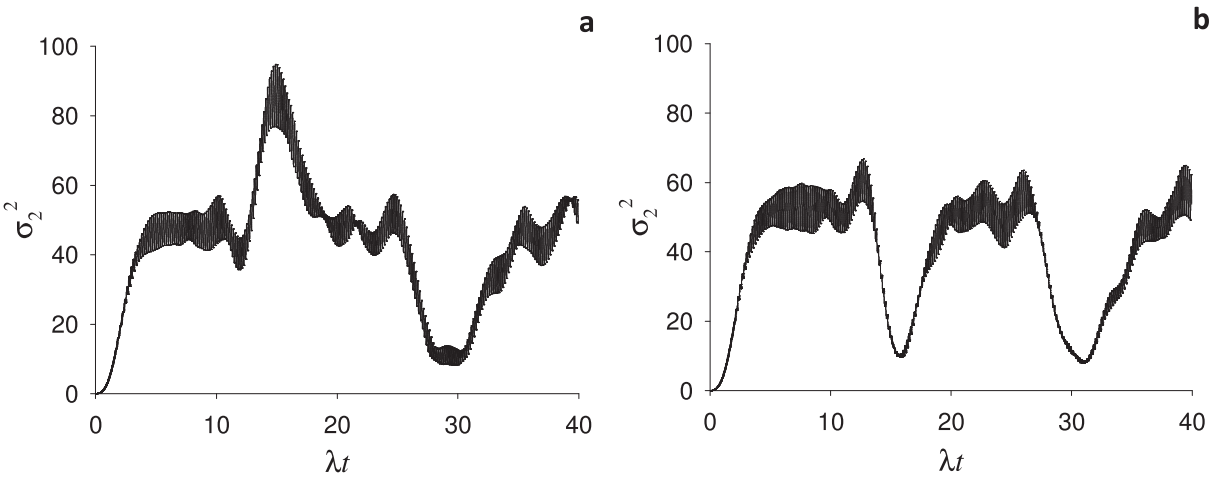

Fig. C1. Time evolution of mode 2 photon number variances for $|\psi(0)\rangle = |n, 0, -\rangle$: σ_2^2 vs λt for (a) $n = 20$ and (b) $n = 21$.

Appendix D

Closed expressions for $\langle S_z(t)\rangle$, $n_1(t)$, $\sigma_1^2(t)$, $\sigma_{12}(t)$ and $\sigma_2^2(t)$ starting from the initial condition $|\psi(0)\rangle = |n, 0, -\rangle$

We obtain the time evolution of the atomic inversion using the unitary operator U and thus Eq. (B11a):

$$\langle S_z(t)\rangle \equiv \langle\psi(t)|S_z|\psi(t)\rangle = \langle\varphi(t)|S_z|\varphi(t)\rangle = -\frac{1}{2^{n+1}}\sum_{k=0}^{n}\binom{n}{k}cos[2f(k)t] \tag{D1}$$

where we used Eq. (B8b). Eq. (D1) is diagrammed in Fig. D1 for $n = 20$ and $n = 21$. For $n = 20$ (cf. Fig. 5 of reference [31] for $n = 100$), Fig. D1 shows a substantial quenching of the atomic inversion dynamics during the plateaus of the photon numbers in the two field modes, as is predicted from the analysis of states $|\psi_a\rangle$ and $|\psi_b\rangle$.

The average photon number in field mode 1 at time t is

$$n_1(t) \equiv \left\langle \widehat{n}_1(t)\right\rangle = \frac{1}{2}\langle\varphi(t)|\widehat{n}_1 + \widehat{n}_2 + i\left(a_1a_2^\dagger - a_1^\dagger a_2\right)|\varphi(t)\rangle = \frac{N-1}{2} - \langle S_z(t)\rangle - \mathrm{Im}\langle\varphi(t)|a_1a_2^\dagger|\varphi(t)\rangle \tag{D2}$$

where the two equalities are obtained by insertion of Eq. (B2) and the constant of motion $\widehat{N}$. $n_1(t)$ can be obtained using Eq. (B11a) in Eq. (D2) [31]. Here, we pursue a different approach, which uses the new polynomials defined in the next section. These polynomials enable a consistent procedure to obtain closed form expressions for the first and second moments of the photon number distributions in the two field modes, and the entropies of the atom and field subsystems.

Summation reducing (SR) polynomial functions

We define the functions

$$\begin{aligned} A_\nu^{(\alpha,\beta)}(x) &= \frac{1}{\nu!}\frac{d^\nu}{dx^\nu}\left[(1-x)^\alpha(1+x)^\beta\right] \\ &= \sum_{j=max\{0,\nu-\beta\}}^{min\{\alpha,\nu\}}\binom{\alpha}{j}\binom{\beta}{\nu-j}(-1)^j(1-x)^{\alpha-j}(1+x)^{\beta-\nu+j} \end{aligned} \tag{D3}$$

where ν is zero or a natural number. The polynomial expression is obtained for integer α, β and holds for $\alpha + \beta \geq \nu$, while $A_\nu^{(\alpha,\beta)}(x) = 0$ for $\alpha + \beta < \nu$. The polynomial expression becomes

$$A_\nu^{(\alpha,\beta)}(x) = \sum_{j=0}^{\nu}\binom{\alpha}{j}\binom{\beta}{\nu-j}(-1)^j(1-x)^{\alpha-j}(1+x)^{\beta-\nu+j} \tag{D4}$$

and is valid for any real α and β by using the generalized binomial coefficients [57]

$$\binom{r}{j} = \begin{cases} r^j/j! & j \geq 0 \\ 0 & j < 0 \end{cases} \tag{D5}$$

in which r is a real number, j is an integer and

$$r^{\underline{j}} = r(r-1)\cdots(r-j+1) \tag{D6}$$

Next, we demonstrate properties of these polynomial functions that allow us to obtain simple closed-form expressions for the physical quantities of interest. For this purpose, we limit our analysis to integer α and β. Eq. (D3) gives

$$\begin{aligned}
&\frac{1}{2^n}\sum_{k=0}^{n}\binom{n}{k}A_p^{(n-k,k+m)}(x)A_{p+r}^{(n-k,k+m)}(y)\\
&=\frac{1}{2^n}\frac{1}{p!(p+r)!}\frac{\partial^{2p+r}}{\partial x^p\partial y^{p+r}}\sum_{k=0}^{n}\binom{n}{k}[(1-x)(1-y)]^{n-k}[(1+x)(1+y)]^k(1+x)^m(1+y)^m\\
&=\frac{1}{p!(p+r)!}\frac{\partial^{2p+r}}{\partial x^p\partial y^{p+r}}[(1+xy)^n(1+x)^m(1+y)^m]\\
&=\frac{1}{p!(p+r)!}\frac{\partial^p}{\partial x^p}\left[(1+x)^m\sum_{j=max\{0,p+r-m\}}^{min\{p+r,n\}}\binom{p+r}{j}\frac{n!}{(n-j)!}x^j(1+xy)^{n-j}\frac{\partial^{p+r-j}}{\partial y^{p+r-j}}(1+y)^m\right]\\
&=\frac{1}{p!}\frac{\partial^p}{\partial x^p}\sum_{l=0}^{m}\sum_{j=max\{0,p+r-m\}}^{min\{p+r,n\}}\frac{1}{(p+r-j)!}\binom{m}{l}\binom{n}{j}x^{j+l}(1+xy)^{n-j}\frac{\partial^{p+r-j}}{\partial y^{p+r-j}}(1+y)^m\\
&=\frac{1}{p!}\frac{\partial^p}{\partial x^p}\sum_{l=0}^{m}\sum_{j=max\{0,m-p-r\}}^{min\{m,n+m-p-r\}}\binom{m}{l}\binom{m}{j}\binom{n}{p+r-m+j}x^{p+r-m+j+l}(1+xy)^{n-p-r+m-j}(1+y)^j
\end{aligned} \tag{D7}$$

in which $r\in\mathbb{Z}$, all other indices are nonnegative integers and $max\{p,p+r\}\le n+m$. The summation on the left-hand side of Eq. (D7) is zero for $max\{p, p+r\} > n+m$. Eq. (D7) gives

$$\begin{aligned}
&\frac{1}{2^n}\sum_{k=0}^{n}\binom{n}{k}A_p^{(n-k,k+m)}(0)A_{p+r}^{(n-k,k+m)}(0)\\
&=\frac{1}{p!}\frac{\partial^p}{\partial x^p}\sum_{l=0}^{m}\sum_{j=max\{0,m-p-r\}}^{min\{m,n+m-p-r\}}\binom{m}{l}\binom{m}{j}\binom{n}{p+r-m+j}x^{p+r-m+j+l}\Bigg|_{x=0}
\end{aligned} \tag{D8}$$

The condition $r-m+j+l=0$ produces the nonzero terms in the right-hand side of Eq. (D8). From the limit values of j and l is easily seen that such terms can only exist for $-m\le r\le m$. Moreover, $r-m+j+l=0$ is compatible with the upper bound of $j=m-r-l$ if $l\ge max\{-r,p-n\}$, namely, $l\ge max\{0,-r,p-n\}$. The lower bound of j leads to either $m>p+r\Rightarrow m-r-l\ge m-p-r\Rightarrow l\le p$ or $m\le p+r\Rightarrow m-r-l\ge 0\Rightarrow l\le m-r$. Using these limitations and the symmetry properties of the binomial coefficients, we obtain

$$\begin{aligned}
&\frac{1}{2^n}\sum_{k=0}^{n}\binom{n}{k}A_p^{(n-k,k+m)}(0)A_{p+r}^{(n-k,k+m)}(0)\\
&=\begin{cases}
\sum_{l=max\{0,-r,p-n\}}^{min\{m,m-r,p\}}\binom{m}{l}\binom{m}{r+l}\binom{n}{p-l} & (-m\le r\le m)\\
0 & (|r|>m)\\
0 & (n+m<max\{p,p+r\})
\end{cases}
\end{aligned} \tag{D9}$$

The left-hand side of Eq. (D9) contains three summations. Therefore, Eq. (D9) describes the simplification of a triple summation to (at most) a single summation. In particular, Eq. (D9) produces the useful relationships

$$\Lambda_{p,r}^{n,m}\equiv\frac{1}{2^n}\sum_{k=0}^{n}\binom{n}{k}A_p^{(n-k,k+m)}(0)A_{p+r}^{(n-k,k+m)}(0)=\begin{cases}
\binom{n}{p} & (r=m)\\
m\binom{n+1}{p} & (r=m-1\ge 0)\\
m\binom{n+1}{p-m+1} & (r=-m+1\le 0)\\
\binom{n}{p-m} & (r=-m)\\
\binom{n+2}{p}+2\binom{n}{p-1} & (m=2,\ r=0)
\end{cases} \tag{D10}$$

for all values of p for which the binomial coefficients are defined. The last expression also holds for $p = 0$ and $p = n+2$ using the definition of generalized binomial coefficient in Eqs. (D5) and (D6), which makes the second binomial coefficient zero for such p values. By combining the relation

$$n(n-1)\cdots(n-j+1)\binom{n-j}{k-j} = \frac{n!}{(k-j)!(n-k)!} = \binom{n}{k}k(k-1)\cdots(k-j+1) \qquad (j \geq 1) \tag{D11}$$

with Eq. (D10), we obtain, for $j \geq 1$ (and the standard definition of the binomial coefficients),

$$\begin{aligned}
&\frac{1}{2^{n-j}}\sum_{k=0}^{n}\binom{n}{k}k(k-1)\cdots(k-j+1)A_p^{(n-k,k-j+m)}(0)A_{p+r}^{(n-k,k-j+m)}(0)\\
&= n(n-1)\cdots(n-j+1)\frac{1}{2^{n-j}}\sum_{k=j}^{n}\binom{n-j}{k-j}A_p^{(n-k,k-j+m)}(0)A_{p+r}^{(n-k,k-j+m)}(0)\\
&= \frac{n!}{(n-j)!}\frac{1}{2^{n-j}}\sum_{k=0}^{n-j}\binom{n-j}{k}A_p^{(n-j-k,k+m)}(0)A_{p+r}^{(n-j-k,k+m)}(0)\\
&= \frac{n!}{(n-j)!}\times\begin{cases}
0 & (|r| > m)\\
\binom{n-j}{p} & (r = m)\\
\binom{n-j}{p-1} & (m = 1,\ r = -1)\\
\binom{n-j+1}{p} & (m = 1,\ r = 0)
\end{cases}
\end{aligned} \tag{D12}$$

Closed-form expression for $n_1(t)$

In order to obtain the time evolution of the average photon number in field mode 1, we consider the density matrix $\rho(t) = |\psi(t)\rangle\langle\psi(t)|$, after rewriting Eq. (7) in the form:

$$|\psi(t)\rangle = \sum_{k=0}^{n} Q_k^{(-)}(t)|n-k,\ k,\ -\rangle + \sum_{k=2}^{n} Q_k^{(+)}(t)|n-k,\ k-2,\ +\rangle \tag{D13}$$

The expressions for the expansion coefficients in Eq. (D13) result from Eqs. (B15) and (B17), that is, $Q_k^{(-)}(t) = P_r^{(-)}(t)$ for $0 \leq k/2 = r \leq r_{max}$ and $Q_k^{(-)}(t) = 0$ for any other integer $k \leq n$, $Q_k^{(+)}(t) = P_s^{(+)}(t)$ for $1 \leq k/2 = s \leq s_{max}$ and $Q_k^{(+)}(t) = 0$ for any other $k \leq n$.

Using Eq. (D13), we write the reduced density matrix of field mode 1 as

$$\rho_1(t) \equiv \mathrm{Tr}_{A,2}\rho(t) = \sum_{k=0}^{n}\left[\left|Q_k^{(-)}(t)\right|^2 + \left|Q_k^{(+)}(t)\right|^2\right]|n-k\rangle\langle n-k| \tag{D14}$$

where we simplified the notation considering that $Q_k^{(+)}(t) = 0$ for $k = 0, 1$. Mode 1 population is then given by

$$n_1(t) = \mathrm{Tr}_1[\rho_1(t)\hat{n}_1] = \sum_{k=0}^{n}\left[\left|Q_k^{(-)}(t)\right|^2 + \left|Q_k^{(+)}(t)\right|^2\right](n-k) = n - \sum_{k=0}^{n}\left|Q_k^{(-)}(t)\right|^2 k - \sum_{k=0}^{n}\left|Q_k^{(+)}(t)\right|^2 k \tag{D15}$$

From Eq. (B15) we obtain

$$\begin{aligned}
&\sum_{k=0}^{n}\left|Q_k^{(-)}(t)\right|^2 k\\
&= \frac{1}{2^{2n}}\sum_{k=0}^{n}\binom{n}{k}k\sum_{j,j'=0}^{n-k}\sum_{l,l'=0}^{k}(-1)^{l+l'}\binom{n-k}{j}\binom{n-k}{j'}\binom{k}{l}\binom{k}{l'}cos[f(j+l)t]cos[f(j'+l')t]
\end{aligned} \tag{D16}$$

To simplify the right-hand side of Eq. (D16), we group the terms with the same arguments of the cosine functions by putting $p = j+l$ and $p + r = j' + l'$. Considering the lower and upper bounds of the summations in Eq. (D16), $-n \leq r = j' + l' - j - l \leq n$. For each value of r, the definitions of p and r

imply that $max\{0,-r\} \le p \le min\{n,n-r\}$; hence, considering the lower and upper bounds of j, $max\{0,p-k\} \le j = p-l \le min\{n-k,p\}$. Similarly, $max\{0,p+r-k\} \le j' \le min\{n-k,p+r\}$. Moreover, $(-1)^{l+l'} = (-1)^{2p+r-j-j'} = (-1)^{r+j+j'}$. Thus, using Eq. (D3), Eq. (D16) is written

$$\begin{aligned}
&\sum_{k=0}^{n} \left|Q_k^{(-)}(t)\right|^2 k \\
&= \frac{1}{2^{2n}} \sum_{r=-n}^{n} (-1)^r \sum_{p=max\{0,-r\}}^{min\{n,n-r\}} cos[f(p)t]cos[f(p+r)t] \sum_{k=0}^{n} \binom{n}{k} k \\
&\times \sum_{j=max\{0,p-k\}}^{min\{n-k,p\}} \binom{n-k}{j} \binom{k}{p-j} (-1)^j \sum_{j'=max\{0,p+r-k\}}^{min\{n-k,p+r\}} \binom{n-k}{j'} \binom{k}{p+r-j'} (-1)^{j'} \\
&= \frac{1}{2^{2n}} \sum_{r=-n}^{n} (-1)^r \sum_{p=max\{0,-r\}}^{min\{n,n-r\}} cos[f(p)t]cos[f(p+r)t] \sum_{k=0}^{n} \binom{n}{k} A_p^{(n-k,k)}(0) A_{p+r}^{(n-k,k)}(0) k
\end{aligned} \tag{D17}$$

Inserting Eq. (D12) with $j = m = 1$ into Eq. (D17), we obtain

$$\begin{aligned}
&\sum_{k=0}^{n} \left|Q_k^{(-)}(t)\right|^2 k = \frac{n}{2^{n+1}} \left\{ -\sum_{p=0}^{n-1} \binom{n-1}{p} cos[f(p)t]cos[f(p+1)t] \right. \\
&\left. - \sum_{p=1}^{n} \binom{n-1}{p-1} cos[f(p-1)t]cos[f(p)t] + \sum_{p=0}^{n} \binom{n}{p} cos^2[f(p)t] \right\} \\
&= \frac{n}{2^{n+1}} \sum_{p=0}^{n} \binom{n}{p} cos^2[f(p)t] - \frac{n}{2^n} \sum_{p=0}^{n-1} \binom{n-1}{p} cos[f(p)t]cos[f(p+1)t]
\end{aligned} \tag{D18}$$

Using Eq. (B17) and proceeding similarly with $p = j+l+1$ and $p + r = j' + l' + 1$, we have

$$\begin{aligned}
&\sum_{k=0}^{n} \left|Q_k^{(+)}(t)\right|^2 k = \frac{1}{2^{2n-2}} \sum_{k=0}^{n} \binom{n}{k} k^2(k-1) \sum_{j,j'=0}^{n-k} \sum_{l,l'=0}^{k-2} (-1)^{l+l'} \binom{n-k}{j} \binom{n-k}{j'} \binom{k-2}{l} \binom{k-2}{l'} \\
&\times \frac{sin[f(j+l+1)t]sin[f(j'+l'+1)t]}{\sqrt{(j+l+1)(n-j-l-1)(j'+l'+1)(n-j'-l'-1)}} \\
&= \frac{1}{2^{2n-2}} \sum_{r=-n+2}^{n-2} (-1)^r \sum_{p=max\{1,1-r\}}^{min\{n-1,n-1-r\}} \frac{sin[f(p)t]sin[f(p+r)t]}{\sqrt{p(n-p)(p+r)(n-p-r)}} \sum_{k=0}^{n} \binom{n}{k} k^2(k-1) \\
&\times \sum_{j=max\{0,p-k+1\}}^{min\{n-k,p-1\}} \binom{n-k}{j} \binom{k-2}{p-1-j} (-1)^j \sum_{j'=max\{0,p+r-k+1\}}^{min\{n-k,p+r-1\}} \binom{n-k}{j'} \binom{k-2}{p+r-1-j'} (-1)^{j'} \\
&= \frac{1}{2^{2n-2}} \sum_{r=-n+2}^{n-2} (-1)^r \sum_{p=max\{1,1-r\}}^{min\{n-1,n-1-r\}} \frac{sin[f(p)t]sin[f(p+r)t]}{\sqrt{p(n-p)(p+r)(n-p-r)}} \\
&\times \sum_{k=2}^{n} \binom{n}{k} k^2(k-1) A_{p-1}^{(n-k,k-2)}(0) A_{p-1+r}^{(n-k,k-2)}(0)
\end{aligned} \tag{D19}$$

At this point, we note that

$$\begin{aligned}
&\frac{1}{2^{n-2}} \sum_{k=2}^{n} \binom{n}{k} k^2(k-1) A_{p-1}^{(n-k,k-2)}(0) A_{p-1+r}^{(n-k,k-2)}(0) \\
&= \frac{n(n-1)}{2^{n-2}} \sum_{k=0}^{n-2} \binom{n-2}{k} k A_{p-1}^{(n-2-k,k)}(0) A_{p-1+r}^{(n-2-k,k)}(0) + 2n(n-1)\Lambda_{p-1,r}^{n-2,0}
\end{aligned} \tag{D20}$$

The first summation on the right-hand side of Eq. (D20) is obtained from Eq. (D12) for $j = m = 1$, by replacing n and p with $n-2$ and $p-1$,

respectively. The second summation is obtained from Eq. (D10). Thus,

$$\frac{1}{2^{n-2}}\sum_{k=2}^{n}\binom{n}{k}k^2(k-1)A_{p-1}^{(n-k,k-2)}(0)A_{p-1+r}^{(n-k,k-2)}(0)$$

$$=\frac{n}{2}\times\begin{cases}(n-1)(n-2)\binom{n-3}{p-2}=(p-1)(n-p)\binom{n-1}{p-1} & (r=-1)\\ (n-1)(n-2)\binom{n-2}{p-1}+4(n-1)\binom{n-2}{p-1}=\frac{n+2}{n}p(n-p)\binom{n}{p} & (r=0)\\ (n-1)(n-2)\binom{n-3}{p-1}=(n-p)(n-p-1)\binom{n-1}{p-1} & (r=1)\end{cases} \tag{D21}$$

$\forall p: max\{1,1-r\}\le p\le min\{n-1,n-1-r\}$. Inserting Eq. (D21) into Eq. (D19), we find

$$\sum_{k=0}^{n}\left|Q_k^{(+)}(t)\right|^2 k=\frac{n}{2^{n+1}}\Bigg\{-\sum_{p=2}^{n-1}\binom{n-1}{p-1}\sqrt{\frac{p-1}{p}\frac{n-p}{n-p+1}}sin[f(p-1)t]sin[f(p)t]$$

$$-\sum_{p=1}^{n-2}\binom{n-1}{p-1}\sqrt{\frac{(n-p)(n-p-1)}{p(p+1)}}sin[f(p)t]sin[f(p+1)t]+\frac{n+2}{n}\sum_{p=1}^{n-1}\binom{n}{p}sin^2[f(p)t]\Bigg\} \tag{D22}$$

$$=\frac{n+2}{2^{n+1}}\sum_{p=0}^{n}\binom{n}{p}sin^2[f(p)t]-\frac{n}{2^n}\sum_{p=0}^{n-1}\binom{n-1}{p}\sqrt{\frac{p}{p+1}\left(1-\frac{1}{n-p}\right)}sin[f(p)t]sin[f(p+1)t]$$

In the last line of Eq. (D22), we used the property $\binom{n-1}{p-1}=\frac{p}{n-p}\binom{n-1}{p}$ and simplified the bounds of the summations considering that $f(0)=f(n)=0$ and that the quantity in the square root vanishes for $p=0$ and $p=n-1$.

Using Eqs. (D1), (D18) and (D22), as well as double angle and difference formulas for cosine, Eq. (D15) finally reads

$$n_1(t)=\frac{n-1}{2}-\langle S_z(t)\rangle+\frac{n}{2^n}\sum_{p=0}^{n-1}\binom{n-1}{p}cos\{[f(p)-f(p+1)]t\}$$

$$+\frac{n}{2^n}\sum_{p=0}^{n-1}\binom{n-1}{p}\left[\sqrt{\frac{p}{p+1}\left(1-\frac{1}{n-p}\right)}-1\right]sin[f(p)t]sin[f(p+1)t] \tag{D23}$$

Eq. (D23) is plotted in Fig. 1a and d for $n=20,21$, while Fig. D2 shows the average photon number in field mode 2, $n_2(t)=n-1-n_1(t)-2\langle S_z(t)\rangle$, and the difference in population between the two field modes, $\Delta\widehat{n}(t)\equiv n_1(t)-n_2(t)$, for $n=20$.

Approximate expression for $n_1(t)$

In this section, we demonstrate the approximate expression for $n_1(t)$ in Eq. (3). To this end, we first show that the last summation on the right-hand side of Eq. (D23) is $\underset{\sim}{<}1$ and therefore can be neglected compared to the large variations of the field mode population for $n\gg1$. Since a binomial distribution function with a mean of $\sim n/2$ has a standard deviation of $\sim\sqrt{n}/2$, in the summation we retain the terms such that $|p-n/2|\le\sqrt{n}/2$. Defining the quantity

$$x=\frac{p-n/2}{n/2}\le n^{-1/2} \tag{D24}$$

we obtain

$$1-\sqrt{\frac{p}{p+1}\left(1-\frac{1}{n-p}\right)}=1-\frac{p}{p+1}\sqrt{1-\frac{4}{n}\left(x+\frac{1}{n}\right)\frac{1}{1-x^2}}$$

$$=1-\frac{p}{p+1}\left(1-\frac{2x}{n}+\ldots\right)=\frac{1}{p+1}+O\left(n^{-3/2}\right) \tag{D25}$$

Therefore, neglecting the $O\left(n^{-3/2}\right)$ term in Eq. (D25), we have

$$\left|\frac{n}{2^n}\sum_{p=0}^{n-1}\binom{n-1}{p}\left[\sqrt{\frac{p}{p+1}\left(1-\frac{1}{n-p}\right)}-1\right]sin[f(p)t]sin[f(p+1)t]\right|$$

$$<\frac{n}{2^n}\sum_{p=0}^{n-1}\binom{n-1}{p}\left[1-\sqrt{\frac{p}{p+1}\left(1-\frac{1}{n-p}\right)}\right]\cong\frac{n}{2^n}\sum_{p=0}^{n-1}\binom{n-1}{p}\frac{1}{p+1} \tag{D26}$$

$$=\frac{1}{2^n}\sum_{p=0}^{n-1}\binom{n}{p+1}=\frac{1}{2^n}(2^n-1)\cong 1$$

With similar analysis, and using Eq. (B11b), the argument of the cosine in the first summation of Eq. (D23) is written

$$f(p)-f(p+1)=2\lambda\sqrt{p(n-p)}\left(1-\sqrt{\frac{p+1}{p}\frac{n-p-1}{n-p}}\right)$$

$$=\lambda n\sqrt{1-x^2}\left[1-\sqrt{1-\frac{4}{n}\left(x+\frac{1}{n}\right)\frac{1}{1-x^2}}\right]=\lambda n\left[\frac{2x}{n}+\frac{2}{n^2}+O\left(n^{-5/2}\right)\right] \tag{D27}$$

$$=\frac{2\lambda}{n}\left[2p-n+1+O\left(n^{-1/2}\right)\right]$$

Then, for $\lambda t\ll n^{3/2}/2$,

$$n_1(t)\cong\frac{n}{2}\left\{1+\frac{1}{2^{n-1}}\sum_{p=0}^{n-1}\binom{n-1}{p}cos\left[\frac{2\lambda t}{n}(2p-n+1)\right]\right\} \tag{D28}$$

where we also disregarded the quantity $-\langle S_z(t)\rangle-1/2$, which is between -1 and 0 at any t. Exploiting the identity [58]

$$\sum_{p=0}^{n}\binom{n}{p}cos(ap+b)=2^n cos^n\left(\frac{a}{2}\right)cos\left(a\frac{n}{2}+b\right) \tag{D29}$$

Eq. (D28) reduces to Eq. (3).

Closed-form expression for $\sigma_1^2(t)$

The variance of the photon distribution in field mode 1 can be written as

$$\sigma_1^2(t)=\sum_{k=0}^{n}\left[\left|Q_k^{(-)}(t)\right|^2+\left|Q_k^{(+)}(t)\right|^2\right](n-k)^2-n_1^2(t)$$

$$=\sum_{k=0}^{n}\left|Q_k^{(-)}(t)\right|^2k(k-1)+\sum_{k=0}^{n}\left|Q_k^{(+)}(t)\right|^2k(k-1)-[n-n_1(t)][n-1-n_1(t)] \tag{D30}$$

The last line of Eq. (D30) was obtained inserting the expression for $n-n_1(t)$ that results from Eq. (D15) and using the normalization of the state vector. Next, we elaborate the expression for $\sum_{k=0}^{n}\left|Q_k^{(-)}(t)\right|^2k(k-1)$ similarly to Eq. (D17), by means of equations (D9) and (D10) with n replaced by $n-2$:

$$\sum_{k=0}^{n}\left|Q_k^{(-)}(t)\right|^2k(k-1)$$

$$=\frac{1}{2^{2n}}\sum_{r=-n}^{n}(-1)^r\sum_{p=max\{0,-r\}}^{min\{n,n-r\}}cos[f(p)t]cos[f(p+r)t]\sum_{k=0}^{n}\binom{n}{k}A_p^{(n-k,k)}(0)A_{p+r}^{(n-k,k)}(0)k(k-1) \tag{D31}$$

$$=\frac{n(n-1)}{2^{n+2}}\sum_{r=-n}^{n}(-1)^r\sum_{p=max\{0,-r\}}^{min\{n,n-r\}}cos[f(p)t]cos[f(p+r)t]\Lambda_{p,r}^{n-2,2}$$

The last expression in Eq. (D31) is readily obtained by repeated application of the substitution $k\to k+1$. Using Eq. (D10), we can then write

$$\sum_{k=0}^{n}\left|Q_k^{(-)}(t)\right|^2 k(k-1)=\frac{n(n-1)}{2^{n+2}}\Bigg\{\sum_{p=2}^{n}cos[f(p-2)t]cos[f(p)t]\Lambda_{p,-2}^{n-2,2}$$

$$-\sum_{p=1}^{n}cos[f(p-1)t]cos[f(p)t]\Lambda_{p,-1}^{n-2,2}+\sum_{p=0}^{n}cos^2[f(p)t]\Lambda_{p,0}^{n-2,2}$$

$$-\sum_{p=0}^{n-1}cos[f(p)t]cos[f(p+1)t]\Lambda_{p,1}^{n-2,2}+\sum_{p=0}^{n-2}cos[f(p)t]cos[f(p+2)t]\Lambda_{p,2}^{n-2,2}\Bigg\}$$

$$=\frac{n(n-1)}{2^{n+2}}\Bigg\{\sum_{p=2}^{n}\binom{n-2}{p-2}cos[f(p-2)t]cos[f(p)t]-2\sum_{p=1}^{n}\binom{n-1}{p-1}cos[f(p-1)t]cos[f(p)t]$$

$$+\sum_{p=0}^{n}\binom{n}{p}cos^2[f(p)t]+2\sum_{p=1}^{n-1}\binom{n-2}{p-1}cos^2[f(p)t] \tag{D32}$$

$$-2\sum_{p=0}^{n-1}\binom{n-1}{p}cos[f(p)t]cos[f(p+1)t]+\sum_{p=0}^{n-2}\binom{n-2}{p}cos[f(p)t]cos[f(p+2)t]\Bigg\}$$

$$=\frac{n(n-1)}{2^{n+2}}\Bigg\{2\sum_{p=0}^{n-2}\binom{n-2}{p}cos[f(p)t]cos[f(p+2)t]-4\sum_{p=0}^{n-1}\binom{n-1}{p}cos[f(p)t]cos[f(p+1)t]$$

$$+\sum_{p=0}^{n}\binom{n}{p}cos^2[f(p)t]+2\sum_{p=0}^{n-2}\binom{n-2}{p}cos^2[f(p+1)t]\Bigg\}$$

Next, exploiting Eq. (D19), we get

$$\sum_{k=0}^{n}\left|Q_k^{(+)}(t)\right|^2 k(k-1)=\frac{1}{2^{2n-2}}\sum_{r=-n+2}^{n-2}(-1)^r\sum_{p=max\{1,1-r\}}^{min\{n-1,n-1-r\}}\frac{sin[f(p)t]sin[f(p+r)t]}{\sqrt{p(n-p)(p+r)(n-p-r)}} \tag{D33}$$

$$\times\sum_{k=2}^{n}\binom{n}{k}k^2(k-1)^2A_{p-1}^{(n-k,k-2)}(0)A_{p-1+r}^{(n-k,k-2)}(0)$$

Through rearrangement of the binomial coefficients and repeated change of the summation index, the sum of SR polynomials in Eq. (D33) is written

$$\frac{1}{2^{n-2}}\sum_{k=2}^{n}\binom{n}{k}k^2(k-1)^2A_{p-1}^{(n-k,k-2)}(0)A_{p-1+r}^{(n-k,k-2)}(0)$$

$$=\frac{n(n-1)}{2^{n-2}}\sum_{k=0}^{n-2}\binom{n-2}{k}\left(k^2+3k+2\right)A_{p-1}^{(n-2-k,k)}(0)A_{p-1+r}^{(n-2-k,k)}(0)$$

$$=\frac{n(n-1)}{2^{n-2}}\Bigg[\left((n-2)(n-3)\sum_{k=0}^{n-4}\binom{n-4}{k}A_{p-1}^{(n-4-k,k+2)}(0)A_{p-1+r}^{(n-4-k,k+2)}(0)\right. \tag{D34}$$

$$\left.+4(n-2)\sum_{k=0}^{n-3}\binom{n-3}{k}A_{p-1}^{(n-3-k,k+1)}(0)A_{p-1+r}^{(n-3-k,k+1)}(0)+2\sum_{k=0}^{n-2}\binom{n-2}{k}A_{p-1}^{(n-2-k,k)}(0)A_{p-1+r}^{(n-2-k,k)}(0)\right]$$

$$=n(n-1)\left[\frac{(n-2)(n-3)}{4}\Lambda_{p-1,r}^{n-4,2}+2(n-2)\Lambda_{p-1,r}^{n-3,1}+2\Lambda_{p-1,r}^{n-2,0}\right]$$

Then, inserting Eq. (D10) into Eq. (D34) and using the notation

$$\phi(p,p+r)\equiv\frac{n(n-1)}{2^n}\frac{sin[f(p)t]sin[f(p+r)t]}{\sqrt{p(n-p)(p+r)(n-p-r)}} \tag{D35}$$

we recast Eq. (D33) in the form

$$\sum_{k=0}^{n}\left|Q_k^{(+)}(t)\right|^2 k(k-1)$$

$$=\sum_{r=-n+2}^{n-2}(-1)^r\sum_{p=max\{1,1-r\}}^{min\{n-1,n-1-r\}}\phi(p,p+r)\left[\frac{(n-2)(n-3)}{4}\Lambda_{p-1,r}^{n-4,2}+2(n-2)\Lambda_{p-1,r}^{n-3,1}+2\Lambda_{p-1,r}^{n-2,0}\right]$$

$$=\frac{(n-2)(n-3)}{4}\sum_{r=-2}^{2}(-1)^r\sum_{p=max\{1,1-r\}}^{min\{n-1,n-1-r\}}\phi(p,p+r)\Lambda_{p-1,r}^{n-4,2}$$

$$+2(n-2)\sum_{r=-1}^{1}(-1)^r\sum_{p=max\{1,1-r\}}^{min\{n-1,n-1-r\}}\phi(p,p+r)\Lambda_{p-1,r}^{n-3,1}+2\sum_{p=1}^{n-1}\phi(p,p)\Lambda_{p-1,0}^{n-2,0}$$

$$=\frac{(n-2)(n-3)}{4}\left[\sum_{p=3}^{n-1}\phi(p,p-2)\Lambda_{p-1,-2}^{n-4,2}-\sum_{p=2}^{n-1}\phi(p,p-1)\Lambda_{p-1,-1}^{n-4,2}+\sum_{p=1}^{n-1}\phi(p,p)\Lambda_{p-1,0}^{n-4,2}\right.$$

$$\left.-\sum_{p=1}^{n-2}\phi(p,p+1)\Lambda_{p-1,1}^{n-4,2}+\sum_{p=1}^{n-3}\phi(p,p+2)\Lambda_{p-1,2}^{n-4,2}\right]+2(n-2)\left[-\sum_{p=2}^{n-1}\phi(p,p-1)\Lambda_{p-1,-1}^{n-3,1}\right.$$

$$\left.+\sum_{p=1}^{n-1}\phi(p,p)\Lambda_{p-1,0}^{n-3,1}-\sum_{p=1}^{n-2}\phi(p,p+1)\Lambda_{p-1,1}^{n-3,1}\right]+2\sum_{p=1}^{n-1}\phi(p,p)\Lambda_{p-1,0}^{n-2,0}$$

$$=\frac{(n-2)(n-3)}{4}\left[\sum_{p=3}^{n-1}\binom{n-4}{p-3}\phi(p,p-2)-2\sum_{p=2}^{n-1}\binom{n-3}{p-2}\phi(p,p-1)\right.$$

$$+\sum_{p=1}^{n-1}\binom{n-2}{p-1}\phi(p,p)+2\sum_{p=2}^{n-2}\binom{n-4}{p-2}\phi(p,p)-2\sum_{p=1}^{n-2}\binom{n-3}{p-1}\phi(p,p+1) \tag{D36}$$

$$\left.+\sum_{p=1}^{n-3}\binom{n-4}{p-1}\phi(p,p+2)\right]+2(n-2)\left[-\sum_{p=2}^{n-1}\binom{n-3}{p-2}\phi(p,p-1)\right.$$

$$\left.+\sum_{p=1}^{n-1}\binom{n-2}{p-1}\phi(p,p)-\sum_{p=1}^{n-2}\binom{n-3}{p-1}\phi(p,p+1)\right]+2\sum_{p=1}^{n-1}\binom{n-2}{p-1}\phi(p,p)$$

$$=\frac{n^2+3n-2}{4}\sum_{p=0}^{n-2}\binom{n-2}{p}\phi(p+1,p+1)-(n+1)(n-2)\sum_{p=0}^{n-3}\binom{n-3}{p}\phi(p+1,p+2)$$

$$+\frac{(n-2)(n-3)}{2}\sum_{p=0}^{n-4}\binom{n-4}{p}[\phi(p+1,p+3)+\phi(p+2,p+2)]$$

$$=\frac{1}{2^n}\sum_{p=0}^{n}\binom{n}{p}\left[\frac{n^2+3n-2}{4}+\frac{(p-1)(n-1-p)}{2}\right]sin^2[f(p)t]$$

$$-\frac{n(n+1)}{2}\frac{1}{2^{n-1}}\sum_{p=0}^{n-1}\binom{n-1}{p}\sqrt{\frac{p}{p+1}\left(1-\frac{1}{n-p}\right)}sin[f(p)t]sin[f(p+1)t]$$

$$+\frac{n(n-1)}{8}\frac{1}{2^{n-2}}\sum_{p=0}^{n-2}\binom{n-2}{p}\sqrt{\frac{p}{p+2}\left(1-\frac{2}{n-p}\right)}sin[f(p)t]sin[f(p+2)t]$$

In the last expression we used the fact that $sin[f(0)t]=sin[f(n)t]=0$ to extend the lower and upper bounds of the summations. The insertion of Eqs. (D32) and (D36) into equation (D30) gives the variance of the photon number distribution in mode 1 as

$$\sigma_1^2(t) = \frac{n(n-1)}{4} - [n-n_1(t)][n-1-n_1(t)] + \frac{1}{2^n}\sum_{p=0}^{n}\binom{n}{p}\frac{n+np-p^2}{2}sin^2[f(p)t]$$

$$-\frac{n(n-1)}{2}\frac{1}{2^{n-1}}\sum_{p=0}^{n-1}\binom{n-1}{p}\{cos[(f(p)-f(p+1))t]$$

$$+\left[\frac{n+1}{n-1}\sqrt{\frac{p}{p+1}\left(1-\frac{1}{n-p}\right)}-1\right]sin[f(p)t]sin[f(p+1)t]\Bigg\} \tag{D37}$$

$$+\frac{n(n-1)}{8}\frac{1}{2^{n-2}}\sum_{p=0}^{n-2}\binom{n-2}{p}\{cos[(f(p)-f(p+2))t]$$

$$+\left[\sqrt{\frac{p}{p+2}\left(1-\frac{2}{n-p}\right)}-1\right]sin[f(p)t]sin[f(p+2)t]+cos^2[f(p+1)t]\Bigg\}$$

where $n_1(t)$ is given by Eq. (D23).

Closed-form expressions for $\sigma_{12}(t)$ and $\sigma_2^2(t)$

$\sigma_{12}(t)$ can be obtained from Eq. (C6). To this end, we first calculate the field-atom correlation $\left\langle \widehat{n}_1(t)S_z(t)\right\rangle$ using Eq. (D13) and the normalization of the state vector:

$$\left\langle \widehat{n}_1(t)S_z(t)\right\rangle = \langle\psi(t)|\widehat{n}_1 S_z|\psi(t)\rangle = \frac{1}{2}\left[\sum_{k=0}^{n}\left|Q_k^{(-)}(t)\right|^2 k - \sum_{k=0}^{n}\left|Q_k^{(+)}(t)\right|^2 k\right] + \frac{n}{2} - n\sum_{k=0}^{n}\left|Q_k^{(-)}(t)\right|^2 \tag{D38}$$

Proceeding along the lines of Eq. (D17) to express the sum in the last term of Eq. (D38), and using Eqs. (D9) and (D10), we find

$$\begin{aligned}\sum_{k=0}^{n}\left|Q_k^{(-)}(t)\right|^2 &= \frac{1}{2^{2n}}\sum_{r=-n}^{n}(-1)^r\sum_{p=max\{0,-r\}}^{min\{n,n-r\}}cos[f(p)t]cos[f(p+r)t]\sum_{k=0}^{n}\binom{n}{k}A_p^{(n-k,k)}(0)A_{p+r}^{(n-k,k)}(0)\\ &= \frac{1}{2^n}\sum_{p=0}^{n}cos^2[f(p)t]\Lambda_{p,0}^{n,0} = \frac{1}{2^n}\sum_{p=0}^{n}\binom{n}{p}cos^2[f(p)t]\end{aligned} \tag{D39}$$

Inserting Eqs. (D18), (D22) and (D39) into Eq. (D38), we obtain

$$\begin{aligned}\left\langle \widehat{n}_1(t)S_z(t)\right\rangle &= \frac{n-1}{2}\langle S_z(t)\rangle - \frac{n}{4}\frac{1}{2^{n-1}}\sum_{p=0}^{n-1}\binom{n-1}{p}\{cos[(f(p)+f(p+1))t]\\ &\quad +\left[1-\sqrt{\frac{p}{p+1}\left(1-\frac{1}{n-p}\right)}\right]sin[f(p)t]sin[f(p+1)t]\Bigg\} - \frac{1}{4}\end{aligned} \tag{D40}$$

The insertion of Eqs. (D23), (D37) and (D40) into Eq. (C6) gives

$$\sigma_{12}(t) = -\sigma_1^2(t) - 2\left\langle \widehat{n}_1(t)S_z(t)\right\rangle + 2\left\langle \widehat{n}_1(t)\right\rangle\langle S_z(t)\rangle$$

$$= -\sigma_1^2(t) + \frac{n}{2^n}\sum_{p=0}^{n-1}\binom{n-1}{p}\{cos[(f(p)+f(p+1))t] + 2\langle S_z(t)\rangle cos[(f(p)-f(p+1))t] \tag{D41}$$

$$+[1-2\langle S_z(t)\rangle]\left[1-\sqrt{\frac{p}{p+1}\left(1-\frac{1}{n-p}\right)}\right]sin[f(p)t]sin[f(p+1)t]\Bigg\} + \frac{1}{2} - 2\langle S_z(t)\rangle^2$$

At this point, $\sigma_2^2(t)$ is obtained from Eqs. (C2), (C8), (D1), (D37) and (D41) as

$$\sigma_2^2(t) = 1 - 4\langle S_z(t)\rangle^2 - 2\sigma_{12}(t) - \sigma_1^2(t) \tag{D42}$$

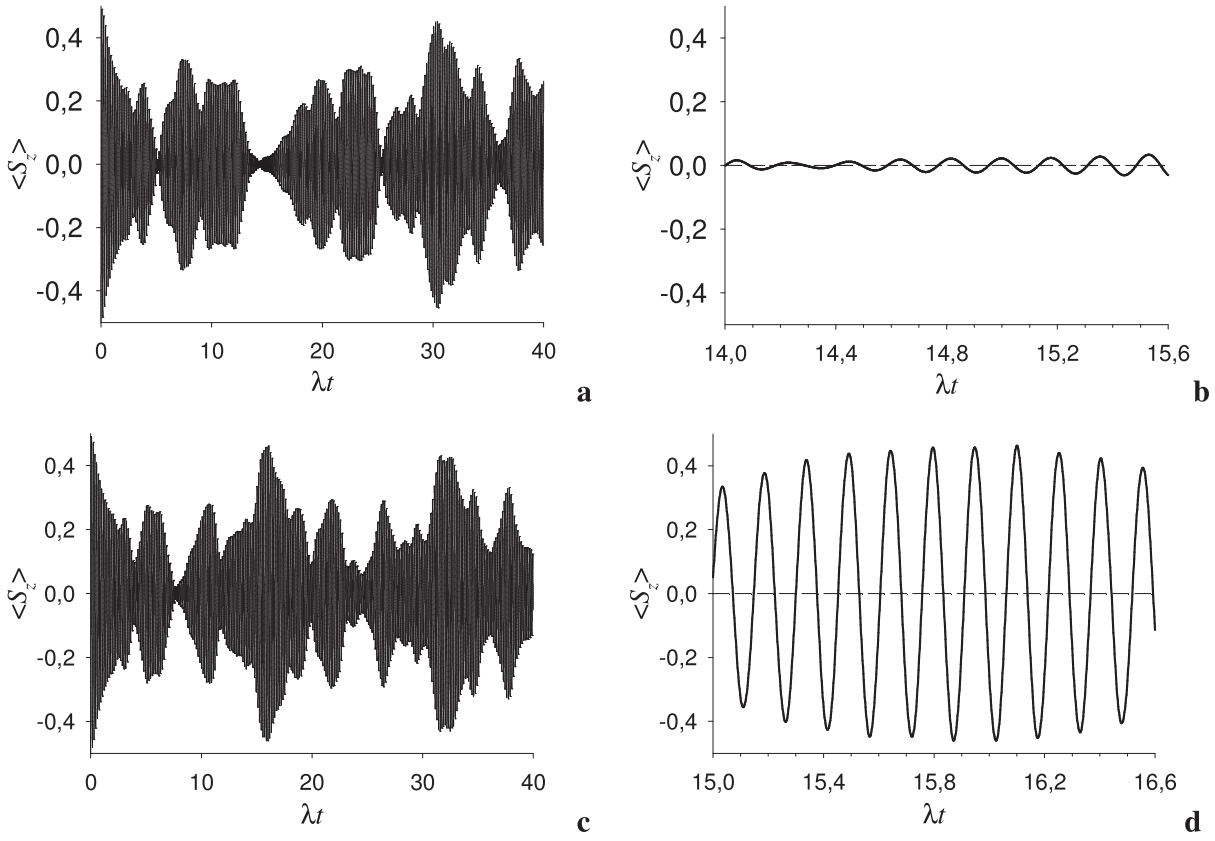

Fig. D1. Time evolution of the atomic inversion for $|\psi(0)\rangle = |n, 0, -\rangle$. (a-d) $\langle S_z \rangle$ versus the effective time λt for (a, b) $n = 20$ and (c, d) $n = 21$. The mid-plateau evolution of $\langle S_z \rangle$ for $n = 20$ agrees with the value of $\langle S_z \rangle = 0.5/(n-1)$ corresponding to the states in Eq. (10). (b) and (d) show the temporal evolution of the atomic inversion around the center of the plateaus in the field mode populations.

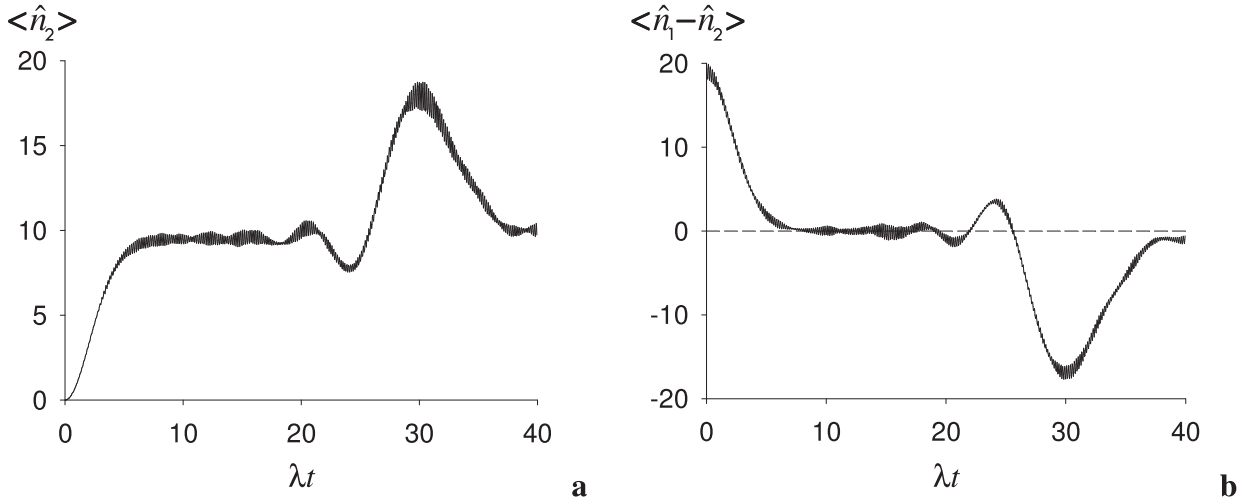

Fig. D2. Dynamics of the field population starting from $|\psi(0)\rangle = |n, 0, -\rangle$. (a) Mean photon number in field mode 1 and (b) difference population of the two modes vs. λt for $n = 20$.

Appendix E

Heisenberg equations of motion

The Heisenberg equation of motion of the photon number operator associated with field mode μ is (in units such that $\hbar = 1$ and omitting the time dependence of the operators to simplify the notation)

$$\frac{d\widehat{n}_\mu}{dt} = i\left[H,\widehat{n}_\mu\right] = i\lambda\left(\left[a_\mu^2,\widehat{n}_\mu\right]S_+ + \left[a_\mu^{\dagger 2},\widehat{n}_\mu\right]S_-\right) = 2i\lambda\left(a_\mu^2 S_+ - a_\mu^{\dagger 2}S_-\right) \quad (\mu = 1,2) \tag{E1}$$

On the other hand, from the constant of motion N we obtain

$$\frac{dS_z}{dt} = -\frac{1}{2}\sum_{\mu=1}^{2}\frac{d\widehat{n}_\mu}{dt} = -i\lambda\sum_{\mu=1}^{2}\left(a_\mu^2 S_+ - a_\mu^{\dagger 2}S_-\right) \tag{E2}$$

and thus

$$\frac{d\widehat{n}_\mu}{dt} = -\frac{d\widehat{n}_\nu}{dt} - 2\frac{dS_z}{dt} = i\lambda\left[\left(a_\mu^2 S_+ - a_\mu^{\dagger 2}S_-\right) - \left(a_\nu^2 S_+ - a_\nu^{\dagger 2}S_-\right)\right] - \frac{dS_z}{dt} \qquad (\nu \neq \mu = 1,2) \tag{E3}$$

whence Eq. (5), namely,

$$\frac{dn_\mu(t)}{dt} \equiv \frac{d\langle\widehat{n}_\mu(t)\rangle}{dt} = -2\lambda\mathrm{Im}\left\langle\left[a_\mu^2(t) - a_\nu^2(t)\right]S_+(t)\right\rangle - \frac{d\langle S_z(t)\rangle}{dt} \qquad (\nu \neq \mu = 1,2) \tag{E4}$$

To analyze the field-atom correlation terms in the right-hand side of Eq. (E4), we make use of Eqs. (B2) and (B6) to write

$$\langle a_1^2(t)S_+(t)\rangle = \langle\psi(t)|a_1^2 S_+|\psi(t)\rangle = \frac{1}{2}\langle\varphi(t)|\left(a_1^2 - a_2^2 - 2ia_1a_2\right)S_+|\varphi(t)\rangle \tag{E5}$$

and consider the initial condition $|\psi(0)\rangle = |n,0,-\rangle$. Then, using Eq. (B11), we obtain

$$a_1^2 S_+|\varphi(t)\rangle = e^{-i(n-1)\omega t}\sum_{k=0}^{n-1}P_k\sqrt{(n-k)(n-k-1)}cos[f(k)t]|n-k-2,k,+\rangle \tag{E6}$$

from which

$$\begin{aligned}\langle\varphi(t)|a_1^2 S_+|\varphi(t)\rangle &= -\sum_{k=0}^{n-2}P_{k+1}^* P_k\sqrt{(n-k)(n-k-1)}cos[f(k)t]sin[f(k+1)t] \\ &= i\frac{n}{2^n}\sum_{k=0}^{n-1}\binom{n-1}{k}\sqrt{\frac{n-k-1}{k+1}}sin[f(k+1)t]cos[f(k)t]\end{aligned} \tag{E7}$$

where we inserted Eq. (B8b). Similarly,

$$\begin{aligned}-\langle\varphi(t)|a_2^2 S_+|\varphi(t)\rangle &= \sum_{k=2}^{n}P_{k-1}^* P_k\sqrt{k(k-1)}cos[f(k)t]sin[f(k-1)t] \\ &= i\frac{n}{2^n}\sum_{k=0}^{n-1}\binom{n-1}{k}\sqrt{\frac{k}{n-k}}sin[f(k)t]cos[f(k+1)t]\end{aligned} \tag{E8}$$

and

$$\begin{aligned}-2i\langle\varphi(t)|a_1a_2 S_+|\varphi(t)\rangle &= \frac{i}{2^n}\sum_{k=0}^{n}\binom{n}{k}\sqrt{k(n-k)}sin[2f(k)t] \\ &= i\frac{n}{2^n}\sum_{k=0}^{n-1}\binom{n-1}{k}\sqrt{\frac{n-k-1}{k+1}}sin[2f(k+1)t]\end{aligned} \tag{E9}$$

Inserting Eqs. (E7) - (E9) into Eq. (E5), one obtains

$$\begin{aligned}\langle a_1^2(t)S_+(t)\rangle &= \frac{1}{2}\langle\varphi(t)|\left(a_1^2 - a_2^2 - 2ia_1a_2\right)S_+|\varphi(t)\rangle \\ &= i\frac{n}{2^{n+1}}\sum_{k=0}^{n-1}\binom{n-1}{k}\left\{\sqrt{\frac{n-k-1}{k+1}}\left[sin(2f(k+1)t) + sin(f(k+1)t)cos(f(k)t)\right]\right. \\ &\left. + \sqrt{\frac{k}{n-k}}sin(f(k)t)cos(f(k+1)t)\right\}\end{aligned} \tag{E10}$$

Similarly, it is

$$\begin{aligned}\langle a_2^2(t)S_+(t)\rangle &= \frac{1}{2}\langle\varphi(t)|\left(a_2^2 - a_1^2 - 2ia_1a_2\right)S_+|\varphi(t)\rangle \\ &= i\frac{n}{2^{n+1}}\sum_{k=0}^{n-1}\binom{n-1}{k}\left\{\sqrt{\frac{n-k-1}{k+1}}\left[sin(2f(k+1)t) - sin(f(k+1)t)cos(f(k)t)\right]\right. \\ &\left. - \sqrt{\frac{k}{n-k}}sin(f(k)t)cos(f(k+1)t)\right\}\end{aligned} \tag{E11}$$

The atom-field correlations in Eqs. (E10) and (E11) are purely imaginary quantities, so that Eq. (E4) can be recast as

$$\frac{dn_\mu(t)}{dt} = 4i\lambda\left\langle a_\mu^2(t)S_+(t)\right\rangle = 2i\lambda\left\langle\left[a_\mu^2(t) - a_\nu^2(t)\right]S_+(t)\right\rangle - \frac{d\langle S_z(t)\rangle}{dt} \qquad (\nu \neq \mu = 1,2) \tag{E12}$$

which also gives Eq. (5). The comparison between the two expressions for $dn_\mu(t)/dt$ in Eq. (E12) highlights the strict link between each mode-atom photon exchange and the difference in the interactions of the two field modes with the atom, when the initial system state is $|\psi(0)\rangle = |n,0,-\rangle$.

The second time derivative of $\hat{n}_1$ is given by

$$\begin{aligned}\frac{d^2\hat{n}_1}{dt^2} &= i\left[H,\frac{d\hat{n}_1}{dt}\right] = 2\lambda\left[a_1^2S_+ - a_1^{\dagger 2}S_-, 2\omega S_z + \omega\sum_{\mu=1}^{2}\hat{n}_\mu + \lambda\sum_{\mu=1}^{2}\left(a_\mu^2S_+ + a_\mu^{\dagger 2}S_-\right)\right] \\ &= -4\lambda\omega\left(a_1^2S_+ + a_1^{\dagger 2}S_-\right) + 4\lambda\omega\left(a_1^2S_+ + a_1^{\dagger 2}S_-\right) + 2\lambda^2\left(\left[a_1^2S_+, a_1^{\dagger 2}S_-\right] + \left[a_1^2S_+, a_2^{\dagger 2}S_-\right]\right. \\ &\left. - \left[a_1^{\dagger 2}S_-, a_1^2S_+\right] - \left[a_1^{\dagger 2}S_-, a_2^2S_+\right]\right) = 4\lambda^2\left[\left(a_1^2a_2^{\dagger 2} + a_1^{\dagger 2}a_2^2\right)S_z + 2\left(\hat{n}_1^2 + \hat{n}_1 + 1\right)S_z + 2\hat{n}_1 + 1\right]\end{aligned} \tag{E13}$$

where we used the commutation rule $[A,BC] = B[A,C] + [A,B]C$, the commutation properties of the photon creation and annihilation operators and of the ½ pseudospin operators that describe the atomic state, as well as the related equalities $S_-S_+ = \frac{1}{2} - S_z$ and $S_+S_- = \frac{1}{2} + S_z$. Given the symmetry of H with respect to the two field modes, the second time derivative of $\hat{n}_2$ is obtained from Eq. (E13) by exchanging the mode indices. Therefore, for $\Delta\hat{n} \equiv \hat{n}_1 - \hat{n}_2$ we find

$$\frac{1}{4\lambda^2}\frac{d^2\Delta\hat{n}}{dt^2} = 2\left(\hat{n}_1^2 - \hat{n}_2^2 + \Delta\hat{n}\right)S_z + 2\Delta\hat{n} = 2\left(\hat{n}_1 + \hat{n}_2 + 1\right)S_z\Delta\hat{n} + 2\Delta\hat{n} = (2NS_z + 1)\Delta\hat{n} \tag{E14}$$

The last equality, which appears in Eq. (6), results from inserting $S_z^2 = \frac{1}{4}$ and the expression for the total excitation number. Making use of Eqs. (C3) and (C9), Eq. (E14) gives

$$\begin{aligned}\frac{1}{4\lambda^2}\frac{d^2\langle\Delta\hat{n}(t)\rangle}{dt^2} &= 2N[\sigma_{1z}(t) - \sigma_{2z}(t)] + [2N\langle S_z(t)\rangle + 1]\langle\Delta\hat{n}(t)\rangle \\ &= N\left[\sigma_2^2(t) - \sigma_1^2(t)\right] + [2N\langle S_z(t)\rangle + 1]\langle\Delta\hat{n}(t)\rangle\end{aligned} \tag{E15}$$

that is, Eq. (6). The comparison with Figs. 1 and D2 highlights that the second term on the right-hand side of Eq. (6) becomes dominant outside the plateaus of the mode populations. This term is negligible at mid-plateau for even n, as both $\langle S_z(t)\rangle$ (Fig. D1) and $\langle\Delta\hat{n}(t)\rangle$ are very small compared to the total excitation number. Therefore, the field-atom correlations described by $2(\sigma_{1z} - \sigma_{2z}) = \sigma_2^2 - \sigma_1^2$, which appear in the first term on the right-hand side of Eq. (E15), essentially cause the changes in $\langle\Delta\hat{n}(t)\rangle$ and its derivatives around mid-plateau (Fig. D2). For odd n, the atom population and depopulation account for a significant portion of the variations in the mid-plateau excitation energy distribution (Fig. D1c), thus reducing the changes in $\langle\Delta\hat{n}(t)\rangle$ and its derivatives.

Appendix F

Maximally symmetric states and evolution of the system at mid-plateau

In this section, we identify mid-plateau eigenstates of the system that are maximally symmetric with respect to the two field modes and yet compatible with the subsequent ability of the system to manifest significant field dynamics, namely, a redistribution of the photons between the two field modes. The symmetry and correlation properties of the mid-plateau states will depend on the initial condition, as is expected to observe the quantum optics parity effect.

By applying the second condition of Eq. (8) to the generic expression for the system state at time t in Eq. (7), we obtain

$$\left\langle\hat{n}_1\,\hat{n}_2\right\rangle = \sum_{r=0}^{r_{max}}\left|P_r^{(-)}\right|^2 2r(n-2r) + \sum_{s=1}^{r_{max}}\left|P_s^{(+)}\right|^2(2s-2)(n-2s) = 0 \tag{F1}$$

All terms in the above summations are nonnegative. Therefore, for odd n, Eq. (F1) is satisfied only if, at some time t, all expansion coefficients except

for $P_0^{(-)}$ and $P_1^{(+)}$ are zero. However, linear combinations of states $|n,\,0,\,-\rangle$ and $|n-2,\,0,\,+\rangle$ clearly cannot satisfy the first condition (8). For even n, $r_{max} = n/2$ and Eq. (F1) requires that only $P_0^{(-)}$, $P_{n/2}^{(-)}$, $P_1^{(+)}$ and $P_{n/2}^{(+)}$ are nonzero. Then, by application of the first condition (8), one obtains the set of normalized states

$$\begin{aligned}\left|\psi_{\varepsilon,q,\theta_1,\theta_2,\theta_3}\right\rangle = &\sqrt{\frac{1}{2}+\frac{n-2}{n}q-\frac{n-1}{n}\varepsilon}|n,0,-\rangle + e^{i\theta_1}\sqrt{\frac{1}{2}-\frac{n-2}{n}q-\frac{1}{n}\varepsilon}|0,n,-\rangle \\ &+e^{i\theta_2}\sqrt{\varepsilon-q}|n-2,0,+\rangle + e^{i\theta_3}\sqrt{q}|0,n-2,+\rangle\end{aligned} \tag{F2}$$

in which θ_1, θ_2 and θ_3 are arbitrary phase factors, and $q = \left|P_{n/2}^{(+)}\right|^2$. If the system is in one of these states, the field-atom correlation terms on the right-hand side of Eq. (5) become

$$\left\langle\psi_{\varepsilon,q,\theta_1,\theta_2,\theta_3}\left|a_1^2 S_+\right|\psi_{\varepsilon,q,\theta_1,\theta_2,\theta_3}\right\rangle = e^{-i\theta_2}\sqrt{n(n-1)\left(\frac{1}{2}+\frac{n-2}{n}q-\frac{n-1}{n}\right)(\varepsilon-q)} \tag{F3a}$$

and

$$\left\langle\psi_{\varepsilon,q,\theta_1,\theta_2,\theta_3}\left|a_2^2 S_+\right|\psi_{\varepsilon,q,\theta_1,\theta_2,\theta_3}\right\rangle = e^{i(\theta_1-\theta_3)}\sqrt{n(n-1)\left(\frac{1}{2}-\frac{n-2}{n}q-\frac{1}{n}\varepsilon\right)q} \tag{F3b}$$

These correlations are zero for $(\varepsilon,q) \in \left\{\left(0,0\right),\ \left(1,\tfrac{1}{2}\right),\ \left(\tfrac{1}{2}\tfrac{n}{n-1},\tfrac{1}{2}\tfrac{n}{n-1}\right),\ \left(\tfrac{1}{2}\tfrac{n}{n-1},0\right)\right\}$, irrespective of the values of the phase factors in Eq. (F2). The last two choices of parameters give

$$\left|\psi_{\theta_3}\right\rangle = \frac{1}{\sqrt{2(n-1)}}\left(\sqrt{n-2}\,|n,\,0,\,-\rangle + e^{i\theta_3}\sqrt{n}\,|0,\,n-2,\,+\rangle\right) \tag{F4a}$$

$$\left|\psi_{\theta_1,\theta_2}\right\rangle = \frac{1}{\sqrt{2(n-1)}}\left[\sqrt{n-2}\,|0,\,n,\,-\rangle + e^{i(\theta_2-\theta_1)}\sqrt{n}\,|n-2,\,0,\,+\rangle\right] \tag{F4b}$$

(a global phase factor $e^{i\theta_1}$ was factored out and removed in Eq. (F4b)). These states correspond to a maximal atom-field mutual entropy (the largest possible value of $2ln2$ is attained for $n\to\infty$, as $\varepsilon = \frac{1}{2}\frac{n}{n-1}\to\frac{1}{2}$) and to the related quenching of the atomic dynamics shown in Fig. D1a-b. $|\psi_{\theta_3}\rangle$ is a linear combination of the basis states associated with the coefficients $P_0^{(-)}$ and $P_{n/2}^{(+)}$ in Eq. (7), while $\left|\psi_{\theta_1,\theta_2}\right\rangle$ is a linear combination of the states corresponding to $P_{n/2}^{(-)}$ and $P_1^{(+)}$. Eqs. (B16) and (B18) provide the exact expressions for the time evolutions of these coefficients when the atom-radiation system starts from state $|\psi(0)\rangle = |n,\,0,\,-\rangle$.

Fig. F1 shows the time evolutions of the products $\mathscr{P}_0^{(-)}(t)\cdot\mathrm{Im}[\mathscr{P}_{n/2}^{(+)}(t)]$ and $\mathscr{P}_{n/2}^{(-)}(t)\cdot\mathrm{Im}[\mathscr{P}_1^{(+)}(t)]$ at mid-plateau, where $\mathscr{P}$ denotes coefficients that differ from the corresponding P's in Eq. (7) by the phase factor $e^{-i(n-1)\,\omega t}$. This factor is shared by all coefficients and is therefore unimportant for the present considerations. The two products of coefficients are relevant to the definition of $|\psi_{\theta_3}\rangle$ and $\left|\psi_{\theta_1,\theta_2}\right\rangle$, respectively. From Fig. F1, it is clear that the $\left\{P_0^{(-)},P_{n/2}^{(+)}\right\}$ and $\left\{P_{n/2}^{(-)},P_1^{(+)}\right\}$ terms alternatively contribute to the mid-plateau time evolution of the system state, which can thus be roughly described as an oscillation between states (F4a-b). Furthermore, at mid-plateau $\mathscr{P}_0^{(-)}(t)$ and $\mathrm{Im}[\mathscr{P}_{n/2}^{(+)}(t)]$ have the same sign, while $\mathscr{P}_{n/2}^{(-)}(t)$ and $\mathrm{Im}[\mathscr{P}_1^{(+)}(t)]$ have opposite signs, which fixes the phases in Eq. (F4a-b) so as to obtain the states $|\psi_a\rangle$ and $|\psi_b\rangle$ of Eq. (10).

Next, we show that the phases in Eqs. (F4a-b) leading to the states in Eq. (10) can be obtained directly using Eqs. (B16) and (B18). The analysis will also show how the frequency $\nu_n \cong n\lambda/\pi$ of mid-plateau oscillation of the system between the states in Eq. (10) emerges from the expressions for the coefficients in Eqs. (B16) and (B18).

Eq. (3) places, approximately, the center of the plateau in the field mode populations at $t \cong t_0$ such that

$$\lambda t_0 = \frac{n}{4}\pi \tag{F5}$$

For even n, Eqs. (B11b) and (B16) give

$$\mathscr{P}_{n/2}^{(-)}(t) = \frac{(-1)^{n/2}}{2^n}\sum_{l=0}^{n}(-1)^l\binom{n}{l}cos[2\lambda\sqrt{l(n-l)}t] \tag{F6}$$

Inserting the quantity x from equation (D24) into Eq. (F6), and for times

$$t = t_0 + \Delta t \tag{F7a}$$

such that

$$\left|nx^2\lambda\Delta t\right| \le \lambda\Delta t << 1 \tag{F7b}$$

we can write

$$\begin{aligned} cos[2\lambda\sqrt{l(n-l)}t] &\cong cos\left[\lambda(t_0+\Delta t)n\left(1-\frac{x^2}{2}\right)\right] \cong cos\left[\frac{n^2\pi}{4}\left(1-\frac{x^2}{2}\right)+n\lambda\Delta t\right] \\ &= cos\left[m^2\pi\left(1-\frac{x^2}{2}\right)\right]cos(n\lambda\Delta t) - sin\left[\pi m^2\left(1-\frac{x^2}{2}\right)\right]sin(n\lambda\Delta t) \\ &= cos(m^2\pi)\left[cos\left(m^2x^2\frac{\pi}{2}\right)cos(n\lambda\Delta t) + sin\left(m^2x^2\frac{\pi}{2}\right)sin(n\lambda\Delta t)\right] \end{aligned} \tag{F8}$$

where we put $n = 2m$. Since $m^2x^2 = (l-m)^2$, Eq. (F8) gives

$$cos[2\lambda\sqrt{l(n-l)}t] \cong \begin{cases} cos(n\lambda\Delta t), & l-\dfrac{n}{2} = \pm 2p \\ sin(n\lambda\Delta t), & l-\dfrac{n}{2} = \pm 2p+1 \end{cases} \tag{F9}$$

where l is limited to the range $0 \le l \le n$. For even $n/2$, Eq. (F9) implies

$$cos[2\lambda\sqrt{l(n-l)}t] \cong \begin{cases} cos(n\lambda\Delta t), & 0 \le l = 2p \le n \\ sin(n\lambda\Delta t), & 1 \le l = 2p+1 \le n-1 \end{cases} \tag{F10}$$

and thus, using formulas 0.15.2 and 0.15.3 of reference [59], Eq. (F6) becomes

$$\begin{aligned} \mathscr{P}^{(-)}_{n/2}(t_0+\Delta t) &\cong \frac{(-1)^{n/2}}{2^n}\left[cos(n\lambda\Delta t)\sum_{p=0}^{n/2}\binom{n}{2p} - sin(n\lambda\Delta t)\sum_{p=0}^{n/2-1}\binom{n}{2p+1}\right] \\ &= \frac{1}{2}[cos(n\lambda\Delta t) - sin(n\lambda\Delta t)] = \frac{1}{\sqrt{2}}cos\left(n\lambda\Delta t+\frac{\pi}{4}\right) \end{aligned} \tag{F11}$$

For odd $n/2$, $cos(n\lambda\Delta t)$ and $sin(n\lambda\Delta t)$ are associated with the odd and even l values, respectively. Thus, since both the sign of $(-1)^{n/2}$ and the signs of the two summations are inverted compared to the case in which $n/2$ is even, we conclude that, for any even n,

$$\mathscr{P}^{(-)}_{n/2}(t_0+\Delta t) \cong \frac{1}{\sqrt{2}}cos\left(n\lambda\Delta t+\frac{\pi}{4}\right) = \frac{1}{\sqrt{2}}cos\left(\pi\nu_n\Delta t+\frac{\pi}{4}\right) \tag{F12}$$

from which

$$\left|\mathscr{P}^{(-)}_{n/2}(t_0+\Delta t)\right|^2 \cong \frac{1}{4}\left[1+cos\left(2\pi\nu_n\Delta t+\frac{\pi}{2}\right)\right] = \frac{1}{4}[1-sin(2\pi\nu_n\Delta t)] \tag{F13}$$

Similarly, we obtain

$$\begin{aligned} \mathscr{P}^{(-)}_{0}(t_0+\Delta t) &= \frac{1}{2^n}\sum_{j=0}^{n}\binom{n}{j}cos[2\lambda\sqrt{j(n-j)}t] \\ &\cong \frac{1}{2}[cos(n\lambda\Delta t) + sin(n\lambda\Delta t)] = \frac{1}{\sqrt{2}}cos\left(n\lambda\Delta t-\frac{\pi}{4}\right) \end{aligned} \tag{F14}$$

whence

$$\left|\mathscr{P}^{(-)}_{0}(t_0+\Delta t)\right|^2 \cong \frac{1}{4}[1+sin(2\pi\nu_n\Delta t)] \tag{F15}$$

Eq. (B18) gives

$$\begin{aligned} \mathscr{P}^{(+)}_{n/2}(t_0+\Delta t) &= -i\frac{(-1)^{n/2}}{2^{n-1}}\sqrt{n(n-1)}\sum_{l=0}^{n-2}(-1)^l\binom{n-2}{l}\frac{sin[f(l+1)t]}{\sqrt{(l+1)(n-l-1)}} \\ &= -i\frac{(-1)^{n/2}}{2^{n-1}}\sqrt{n(n-1)}\sum_{l=1}^{n-1}(-1)^{l-1}\binom{n-2}{l-1}\frac{sin[2\lambda\sqrt{l(n-l)}t]}{\sqrt{l(n-l)}} \end{aligned} \tag{F16}$$

Using again Eq. (D24) and proceeding along the lines of Eqs. (F8) and (F9), one obtains

$$\begin{aligned}
&\sqrt{\frac{n(n-1)}{l(n-l)}}sin[2\lambda\sqrt{l(n-l)}t] \cong 2sin\left[\frac{n^2\pi}{4}\left(1-\frac{x^2}{2}\right)+n\lambda\Delta t\right] \\
&= 2\left\{sin\left[m^2\pi\left(1-\frac{x^2}{2}\right)\right]cos(n\lambda\Delta t)+cos\left[\pi m^2\left(1-\frac{x^2}{2}\right)\right]sin(n\lambda\Delta t)\right\} \\
&= 2\left\{cos(m^2\pi)\left[cos\left(m^2x^2\frac{\pi}{2}\right)sin(n\lambda\Delta t)-sin\left(m^2x^2\frac{\pi}{2}\right)cos(n\lambda\Delta t)\right]\right\} \\
&= 2\times\begin{cases} sin(n\lambda\Delta t), & l-\dfrac{n}{2}=\pm 2p \\ -cos(n\lambda\Delta t), & l-\dfrac{n}{2}=\pm 2p+1 \end{cases}
\end{aligned} \tag{F17}$$

from which

$$\begin{aligned}
\mathscr{P}^{(+)}_{n/2}(t_0+\Delta t) &\cong \frac{i}{2^{n-2}}\left[sin(n\lambda\Delta t)\sum_{p=0}^{n/2-2}\binom{n-2}{2p+1}+cos(n\lambda\Delta t)\sum_{p=0}^{n/2-1}\binom{n-2}{2p}\right] \\
&= \frac{i}{2}[sin(n\lambda\Delta t)+cos(n\lambda\Delta t)] = i\,\mathscr{P}^{(-)}_0(t_0+\Delta t)
\end{aligned} \tag{F18}$$

Similarly,

$$\begin{aligned}
\mathscr{P}^{(+)}_1(t_0+\Delta t) &= \frac{i\sqrt{n(n-1)}}{2^{n-1}}\sum_{j=1}^{n-1}\binom{n-2}{j-1}\frac{sin[2\lambda\sqrt{j(n-j)}t]}{\sqrt{j(n-j)}} \\
&\cong \frac{i}{2}[sin(n\lambda\Delta t)-cos(n\lambda\Delta t)] = -i\,\mathscr{P}^{(-)}_{n/2}(t_0+\Delta t)
\end{aligned} \tag{F19}$$

Eqs. (F11), (F14), (F18) and (F19) confirm, analytically and for any (even) n, the phases leading from Eq. (F4) to Eq. (10), which were deduced for a specific value of n from the numerical analysis in Fig. F1. Using these equations, one obtains

$$c_a(t) = \frac{\sqrt{n-2}+\sqrt{n}}{\sqrt{2(n-1)}}P^{(-)}_0(t) \cong \sqrt{2}P^{(-)}_0(t) \tag{F20a}$$

and

$$c_b(t) = \frac{\sqrt{n-2}+\sqrt{n}}{\sqrt{2(n-1)}}P^{(-)}_{n/2}(t) \cong \sqrt{2}P^{(-)}_{n/2}(t) \tag{F20b}$$

which yield Eq. (12) using (F15) and (F13), respectively.

We conclude showing that the states in Eq. (10) satisfy Eq. (13):

$$\begin{aligned}
&\langle\psi_b|a_1^2S_+|\psi_a\rangle \\
&= \frac{1}{2(n-1)}\left(\sqrt{n-2}\,\langle 0,\,n,\,-|+i\sqrt{n}\,\langle n-2,\,0,\,+|\right)a_1^2S_+\left(\sqrt{n-2}\,|n,\,0,\,-\rangle+i\sqrt{n}\,|0,\,n-2,\,+\rangle\right) \\
&= i\frac{\sqrt{n(n-2)}}{2(n-1)}\langle n-2,\,0,\,+|a_1^2S_+|n,\,0,\,-\rangle = i\frac{n}{2}\sqrt{\frac{n-2}{n-1}}
\end{aligned} \tag{F21}$$

$$\langle\psi_b|a_1^{\dagger 2}S_-|\psi_a\rangle = i\frac{\sqrt{n(n-2)}}{2(n-1)}\langle 0,\,n,\,-|a_1^{\dagger 2}S_-|0,\,n-2,\,+\rangle = \frac{i}{n-1}\sqrt{\frac{n(n-2)}{2}}\langle 0,\,n|2,\,n-2\rangle = 0 \tag{F22}$$

$$\langle\psi_b|a_2^2S_+|\psi_a\rangle = 0 \tag{F23}$$

and

$$\langle\psi_b|a_2^{\dagger 2}S_-|\psi_a\rangle = i\frac{\sqrt{n(n-2)}}{2(n-1)}\langle 0,\,n,\,-|a_2^{\dagger 2}S_-|0,\,n-2,\,+\rangle = i\frac{n}{2}\sqrt{\frac{n-2}{n-1}} = \langle\psi_b|a_1^2S_+|\psi_a\rangle \tag{F24}$$

from which

$$\frac{1}{\lambda}\langle\psi_b|H_{\rm int}|\psi_a\rangle = \langle\psi_b|\sum_{\mu=1}^{2}\left(a_\mu^2 S_+ + a_\mu^{\dagger 2} S_-\right)|\psi_a\rangle = in\sqrt{\frac{n-2}{n-1}} \tag{F25}$$

Note that only $a_1^2 S_+$ and $a_2^{\dagger 2} S_-$ can lead from ψ_a to ψ_b, while the transition matrix elements of $a_1^{\dagger 2} S_-$ and $a_2^2 S_+$ are zero. The converse holds for transitions from ψ_b to ψ_a.

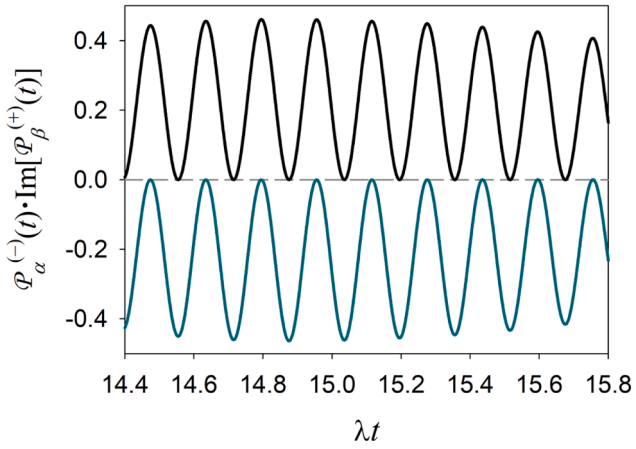

Fig. F1. Temporal evolution of the predominant coefficients in the system state at mid-plateau. We show $\mathscr{P}_\alpha^{(-)}\cdot\mathrm{Im}\,(\mathscr{P}_\beta^{(+)})$ vs. λt for $\{\alpha,\beta\} = \{0, n/2\}, \{n/2, 1\}$ and $n = 20$.

Appendix G

Atom-radiation field correlations at mid-plateau

In this section we provide closed-form expressions for the differences in the correlations between the two field modes and the atom, which appear in the equations of motion (5) and (6).

Using Eq. (D40) and considering that $\langle S_z^2(t)\rangle = 1/4$ and $\widehat{n}_2 = \widehat{N} - \widehat{n}_1 - 2S_z - 1$, we obtain

$$\begin{aligned}\langle S_z(t)\Delta\widehat{n}(t)\rangle &= \left\langle\left[2\widehat{n}_1(t) - \widehat{N} + 2S_z(t) + 1\right]S_z(t)\right\rangle = 2\left\langle\widehat{n}_1(t)S_z(t)\right\rangle + (1-n)\langle S_z(t)\rangle + \frac{1}{2}\\ &= -\frac{n}{2^n}\sum_{p=0}^{n-1}\binom{n-1}{p}\Big\{cos[(f(p)+f(p+1))t]\\ &\quad + \left[1 - \sqrt{\frac{p}{p+1}\left(1-\frac{1}{n-p}\right)}\right]sin[f(p)t]sin[f(p+1)t]\Big\}\\ &= \frac{n}{2^n}\sum_{p=0}^{n-1}\binom{n-1}{p}\left\{\sqrt{\frac{p}{p+1}\left(1-\frac{1}{n-p}\right)}\,sin[f(p)t]sin[f(p+1)t] - cos[f(p)t]cos[f(p+1)t]\right\}\end{aligned} \tag{G1}$$

that is, Eq. (14). For even n, using the mid-plateau approximation

$$|\psi(t)\rangle \cong |\psi(t)\rangle_{\text{two-state}} = c_a(t)|\psi_a\rangle + c_b(t)|\psi_b\rangle \tag{G2}$$

one finds

$$\begin{aligned}<S_z(t)\,\Delta\widehat{n}(t)>_{\text{two-state}} &= c_a^2(t)\langle\psi_a|S_z\Delta\widehat{n}|\psi_a\rangle + c_b^2(t)\langle\psi_b|S_z\Delta\widehat{n}|\psi_b\rangle\\ &\cong -\frac{n}{2}sin[2\pi\nu_n(t - n\pi/4\lambda)] = \frac{n}{2}sin[2\pi\nu_n(t - n\pi/4\lambda) + \pi]\end{aligned} \tag{G3}$$

that is, the second Eq. (15).

Eq. (16) is obtained by subtracting the quantities in Eqs. (E10) and (E11). Next, we calculate such quantities using Eq. (G2). Since the expectation values of $a_1^2 S_+$ and $a_2^2 S_+$ in states $|\psi_a\rangle$ and $|\psi_b\rangle$ are zero by construction, using Eqs. (F12), (F14), (F20) with $t_0 = 0$, (F21) to (F24) and their complex conjugates, one obtains

$$\begin{aligned}\left\langle a_1^2(t)\, S_+(t)\right\rangle_{\text{two-state}} &= c_a(t)c_b(t)\langle\psi_b|a_1^2 S_+|\psi_a\rangle \\ &= i\frac{n}{2}\sqrt{\frac{n-2}{n-1}}cos\left(\pi\nu_n\Delta t-\frac{\pi}{4}\right)cos\left(\pi\nu_n\Delta t+\frac{\pi}{4}\right) \\ &= i\frac{n}{4}\sqrt{\frac{n-2}{n-1}}cos[2\pi\nu_n(t-n\pi/4\lambda)] = -<a_2^2(t)\, S_+(t)>_{\text{two-state}}\end{aligned} \tag{G4}$$

from which

$$\text{Im}\left\langle\left[a_1^2(t)-a_2^2(t)\right]S_+(t)\right\rangle_{\text{two-state}} \cong \frac{n}{2}cos[2\pi\nu_n(t-n\pi/4\lambda)] \tag{G5}$$

that is, the second Eq. (17).

Appendix H

Entropy expressions

To obtain the closed-form expression for the von Neumann entropy associated with the atom, we first write the reduced density matrix of the atom as

$$\rho_A(t) = \text{Tr}_F|\psi(t)\rangle\langle\psi(t)| = \sum_{k=0}^{n}\left|Q_k^{(-)}(t)\right|^2|-\rangle\langle-|+\sum_{k=2}^{n}\left|Q_k^{(+)}(t)\right|^2|+\rangle\langle+| \tag{H1}$$

where we used Eq. (D13). Eq. (H1) describes a statistical mixture of atomic states $|-\rangle$ and $|+\rangle$. The first coefficient is provided by Eq. (D39). The second coefficient can be deduced from the state normalization condition or derived directly as follows.

Proceeding along the lines of equation (D19), we can write

$$\begin{aligned}\sum_{k=0}^{n}\left|Q_k^{(+)}(t)\right|^2 &= \frac{1}{2^{2n-2}}\sum_{r=-n+2}^{n-2}(-1)^r\sum_{p=max\{1,1-r\}}^{min\{n-1,n-1-r\}}\frac{sin[f(p)t]sin[f(p+r)t]}{\sqrt{p(n-p)(p+r)(n-p-r)}} \\ &\times\sum_{k=0}^{n}\binom{n}{k}k(k-1)A_{p-1}^{(n-k,k-2)}(0)A_{p-1+r}^{(n-k,k-2)}(0)\end{aligned} \tag{H2}$$

The last summation is given by Eq. (D12) with $j = 2, m = 0$, and p replaced by $p-1$; hence, it does not vanish only for $r = m = 0$. Therefore, Eq. (D19) becomes

$$\begin{aligned}\sum_{k=0}^{n}\left|Q_k^{(+)}(t)\right|^2 &= \frac{1}{2^{2n-2}}\sum_{r=-n+2}^{n-2}(-1)^r\sum_{p=max\{1,1-r\}}^{min\{n-1,n-1-r\}}\frac{sin[f(p)t]sin[f(p+r)t]}{\sqrt{p(n-p)(p+r)(n-p-r)}} \\ &\times\sum_{k=0}^{n}\binom{n}{k}k(k-1)A_{p-1}^{(n-k,k-2)}(0)A_{p-1+r}^{(n-k,k-2)}(0) = \frac{1}{2^n}\sum_{p=1}^{n-1}\frac{n!}{(n-2)!p(n-p)}\binom{n-2}{p-1}sin^2[f(p)t] \\ &= \frac{1}{2^n}\sum_{p=0}^{n}\binom{n}{p}sin^2[f(p)t]\end{aligned} \tag{H3}$$

The extension of the last summation to $p = 0$ and n exploits the fact that $f(0) = f(n) = 0$. Inserting Eqs. (H2) and (H3) into Eq. (H1), we obtain

$$\rho_A(t) = \frac{1}{2^n}\sum_{p=0}^{n}\binom{n}{p}cos^2[f(p)t]|-\rangle\langle-|+\frac{1}{2^n}\sum_{p=0}^{n}\binom{n}{p}sin^2[f(p)t]|+\rangle\langle+| \tag{H4}$$

Then, the corresponding entropy is [36,60]

$$S_A(t) = -\frac{1}{2^n}\sum_{p=0}^{n}\binom{n}{p}cos^2[f(p)t]ln\left\{\frac{1}{2^n}\sum_{p=0}^{n}\binom{n}{p}cos^2[f(p)t]\right\} - \frac{1}{2^n}\sum_{p=0}^{n}\binom{n}{p}sin^2[f(p)t]ln\left\{\frac{1}{2^n}\sum_{p=0}^{n}\binom{n}{p}sin^2[f(p)t]\right\} \tag{H5}$$

Since the atom-radiation system is in the pure state given by Eq. (7), its total entropy is zero and the lower Araki-Lieb inequality gives

$$S_{AF}(t) = |S_A(t) - S_F(t)| = 0 \Rightarrow S_A(t) = S_F(t) \quad \forall t \tag{H6}$$

which implies

$$S_{A:F}(t) = S_A(t) + S_F(t) - S_{AF}(t) = 2S_A(t) = 2S_F(t) \tag{H7}$$

Eqs. (H5) and (H7) yield Eq. (18).

Next, we consider the reduced density matrix and the von Neumann entropy for each radiation field mode. The reduced density matrix of field mode 1 was given by Eq. (D14), and it can be equivalently written using Eqs. (B16) and (B18) as

$$\rho_1(t) = \left|P_0^{(-)}(t)\right|^2|n\rangle\langle n| + \sum_{r=1}^{r_{max}}\left[\left|P_r^{(-)}(t)\right|^2 + \left|P_r^{(+)}(t)\right|^2\right]|n-2r\rangle\langle n-2r| \tag{H8}$$

Similarly, the reduced density matrix of field mode 2 can be written

$$\rho_2(t) = \left|P_{r_{max}}^{(-)}(t)\right|^2|2r_{max}\rangle\langle 2r_{max}| + \sum_{r=0}^{r_{max}-1}\left[\left|P_r^{(-)}(t)\right|^2 + \left|P_{r+1}^{(+)}(t)\right|^2\right]|2r\rangle\langle 2r| \tag{H9}$$

Therefore, the entropies of the two modes are

$$S_1(t) = -\left|P_0^{(-)}(t)\right|^2 ln\left|P_0^{(-)}(t)\right|^2 - \sum_{r=1}^{r_{max}}\left[\left|P_r^{(-)}(t)\right|^2 + \left|P_r^{(+)}(t)\right|^2\right]ln\left[\left|P_r^{(-)}(t)\right|^2 + \left|P_r^{(+)}(t)\right|^2\right] \tag{H10}$$

and

$$S_2(t) = -\left|P_{r_{max}}^{(-)}(t)\right|^2 ln\left|P_{r_{max}}^{(-)}(t)\right|^2 - \sum_{r=0}^{r_{max}-1}\left[\left|P_r^{(-)}(t)\right|^2 + \left|P_{r+1}^{(+)}(t)\right|^2\right]ln\left[\left|P_r^{(-)}(t)\right|^2 + \left|P_{r+1}^{(+)}(t)\right|^2\right] \tag{H11}$$

which are plotted in Figs. 6 and H1. Clearly, $S_{1:2} = S_1 + S_2 - S_F$, with $S_F = S_A$.

We conclude this section demonstrating Eq. (9). Considering the total excitation number, the first Eq. (8) implies $\langle S_z\rangle = \varepsilon - 1/2$, that is,

$$\frac{1}{2}\left[\sum_{k=2}^{n}\left|Q_k^{(+)}(t)\right|^2 - \sum_{k=0}^{n}\left|Q_k^{(-)}(t)\right|^2\right] = \varepsilon - \frac{1}{2} \tag{H12}$$

Eq. (H12) and the state normalization condition

$$\sum_{k=2}^{n}\left|Q_k^{(+)}(t)\right|^2 + \sum_{k=0}^{n}\left|Q_k^{(-)}(t)\right|^2 = 1 \tag{H13}$$

yield

$$\sum_{k=2}^{n}\left|Q_k^{(+)}(t)\right|^2 = \varepsilon = 1 - \sum_{k=0}^{n}\left|Q_k^{(-)}(t)\right|^2 \tag{H14}$$

from which

$$S_{A:F}(\varepsilon) = 2S_A(\varepsilon) = -2[\varepsilon ln\varepsilon + (1-\varepsilon)ln(1-\varepsilon)] \tag{H15}$$

namely, Eq. (9).

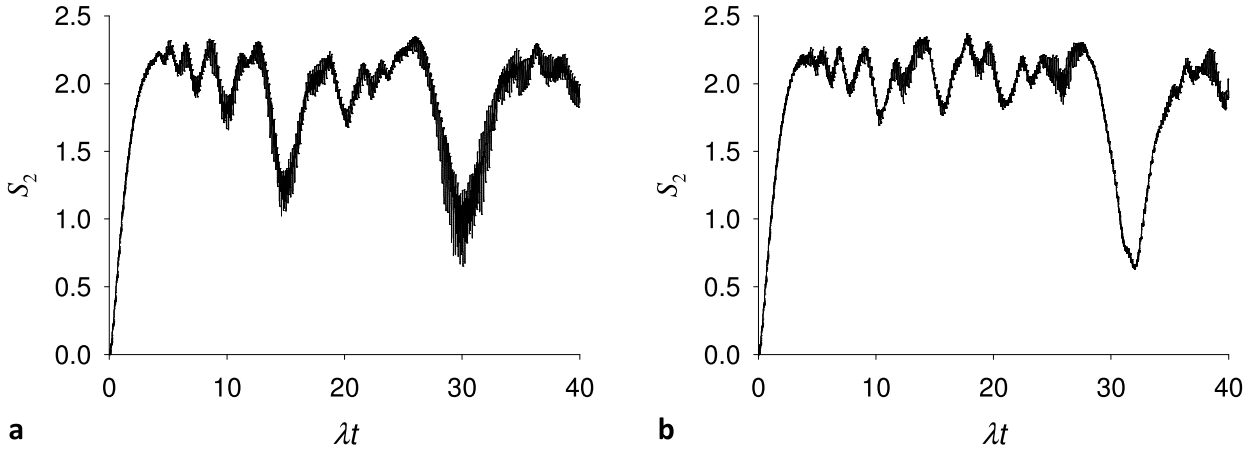

Fig. H1. Entropy in field mode 2, S_2, vs. λt for (a) $n = 20$ and (b) $n = 21$.

Appendix I

Closed-form expressions for $\langle S_z(t)\rangle$ *and* $n_1(t)$ *for* $|\psi(0)\rangle = |n, m, -\rangle$

To obtain closed-form expressions for $\langle S_z(t)\rangle$ and $\langle n_1(t)\rangle$ when the initial state of the system is given by Eq. (4), we use the unitary operator in Eq. (B1). The transformed of the initial state is

$$\begin{aligned}
|\varphi_m(0)\rangle &= U^\dagger|n,m,-\rangle = U^\dagger\frac{(a_1^\dagger)^n(a_2^\dagger)^m}{\sqrt{n!m!}}UU^\dagger|0,0,-\rangle = \frac{(a_1^\dagger+ia_2^\dagger)^n(a_2^\dagger+ia_1^\dagger)^m}{\sqrt{2^{n+m}n!m!}}|0,0,-\rangle \\
&= \frac{1}{\sqrt{2^{n+m}n!m!}}\sum_{j=0}^{n}\sum_{k=0}^{m} i^{j+k}\binom{n}{j}\binom{m}{k}(a_1^\dagger)^{n-j+k}(a_2^\dagger)^{m-k+j}|0,0,-\rangle \\
&= \sum_{j=0}^{n}\sum_{k=0}^{m} i^{j+k}\binom{n}{j}\binom{m}{k}\left[\tfrac{1}{2^{n+m}}\tfrac{(n-j+k)!(m-k+j)!}{n!m!}\right]^{1/2}|n-j+k,m-k+j,-\rangle \\
&= \sum_{j=0}^{n}\sum_{k=0}^{m} P_{jk}^{(n,m)}|n-j+k,m-k+j,-\rangle
\end{aligned} \tag{I1}$$

with the expression for $P_{jk}^{(n,m)}$ given by Eq. (B14b). Through the same procedure leading from Eq. (B8) to Eq. (B11), we obtain

$$\begin{aligned}
|\varphi_m(t)\rangle &= e^{-i(n+m-1)\omega t}\left\{\sum_{j=0}^{n}\sum_{k=0}^{m} P_{jk}^{(n,m)}cos[\phi(j,k)t]|n-j+k,m-k+j,-\rangle\right. \\
&\left. -\sum_{j=0}^{n}\sum_{k=\delta_{j0}}^{m-\delta_{jn}} P_{jk}^{(n,m)}sin[\phi(j,k)t]|n-j+k-1,m-k+j-1,+\rangle\right\}
\end{aligned} \tag{I2a}$$

where

$$\phi(j,k) = 2\lambda\sqrt{(n-j+k)(m-k+j)} \tag{I2b}$$

Note that the second double summation of Eq. (I2a) excludes the $\{j,k\} = \{0,m\},\{n,0\}$ terms, for which the corresponding Fock states in the sum cannot be defined. However, next we will use the fact that $sin[\phi(0,m)t] = sin[\phi(n,0)t] = 0$ to simplify the expression of $\langle S_z(t)\rangle$.

The expectation value of the atomic inversion operator, as a function of time, is

$$\begin{aligned}
\langle S_z(t)\rangle &= \langle\varphi_m(t)|S_z|\varphi_m(t)\rangle \\
&= -\frac{1}{2}\sum_{j,j'=0}^{n}\sum_{k,k'=0}^{m} P_{jk}^{(n,m)*}P_{j'k'}^{(n,m)}\{cos[\phi(j,k)t]cos[\phi(j',k')t] - sin[\phi(j,k)t]sin[\phi(j',k')t]\}\delta_{j'-j,k'-k} \\
&= -\frac{1}{2}\sum_{j,j'=0}^{n}\sum_{k,k'=0}^{m} P_{jk}^{(n,m)*}P_{j'k'}^{(n,m)}cos\{[\phi(j,k)+\phi(j',k')]\,t\}\delta_{j'-j,k'-k}
\end{aligned} \tag{I3}$$

We put $j^{'}-j=k^{'}-k=l$. Since $0\le k^{'}=k+l\le m$, it is $-k\le l\le m-k$. On the other hand, j has to satisfy the two conditions $0\le j\le n$ and $0\le j^{'}=j+l\le n$, and thus $max\{0,-l\}\le j\le min\{n,n-l\}$. Here, we limit our analysis to $n\ge m$, so that $n-l\ge 0$ irrespective of the k value. For $n\le m$, the analysis in this section can be repeated by exchanging field modes 1 and 2. Alternatively, one can set the upper bound for j to the maximum of 0 and $min\{n,n-l\}$. Based on these considerations and on the fact that

$$\begin{aligned}P_{jk}^{(n,m)*}P_{j+l,k+l}^{(n,m)} &= \frac{(-1)^l}{2^{n+m}}\left[\binom{n}{j}\binom{m}{k}\binom{n-j+k}{k}\binom{m-k+j}{j}\right.\\ &\left.\times\binom{n}{j+l}\binom{m}{k+l}\binom{n-j+k}{k+l}\binom{m-k+j}{j+l}\right]^{1/2}\\ &= \frac{(-1)^l}{2^{n+m}}\left[\binom{n}{j+l}\binom{m}{k+l}\binom{n-j+k}{k}\binom{m-k+j}{j}\right.\\ &\left.\times\frac{n!m!(n-j+k)!(m-k+j)!}{j!(n-j)!k!(m-k)!(k+l)!(n-j-l)!(j+l)!(m-k-l)!}\right]^{1/2}\\ &= \frac{(-1)^l}{2^{n+m}}\binom{n}{j+l}\binom{m}{k+l}\binom{n-j+k}{k}\binom{m-k+j}{j}\end{aligned} \tag{I4}$$

and that $\phi(j,k)=\phi(j+l,k+l)\ \forall l$, Eq. (I3) can be recast in the form

$$\begin{aligned}\langle S_z(t)\rangle &= -\frac{1}{2^{m+n+1}}\sum_{k=0}^{m}\sum_{l=-k}^{m-k}\sum_{j=max\{0,-l\}}^{min\{n,n-l\}}(-1)^l\binom{n}{j+l}\binom{m}{k+l}\binom{n-j+k}{k}\binom{m-k+j}{j}cos[2\phi(j,k)t]\\ &= -\frac{1}{2^{n+m+1}}\sum_{k,l=0}^{m}\sum_{j=max\{0,-l+k\}}^{min\{n,n-l+k\}}(-1)^{l-k}\binom{n}{j+l-k}\binom{m}{l}\binom{n-j+k}{k}\binom{m-k+j}{j}cos[2\phi(j,k)t]\end{aligned} \tag{I5}$$

where the last equality was obtained through the change of index $l\to l^{'}=l+k$ ($l^{'}$ was then renamed l).

To find a closed-form expression for $n_1(t)\equiv\left\langle\widehat{n}_1(t)\right\rangle$, we use Eq. (D2) with $N=n+m$, that is,

$$n_1(t)=\frac{n+m-1}{2}-\langle S_z(t)\rangle-\mathrm{Im}\langle\varphi_m(t)|a_1a_2^{\dagger}|\varphi_m(t)\rangle \tag{I6}$$

Using Eq. (I2), the last term on the right-hand side of Eq. (I6) is written

$$\begin{aligned}\langle\varphi_m(t)|a_1a_2^{\dagger}|\varphi_m(t)\rangle &= \sum_{j,j^{'}=0}^{n}\sum_{k,k^{'}=0}^{m}\left\{\sqrt{(n-j+k)(m-k+j+1)}\,cos[\phi(j,k)t]cos[\phi(j^{'},k^{'})t]\right.\\ &\left.+\sqrt{(n-j+k-1)(m-k+j)}\,sin[\phi(j,k)t]sin[\phi(j^{'},k^{'})t]\right\}P_{j^{'}k^{'}}^{(n,m)*}P_{jk}^{(n,m)}\delta_{j^{'}-j-1,k^{'}-k}\end{aligned} \tag{I7}$$

By putting $j^{'}-j-1=k^{'}-k=l$, we obtain $-k\le l\le m-k$, $max\{0,-l-1\}\le j\le min\{n,n-l-1\}$ and $\phi(j+l+1,k+l)=\phi(j+1,k)\ \forall l$. Furthermore,

$$\begin{aligned}P_{j+l+1,k+l}^{(n,m)}{}^{*}P_{jk}^{(n,m)}\sqrt{(n-j+k)(m-k+j+1)} &= \frac{-i(-1)^l}{2^{n+m}}[(n-j+k)(m-k+j+1)\\ &\times\binom{n}{j}\binom{m}{k}\binom{n-j+k}{k}\binom{m-k+j}{j}\binom{n}{j+l+1}\binom{m}{k+l}\binom{n-j-1+k}{k+l}\binom{m-k+1+j}{j+l+1}\Big]^{1/2}\\ &= -i(-1)^l\frac{m-k+j+1}{2^{n+m}}\left[\binom{n}{j+l+1}\binom{m}{k+l}\binom{n-j+k}{k}\binom{m-k+j}{j}\right.\\ &\left.\times\frac{n!m!(n-j+k)!(m-k+j)!}{j!(n-j)!k!(m-k)!(k+l)!(n-j-1-l)!(j+l+1)!(m-k-l)!}\right]^{1/2}\\ &= -i(-1)^l\frac{m-k+j+1}{2^{n+m}}\binom{n}{j+l+1}\binom{m}{k+l}\binom{n-j+k}{k}\binom{m-k+j}{j}\end{aligned} \tag{I8}$$

Therefore,

$$\langle\varphi_m(t)|a_1a_2^{\dagger}|\varphi_m(t)\rangle = -i\sum_{k=0}^{m}\sum_{l=-k}^{m-k}\sum_{j=max\{0,-1-l\}}^{min\{n,n-1-l\}}(-1)^l\frac{m-k+j+1}{2^{n+m}}$$

$$\times\binom{n}{j+l+1}\binom{m}{k+l}\binom{n-j+k}{k}\binom{m-k+j}{j}\{cos[\phi(j,k)t]cos[\phi(j+1,k)t]$$

$$+\sqrt{\left(1-\frac{1}{n-j+k}\right)\left(1-\frac{1}{m-k+j+1}\right)}\,sin[\phi(j,k)t]sin[\phi(j+1,k)t]\Bigg\} \tag{I9}$$

$$= -i\sum_{k,l=0}^{m}\sum_{j=max\{0,-1-l+k\}}^{min\{n,n-1-l+k\}}(-1)^{l-k}\frac{m-k+j+1}{2^{n+m}}$$

$$\times\binom{n}{j+l-k+1}\binom{m}{l}\binom{n-j+k}{k}\binom{m-k+j}{j}\{cos[\phi(j,k)t]cos[\phi(j+1,k)t]$$

$$+\sqrt{\left(1-\frac{1}{n-j+k}\right)\left(1-\frac{1}{m-k+j+1}\right)}\,sin[\phi(j,k)t]sin[\phi(j+1,k)t]\Bigg\}$$

Inserting Eq. (I9) into Eq. (I6), we obtain

$$n_1(t) = \frac{n+m-1}{2} - \langle S_z(t)\rangle + \sum_{k,l=0}^{m}\sum_{j=max\{0,-1-l+k\}}^{min\{n,n-1-l+k\}}(-1)^{l-k}\frac{m-k+j+1}{2^{n+m}}$$

$$\times\binom{n}{j+l-k+1}\binom{m}{l}\binom{n-j+k}{k}\binom{m-k+j}{j}\{cos[\phi(j,k)t]cos[\phi(j+1,k)t] \tag{I10}$$

$$+\sqrt{\left(1-\frac{1}{n-j+k}\right)\left(1-\frac{1}{m-k+j+1}\right)}\,sin[\phi(j,k)t]sin[\phi(j+1,k)t]\Bigg\}$$

with $\langle S_z(t)\rangle$ given by Eq. (I5). For $m = 1$,

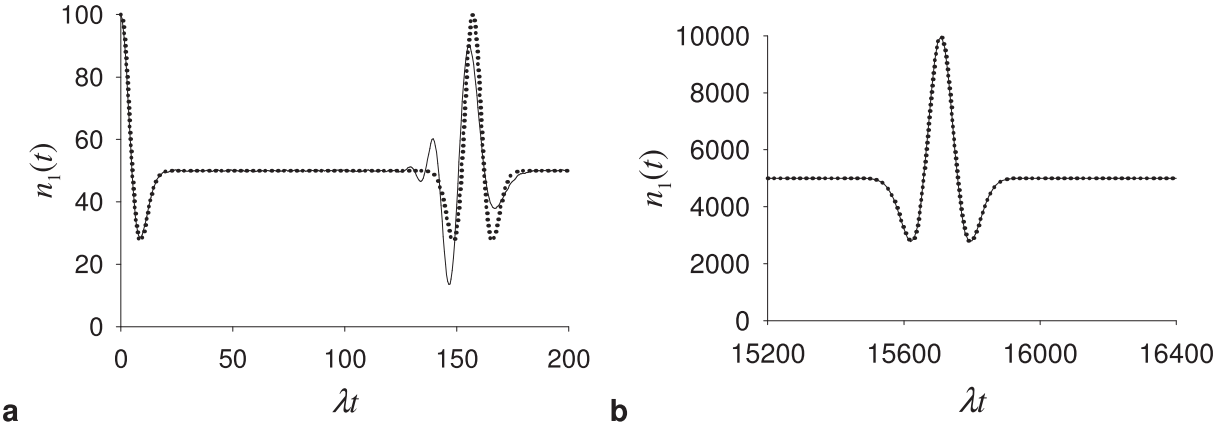

Fig. I1. Exact and approximate evolution of $n_1(t)$ for $|\psi(0)\rangle = |n, 1, -\rangle$, namely, plot of Eqs. (I11) (solid line) and (I19) (dotted line) for (a) $n = 100$ and (b) for $n = 10^4$. The relatively narrow time range diagrammed in panel (b) displays that the approximate Eq. (I19) also accurately describes the first revival of field mode 1 population for the larger n value.

$$
\begin{aligned}
n_1(t) &= \frac{n}{2} - \langle S_z(t)\rangle + \sum_{k,l=0}^{1} \sum_{j=max\{0,-1-l+k\}}^{min\{n,n-1-l+k\}} (-1)^{l-k} \frac{2-k+j}{2^{n+1}} \\
&\times \binom{n}{j+l-k+1} \binom{n-j+k}{k} \binom{1-k+j}{j} \{cos[\phi(j,k)t] cos[\phi(j+1,k)t] \\
&+ \sqrt{\left(1-\frac{1}{n-j+k}\right)\left(1-\frac{1}{2-k+j}\right)}\, sin[\phi(j,k)t] sin[\phi(j+1,k)t] \Big\} \\
&= \frac{n}{2} - \langle S_z(t)\rangle + \frac{1}{2^{n+1}} \sum_{j=0}^{n-1} \binom{n}{j} (j+2)(n-j) \{cos[\phi(j,0)t] cos[\phi(j+1,0)t] \\
&+ \sqrt{\left(1-\frac{1}{n-j}\right)\left(1-\frac{1}{j+2}\right)}\, sin[\phi(j,0)t] sin[\phi(j+1,0)t] \Big\} \\
&- \frac{1}{2^{n+1}} \sum_{j=0}^{n-2} \binom{n}{j} (n-j)(n-j-1) \{cos[\phi(j,0)t] cos[\phi(j+1,0)t] \\
&+ \sqrt{\left(1-\frac{1}{n-j}\right)\left(1-\frac{1}{j+2}\right)}\, sin[\phi(j,0)t] sin[\phi(j+1,0)t] \Big\} \\
&- \frac{1}{2^{n+1}} \sum_{j=0}^{n} \binom{n}{j} (j+1)(n-j+1) \{cos[\phi(j,1)t] cos[\phi(j+1,1)t] \\
&+ \sqrt{\left(1-\frac{1}{n+1-j}\right)\left(1-\frac{1}{j+1}\right)}\, sin[\phi(j,1)t] sin[\phi(j+1,1)t] \Big\} \\
&+ \frac{1}{2^{n+1}} \sum_{j=0}^{n-1} \binom{n}{j} (n-j+1)(n-j) \{cos[\phi(j,1)t] cos[\phi(j+1,1)t] \\
&+ \sqrt{\left(1-\frac{1}{n+1-j}\right)\left(1-\frac{1}{j+1}\right)}\, sin[\phi(j,1)t] sin[\phi(j+1,1)t] \Big\} \\
&= \frac{n}{2} - \langle S_z(t)\rangle + \frac{1}{2^{n+1}} \sum_{j=0}^{n-1} \binom{n}{j} (n-j)(2j+3-n) \{cos[\phi(j,0)t] cos[\phi(j+1,0)t] \\
&+ \sqrt{\left(1-\frac{1}{n-j}\right)\left(1-\frac{1}{j+2}\right)}\, sin[\phi(j,0)t] sin[\phi(j+1,0)t] \Big\} \\
&- \frac{1}{2^{n+1}} \sum_{j=1}^{n} \binom{n}{j} (n-j+1)(2j+1-n) \{cos[\phi(j,1)t] cos[\phi(j+1,1)t] \\
&+ \sqrt{\left(1-\frac{1}{n+1-j}\right)\left(1-\frac{1}{j+1}\right)}\, sin[\phi(j,1)t] sin[\phi(j+1,1)t] \Big\} \\
&= \frac{n}{2} - \langle S_z(t)\rangle + \frac{n}{2^{n+1}} \sum_{j=0}^{n-1} \binom{n-1}{j} \frac{(n-2j-1)(n-2j-3)}{j+1} \{cos[\theta(j)t] cos[\theta(j+1)t] \\
&+ \sqrt{\frac{j+1}{j+2}\left(1-\frac{1}{n-j}\right)}\, sin[\theta(j)t] sin[\theta(j+1)t] \Big\} \\
&= \frac{n}{2} - \langle S_z(t)\rangle + \frac{n}{2^{n+1}} \sum_{j=0}^{n-1} \binom{n-1}{j} \frac{(n-2j-1)(n-2j-3)}{j+1} \{cos[(\theta(j)-\theta(j+1))t] \\
&+ \left[\sqrt{\frac{j+1}{j+2}\left(1-\frac{1}{n-j}\right)} - 1\right] sin[\theta(j)t] sin[\theta(j+1)t] \Big\}
\end{aligned}
\tag{I11}
$$

with

$$\theta(j) \equiv \phi(j,0) = 2\lambda\sqrt{(j+1)(n-j)} \tag{I12}$$

Next, we construct an approximate expression for $n_1(t)$ that highlights the generalized parity effect in the $m = 1$ case. Considering that the mean of the binomial distribution with probability 1/2 is $n/2$, and using the same kind of approximation as in Eq. (D25), it is easy to demonstrate that the sum of sine functions in Eq. (I11) is less than 1. To obtain an analytical approximation for the cosine summation, we first derive expressions for p and $n-p$ from Eq. (D24) to write

$$\begin{aligned}\theta(p) - \theta(p+1) &= 2\lambda\left[\sqrt{(p+1)(n-p)} - \sqrt{(p+2)(n-p-1)}\right] \\ &= n\lambda\left(\sqrt{1+\frac{2}{n}-\frac{2x}{n}-x^2} - \sqrt{1+\frac{2}{n}-\frac{8}{n^2}-\frac{6x}{n}-x^2}\right) \cong \frac{2\lambda}{n}(2p-n+2)\end{aligned} \tag{I13}$$

where the approximation neglects $O(n^{-3/2})$ terms, that is, it is valid for $\lambda t \ll n^{3/2}$. Then, with the shorthand notation

$$g(p) = cos\left[\frac{2\lambda t}{n}(2p-n+2)\right] \tag{I14}$$

we elaborate on the summation as follows:

$$\begin{aligned}&\frac{n}{2^{n+1}}\sum_{p=0}^{n-1}\binom{n-1}{p}\frac{(n-2p-1)(n-2p-3)}{p+1}g(p) = \frac{1}{2^{n+1}}\sum_{p=0}^{n-1}\binom{n}{p+1}(n-2p-1)(n-2p-3)g(p) \\ &= \frac{1}{2^{n+1}}\sum_{p=1}^{n}\binom{n}{p}(n-2p+1)(n-2p-1)g(p-1) \\ &= \frac{n^2-1}{2^{n+1}}\sum_{p=1}^{n}\binom{n}{p}g(p-1) - \frac{n-1}{2^{n-1}}\sum_{p=1}^{n}\binom{n}{p}p\,g(p-1) + \frac{1}{2^{n-1}}\sum_{p=2}^{n}\binom{n}{p}p(p-1)g(p-1) \\ &\cong \frac{n^2}{2^{n+1}}\sum_{p=0}^{n}\binom{n}{p}g(p-1) - \frac{n(n-1)}{2^{n-1}}\sum_{p=0}^{n-1}\binom{n-1}{p}g(p) + \frac{n(n-1)}{2^{n-1}}\sum_{p=0}^{n-2}\binom{n-2}{p}g(p+1)\end{aligned} \tag{I15}$$

The last approximate expression of Eq. (I15) uses Eq. (I14) to define $g(-1) = cos(2\lambda t)$ and considers that the additional $p = 0$ term in the first summation is negligible even compared to 1 for sufficiently large n. Furthermore, as we disregard the terms of the order of 1, we put $n^2 - 1 \cong n^2$. The first summation in the last line of Eq. (I15) is calculated by means of the identity (D29) [58] with $a = 4\lambda t/n$ and $b = -2\lambda t$:

$$\frac{1}{2^{n+1}}\sum_{p=0}^{n}\binom{n}{p}g(p-1) = \frac{1}{2^{n+1}}\sum_{p=0}^{n}\binom{n}{p}cos\left[\frac{2\lambda t}{n}(2p-n)\right] = \frac{1}{2}cos^n\left(\frac{2\lambda t}{n}\right) \tag{I16}$$

Similarly, the upper bound of the second summation is $n-1$ and $b = -2\lambda t + 4\lambda t/n$, whence

$$\frac{1}{2^{n-1}}\sum_{p=0}^{n-1}\binom{n-1}{p}g(p) = cos^{n-1}\left(\frac{2\lambda t}{n}\right)cos\left[\frac{2\lambda t}{n}(n-1) - 2\lambda t + \frac{4\lambda t}{n}\right] = cos^n\left(\frac{2\lambda t}{n}\right) \tag{I17}$$

while

$$\begin{aligned}&\frac{1}{2^{n-1}}\sum_{p=0}^{n-2}\binom{n-2}{p}g(p+1) = \frac{1}{2}cos^{n-2}\left(\frac{2\lambda t}{n}\right)cos\left[\frac{2\lambda t}{n}(n-2) - 2\lambda t + \frac{8\lambda t}{n}\right] \\ &= \frac{1}{2}cos^{n-2}\left(\frac{2\lambda t}{n}\right)\left[2cos^2\left(\frac{2\lambda t}{n}\right) - 1\right] = cos^n\left(\frac{2\lambda t}{n}\right) - \frac{1}{2}cos^{n-2}\left(\frac{2\lambda t}{n}\right)\end{aligned} \tag{I18}$$

Finally, neglecting terms of the order of 1 or less, Eq. (I11) gives Eq. (24), namely,

$$\begin{aligned}n_1(t) \;&\cong \frac{n}{2} + \frac{n^2}{2}cos^n\left(\frac{2\lambda t}{n}\right) - n(n-1)cos^n\left(\frac{2\lambda t}{n}\right) + n(n-1)cos^n\left(\frac{2\lambda t}{n}\right) - \frac{n(n-1)}{2}cos^{n-2}\left(\frac{2\lambda t}{n}\right) \\ &= \frac{n}{2} + \frac{n}{2}cos^{n-2}\left(\frac{2\lambda t}{n}\right)\left[ncos^2\left(\frac{2\lambda t}{n}\right) - n + 1\right] = \frac{n}{2} + \frac{n}{2}cos^{n-2}\left(\frac{2\lambda t}{n}\right)\left[1 - nsin^2\left(\frac{2\lambda t}{n}\right)\right]\end{aligned} \tag{I19}$$

Eq. (I19) implies the repopulation (emptying) of radiation field mode 1 for odd (even) $n+1$, with the mid-plateau turning point at $\lambda t = \pi n/2$, thus exemplifying the generalized parity effect. The comparison between the exact expression for $n_1(t)$ in Eq. (I11) and its approximation (I19) is shown in Fig. I1.

Appendix J

Experimental observability of the generalized parity effect.

Changing from atomic to SI units, Eq. (A34) gives an atom-field interaction strength parameter such that

$$\lambda \approx \frac{2\pi d^2}{\varepsilon_0 V \hbar} \frac{\omega_F}{\Delta} \tag{J1}$$

where d (which is equal to either d_- or d_+) defines the size of the atomic transition dipole moments, and ε_0 is the permittivity of vacuum. Using the dipole moment of cesium or rubidium (namely, alkali atoms frequently used in cavity QED [44]), which is on the order of 10^{-29} C m, as an approximation to d, considering a volume $V \sim 10^{-15}\mathrm{m}^3$ (as for optical cavities used in cold atom experiments [44,61]) and an angular frequency $\omega_F = 2\pi\nu/2$, with the value $\nu \cong 352$ THz of cesium D2 line [44,62], and estimating the detuning Δ as the corresponding natural line width of cesium, $\Delta \cong 32$ MHz [62,63], one obtains

$$\lambda \approx 2 \times 10^{-5}\omega_F \cong 2 \times 10^{10}\ \mathrm{s}^{-1} \tag{J2}$$

For $n = 20$ photons, Eq. (J2) implies that the parity effect is observable on a timescale

$$\tau \cong \frac{n}{\lambda} = 1\ \mathrm{ns} \tag{J3}$$

using well-feasible cavities [41,42] with Q factors on the order of 10^7. Clearly, the use of resonators with higher Q factors would produce larger λ values that still allow the rotating-wave approximation and are well below the limit of spectral collapse [40].

References

[1] Scholes GD, Fleming GR, Chen LX, Aspuru-Guzik A, Buchleitner A, Coker DF, et al. Nature 2017;543:647.
[2] Panitchayangkoon G, Hayes D, Fransted KA, Caram JR, Harel E, Wen JZ, et al. Proc Natl Acad Sci USA 2010;107:12766.
[3] Duan HG, Prokhorenko VI, Cogdell RJ, Ashraf K, Stevens AL, Thorwart M, et al. Proc Natl Acad Sci USA 2017;114:8493.
[4] Wang LL, Allodi MA, Engel GS. Nat Rev Chem 2019;3:477.
[5] Marais A, Adams B, Ringsmuth AK, Ferretti M, Gruber JM, Hendrikx R, et al. J R Soc Interface 2018;15:20180640.
[6] Schafer C, Ruggenthaler M, Appel H, Rubio A. Proc Natl Acad Sci USA 2019;116:4883.
[7] Hong XP, Kim J, Shi SF, Zhang Y, Jin CH, Sun YH, et al. Nat Nanotechnol 2014;9:682.
[8] Gao SY, Yang L, Spataru CD. Nano Lett 2017;17:7809.
[9] Manzeli S, Ovchinnikov D, Pasquier D, Yazyev OV, Kis A. Nat Rev Mater 2017;2:17033.
[10] Stanford MG, Rack PD, Jariwala D. npj 2D Mater Appl 2018;2:20.
[11] Ye M, Seo H. Galli G. npj Comput Mater 2019;5:44.
[12] Ambrosetti A, Ferri N, DiStasio RA, Tkatchenko A. Science 2016;351:1171.
[13] Gagliardi CJ, Wang L, Dongare P, Brennaman MK, Papanikolas JM, Meyer TJ, et al. Proc Natl Acad Sci USA 2016;113:11106.
[14] Mirhosseini M, Kim E, Zhang XY, Sipahigil A, Dieterle PB, Keller AJ, et al. Nature 2019;569:692.
[15] Hertzog M, Wang M, Mony J, Borjesson K. Chem Soc Rev 2019;48:937.
[16] Aeschlimann M, Brixner T, Differt D, Heinzmann U, Hensen M, Kramer C, et al. Nat Photonics 2015;9:663.
[17] Hagglund C, Apell SP, Kasemo B. Nano Lett 2010;10:3135.
[18] Chakraborty C, Vamivakas N, Englund D. Nanophotonics 2019;8:2017.
[19] Srivastava A, Sidler M, Allain AV, Lembke DS, Kis A, Imamoglu A. Nat Nanotechnol 2015;10:491.
[20] He YM, Clark G, Schaibley JR, He Y, Chen MC, Wei YJ, et al. Nat Nanotechnol 2015;10:497.
[21] Chakraborty C, Kinnischtzke L, Goodfellow KM, Beams R, Vamivakas AN. Nat Nanotechnol 2015;10:507.
[22] Jaynes ET, Cummings FW. Proc IEEE 1963;51:89.
[23] Chang DE, Jiang L, Gorshkov AV, Kimble HJ. New J Phys 2012;14:063003.
[24] Zavatta A, Parigi V, Kim MS, Bellini M. AIP Conf Proc 2009;1110:193.
[25] Zavatta A, Viciani S, Bellini M. Science 2004;306:660.
[26] Costanzo LS, Coelho AS, Pellegrino D, Mendes MS, Acioli L, Cassemiro KN, et al. Phys Rev Lett 2016;116:023602.
[27] Zavatta A, Bellini M. Nat Photonics 2012;6:350.
[28] Dell'Anno F, De Siena S, Illuminati F. Phys Rep 2006;428:53.
[29] Marian P, Marian TA. Phys Rev A 2016;93.
[30] Rehacek J, Hradil Z, Klimov AB, Leuchs G, Sanchez-Soto LL. Phys Rev A 2013;88.
[31] Napoli A, Messina A. J Electron Spectrosc Relat Phenom 1996;79:319.
[32] Napoli A, Messina A. Quantum Semiclass Opt 1997;9:587.
[33] Cerf NJ, Adami C. Phys Rev Lett 1997;79:5194.
[34] Wang DQ, Kelkar H, Martin-Cano D, Rattenbacher D, Shkarin A, Utikal T, et al. Nat Phys 2019;15:483.
[35] Cerf NJ, Adami C. Physica D 1998;120:62.
[36] Jaeger G. Quantum Information: An overview. New York: Springer; 2007.
[37] Roa L, Pozo-Gonzalez R, Schaefer M, Utreras-SM P. Phys Rev A 2007;75:062316.
[38] Furuichi S, Ohya M. Lett Math Phys 1999;49:279.
[39] Zhu BH, Liu SJ, Xiong HW. Chin Phys Lett 2011;28:090303.
[40] Felicetti S, Rossatto DZ, Rico E, Solano E, Forn-Diaz P. Phys Rev A 2018;97:013851.
[41] Puckett MW, Liu KK, Chauhan N, Zhao QC, Jin NJ, Cheng HT, et al. Nat Commun 2021;12:934.
[42] Srinivasan K, Borselli M, Johnson TJ, Barclay PE, Painter O, Stintz A, et al. Appl Phys Lett 2005;86:151106.
[43] Uria M, Solano P, Hermann-Avigliano C. Deterministic Generation of Large Fock States. Phys Rev Lett 2020;125:093603.
[44] Forn-Díaz P, Lamata L, Rico E, Kono J, Solano E. Rev Mod Phys 2019;91:025005.
[45] Gyger S, Zichi J, Schweickert L, Elshaari AW, Steinhauer S, da Silva SFC, et al. Nat Commun 2021;12:1408.
[46] Biagi N, Costanzo LS, Bellini M, Zavatta A. Adv Quantum Technol 2021;2000141.
[47] Biagi N, Costanzo LS, Bellini M, Zavatta A. Phys Rev Lett 2020;124:033604.
[48] Kocsis S, Braverman B, Ravets S, Stevens MJ, Mirin RP, Shalm LK, et al. Science 2011;332:1170.
[49] Wang Y, Lu YH, Mei F, Gao J, Li ZM, Tang H, et al. Phys Rev Lett 2019;122:193903.
[50] Kimble HJ. Nature 2008;453:1023.
[51] Law S, Kokkelmans S. J Appl Phys 2021;129.
[52] Weissbluth M. Atoms and Molecules. New York: Academic Press; 1978.
[53] Göppert-Mayer M. Ann Phys (Berlin) 2009;18:466.
[54] Schubert M, Wilhelmi B. Nonlinear optics and quantum electronics. New York: John Wiley & Sons, Inc.; 1986.
[55] Benivegna G, Messina A. Phys Rev A 1988;37:4747.
[56] Louisell WH. Quantum Statistical Properties of Radiation. New York: John Wiley & Sons, Inc.; 1973.
[57] Graham RL, Knuth DE, Patashnik O. Concrete mathematics: a foundation for computer science. 2nd ed. Addison-Wesley; 1994.
[58] Prudnikov AP, Brychkov YA, Marichev OJ. Integrals and Series. New York: Gordon and Breach Science Publishers; 1986.
[59] Gradshteyn IS, Ryzhik IM. Table of integrals, series, and products. 7th ed. United States of America: Elsevier Inc.; 2007.
[60] Wehrl A. Rev Mod Phys 1978;50:221.
[61] Rempe G, Thompson RJ, Kimble HJ, Lalezari R. Opt Lett 1992;17:363.
[62] Steck DA. 2019:Available online at http://steck.us/alkalidata.
[63] Arora P, Jha P, Agarwal A, Gupta AS. Indian J Pure Appl Phys 2012;50:295.